LOW COST ALGORITHMS FOR IMAGE/VIDEO CODING AND RATE CONTROL

CHRISTOS GRECOS

A submission presented in partial fulfilment of the requirements of the University of Glamorgan/Prifysgol Morgannwg for the degree of Doctor of Philosophy

March 2001

Abstract

This thesis is focused on low computational cost and low encoding delay algorithms for image/video coding and for the rate control problem. Ten algorithms and four estimates are proposed which can be classified along three main streams. In the first stream, three algorithms are designed for indirectly optimizing the visual quality for JPEG-LS for the same compression rates as the standard. They are based on the different tolerance of HVS across different textures and they exploit the prediction scheme of JPEG-LS for accurate texture identification. In the second stream, pixel trend variation is used in the design of two algorithms in order to improve the compression rates by up to 9% in the padding problem of boundary macroblocks in MPEG-4. Pixel trend variation is also used through two novel algorithms in order to reduce the MSE error by up to 3% for the same compression rates in the case of diagonal edge detection in JPEG-LS. In the third stream, four novel estimates are proposed to optimize "on-the-fly" the R-D performance of the MPEG-2 rate control scheme. This is achievable through exponential modulation, non-variance based activity estimates and local activity estimation. Improvements by up to 3.5db for the same bit rates as the standard were observed. Finally, two algorithms that improve the "rate only" MPEG-2 rate control scheme in R-D terms, by explicitly considering distortion in the quantization step size assignment through a Lagrangian based local optimization are proposed. The proposed schemes achieve improvements of 0.5-1db as compared to the 1db improvements of traditional R-D optimization techniques for the same compression rates as the standard but with just a small fraction of the operations needed.

All the algorithms and the estimates proposed are ideal for online compression applications where low computational complexity and encoding delay are of prime importance.

Acknowledgements

I would like to express my deepest gratitude and respect to my supervisor, Professor Jianmin Jiang. Jianmin was, and still is, a continuous source of inspiration for me. He taught me apart from compression, to appreciate the values of hard work and professionalism and I will always be indebted to him for that. Without his superb guidance, constant encouragement and patience, this thesis would have never been completed. I would also like to thank my second supervisor Dr Mike Reddy for his valuable comments and suggestions, especially in the writing up phase of this thesis.

My thanks are also due to Pat Bailey from the administrative staff of the School of Computing and to Keith Norris along with Dave Eyres from the academic staff, for their help regarding part time teaching issues. I am also indebted to Kevin Sewell for his excellent technical support of the UNIX research servers.

I would also like to thank my dear friend Dr Eran Edirisinghe from Loughborough University for all the research discussions we had and my fellow research students in the School of Computing for their friendship and comradeship.

Last but not least, a very special thank you goes to my parents Dimitrios and Anastasia and to my brother Constantinos. This thesis is especially dedicated to them for all their love and encouragement that they have shown to me during the years.

Table of Contents

Abstract I

Acknowledgements II

List of Figures and Tables VII

CHAPTER 1 – INTRODUCTION

1.1 Introduction to image and video coding 1

1.2 Research Objectives 2

1.3 An Overview of the Thesis 3

1.4 Research contributions 4

CHAPTER 2 - AN OVERVIEW OF IMAGE/VIDEO COMPRESSION ALGORITHMS

2.1 The Human Visual System 7

2.2 Image and Video coding standards 8

2.2.1 Image coding 8

2.2.2 Video coding 10

2.3 Wavelet based/image video coding 13

2.4 Motion estimation and segmentation 18

2.5 Adaptive quantization 21

2.6 Lossless data compression 29

2.7 Empirical versus model based R-D approaches 34

2.8 Rate Distortion and complexity 43

CHAPTER 2 - LOW COST RATE CONTROL ALGORITHMS FOR IMAGE CODING IN A JPEG-LS FRAMEWORK

3.1 Introduction to JPEG-LS 45

3.2 Multilevel information loss in JPEG-LS image compression 48

3.3 Low cost algorithms for Rate Control in still image compression 57

3.3.1 1st Algorithm proposed 57

3.3.2 Experimental evaluation for the proposed scheme 65

3.3.3 2nd Algorithm proposed 67

3.3.4 Experimental evaluation and analysis of the proposed scheme 76

3.4 Applications in medical imaging 86

3.5 Conclusions 90

CHAPTER 4 - LOW COST, PIXEL TREND BASED IMPROVEMENTS OF COMPRESSION RATES AND QUALITY IN IMAGE/VIDEO CODING

4.1 Introduction 92

4.2 Overview of the MPEG-4 standard 92

4.3	Reference VOP Padding	94
4.4	Drawback of the MPEG-4 Padding technique and Proposed Linear Extrapolated Padding Technique (LEP)	96
4.5	Experimental Results for LEP	101
4.6	Extrapolated Average Padding	102
4.7	A Hybrid Padding Scheme combining LEP and EAP	105
4.8	Experimental results and analysis of the hybrid scheme	106
4.9	The edge detection scheme of JPEG-LS and its assessment	107
4.10	Two algorithms for low cost diagonal edge detection in JPEG-LS	110
	4.10.1 Weight based diagonal edge detection	112
	4.10.2 Including pixel a in the prediction	114
	4.10.3 Experiments for the two proposed algorithms	115
4.11	Conclusions	120

CHAPTER 5 - LOW COMPUTATIONAL COST R-D IMPROVEMENTS IN MPEG-2 VIDEO CODING

5.1	Introduction	122
5.2	Review of the MPEG-2 rate control algorithm	124
	5.2.1 Drawbacks of the MPEG-2 rate control scheme	127
5.3	Improving the rate distortion performance by using a local activity estimate	128

5.4 Improving the rate distortion performance by using a family of exponential modulators 137

5.5 Low computational cost activity estimates 145

5.6 Review of the R-D approaches in the context of video coding 153

5.6.1 Analytic model based approaches 153

5.6.2 Empirical approaches 155

5.7 Towards online rate control using the Lagrange multiplier method in MPEG-2 159

5.7.1 Complexity analysis 169

5.7.2 Experiments 175

5.8 Conclusions 182

CHAPTER 6 - THESIS CONCLUSION AND FURTHER RESEARCH 184

References 189

List of Figures & Tables

Figures

Figure 2.1	Scanning route	14
Figure 2.2	Dominant pass	15
Figure 2.3	Subordinate pass	16
Figure 2.4	Empirical R-D approaches	34
Figure 3.1	Predictive pattern in JPEG-LS	45
Figure 3.2(a, b)	Predictive value for horizontal/vertical edge prediction	46
Figure 3.3	Modified information loss distribution in JPEG-LS	50
Figure 3.4(a)	Original "test8.pgm"	53
Figure 3.4(b)	Smooth part of test8.pgm blown up	53
Figure 3.4(c)	Reconstructed by JPEG-LS (NEAR=4)	54
Figure 3.4(d)	Reconstructed by the proposed scheme (NEAR_L=1,NEAR_M=5,NEAR_H=5)	54
Figure 3.4(e)	Reconstructed by JPEG-LS (NEAR=2)	55
Figure 3.4(f)	Reconstructed by the proposed scheme (NEAR_L=1,NEAR_M=2,NEAR_H=5)	55
Figure 3.4(g)	Reconstructed by JPEG-LS (NEAR=3)	56
Figure 3.4(h)	Reconstructed by the proposed scheme (NEAR_L=1,NEAR_M=4,NEAR_H=5)	56
Figure 3.5	The change of the NEAR values along with their thresholds in the proposed rate control scheme	60
Figure 3.6(a)	A flow chart for the rate control algorithm design when OCR < TCR	62
Figure 3.6(b)	A flow chart for the rate control algorithm design when OCR > TCR	62
Figure 3.7	Line fitting prediction with two points (d=3)	68

Figure 3.8	Initial state of parameters	71
Figure 3.9	Algorithm flow chart	71
Figure 3.10	An example of rate control for the sequence: I, I, D, D, D, D, I, I, I	74-75
Figure 3.11	Rate control with delayed action for parameter L	75
Figure 3.12(a)	Original "test8.pgm"	82
Figure 3.12(b)	Smooth part of test8.pgm blown up	82
Figure 3.12(c)	Reconstructed test8 by JPEG-LS with NEAR parameter equal to 3	83
Figure 3.12(d)	Reconstructed test8 by the proposed algorithm with the same compression ratio as in (c)	83
Figure 3.12(e)	Reconstructed test8 by JPEG-LS with NEAR parameter equal to 4	84
Figure 3.12(f)	Reconstructed test8 by the proposed algorithm with the same compression ratio as in (e)	84
Figure 3.12(g)	Reconstructed test8 by JPEG-LS with NEAR parameter equal to 5	85
Figure 3.12(h)	Reconstructed test8 by the proposed algorithm with the same compression ratio as in (g)	85
Figure 3.12	Visual comparison of test8 between JPEG-LS and the proposed rate-controlled JPEG-LS	85
Figure 3.13(a)	Original wound image	88
Figure 3.13(b)	Blown up part of original wound image	88
Figure 3.13 (c)	Blown up part of reconstructed wound image by JPEG-LS with NEAR=7	88
Figure 3.13(d)	Reconstructed wound image by the proposed scheme. (L,M,H) = (1,5,5) , TCR= Rate produced by JPEG-LS with NEAR=7	88
Figure 3.14(a)	Original rash image	89
Figure 3.14(b)	Blown up part of the original rash image	89

Figure 3.14 (c)	Blown up part of the rash image, reconstructed by JPEG-LS with NEAR=6	89
Figure 3.14(d)	Blown up part of the rash image reconstructed by the proposed scheme. (L,M,H) = (2,3,6) , TCR= Rate produced by JPEG-LS with NEAR=6	89
Figure 4.1	Macroblock classification scheme in a VOP. I denotes internal macroblocks, E external macroblocks, B boundary macroblocks	94
Figure 4.2	MPEG-4 Padding Scheme	95
Figure 4.3	Priority of boundary macroblocks	96
Figure 4.4	Error block formation in boundary blocks when the shape of the block to be encoded is inside the shape of the reference block	97
Figure 4.5	Error block formation in boundary blocks when the shape of the block to be encoded encompasses the shape of the boundary block	97
Figure 4.6	Interior/projected pixels	99
Figure 4.7	Modified padding	100
Figure 4.8	Error block formation in severely distorted boundary blocks	103
Figure 4.9	Extrapolated Average Padding	104
Figure 4.10	Matching geometry under which EAP would be more efficient than LEP	106
Figure 4.11	Predictive pattern in JPEG-LS	108
Figure 4.12(a)	Edge detection for c>=max(a,b)	109
Figure 4.12(b)	Edge detection for c<=min(a,b)	109
Figure 4.13	Possible forms of diagonal edges	112
Figure 4.14	Possible forms of pixel intensities in diagonal edges	112
Figure 5.1(a)	Normalised activity as a function of average activity of previous frame	126
Figure 5.1	Luma component of miss america sequence (loc. act. est)	132
Figure 5.2	Luma component of calendar sequence (loc. act. est)	132

Figure 5.3	Luma component of susie sequence (loc. act. est.)	133
Figure 5.4	Luma component of salesman sequence (loc. act. est.)	133
Figure 5.5	Luma component of trevor sequence (loc. act. est.)	134
Figure 5.6	U Chroma component of salesman sequence (loc. act. est.)	134
Figure 5.7	V Chroma component of salesman sequence (loc. act. est.)	135
Figure 5.8	U Chroma component of calendar sequence (loc. act. est.)	135
Figure 5.9	V Chroma component of calendar sequence (loc. act. est.)	136
Figure 5.10	Luma component of miss america sequence (exp. mod)	140
Figure 5.11	Luma component of calendar sequence (exp. mod)	140
Figure 5.12	Luma component of susie sequence (exp. mod)	141
Figure 5.13	Luma component of salesman sequence (exp. mod)	141
Figure 5.14	Luma component of trevor sequence (exp. mod)	142
Figure 5.15	U Chroma component of salesman sequence (exp. mod)	142
Figure 5.16	V Chroma component of salesman sequence (exp. mod)	143
Figure 5.17	U Chroma component of calendar sequence (exp. mod)	143
Figure 5.18	V Chroma component of calendar sequence (exp. mod)	144
Figure 5.19	Luma component of miss america sequence (std. dev.)	147
Figure 5.20	Luma component of miss america sequence (SAD)	147
Figure 5.21	Luma component of calendar sequence (std. dev.)	148
Figure 5.22	Luma component of calendar sequence (SAD)	148
Figure 5.23	Luma component of susie sequence (std. dev.)	149
Figure 5.24	Luma component of susie sequence (SAD)	149
Figure 5.25	Luma component of salesman sequence (std. dev.)	150
Figure 5.26	Luma component of salesman sequence (SAD)	150
Figure 5.27	Luma component of trevor sequence (std. dev.)	151

Figure 5.28 Luma component of trevor sequence (SAD) 151

Figure 5.29 Luma component of miss america sequence (MSE R-D imp) 177

Figure 5.30 Luma component of calendar sequence (MSE R-D imp) 177

Figure 5.31 Luma component of susie sequence (MSE R-D imp) 178

Figure 5.32 Luma component of salesman sequence (MSE R-D imp) 178

Figure 5.33 Luma component of trevor sequence (MSE R-D imp) 179

Figure 5.34 Luma component of miss america sequence (Q step R-D imp) 179

Figure 5.35 Luma component of calendar sequence (Q step R-D imp) 180

Figure 5.36 Luma component of susie sequence (Q step R-D imp) 180

Figure 5.37 Luma component of salesman sequence (Q step R-D imp) 181

Figure 5.38 Luma component of trevor sequence (Q step R-D imp) 181

Tables

Table 3.1 Phase 1 of experiments for test8.pgm 50

Table 3.2 Phase 2 of experiments for test8.pgm 52

Table 3.3 Rate Control Experimental Results (TCR = 2:1) 66

Table 3.4 Rate Control Experimental Results (TCR = 3:1) 66

Table 3.5 Initial NEAR Values 66

Table 3.6 Results of Compressed Image Quality (PSNR) 66

Table 3.7 Rate Control Experimental Results (Initial L, M, H = 1,8,9) 80

Table 3.8 Visual Perception Quality Rating Test Results 80

Table 3.9(a) Phase-2 Rate Control Experimental Results (Initial L, M, H = 0,0,2 and Target-Compression-Ratio = 2:1) 80

Table 3.9(b) Rate Control Experimental Results (Initial L, M, H = 1,8,9 and Target-Compression-Ratio = 3:1) 81

Table 3.10(a) Rate Control Experimental Results for Figure 2.13(a)

	(Initial L, M, H = 1,5,5)	87
Table 3.10(b)	Rate Control Experimental Results for Figure 2.14(a) (Initial L, M, H = 2,3,6)	87
Table 4.1	Experimental results	101
Table 4.2	Experimental results	107
Table 4.3	Experimental Results for weighted predictive scheme (T1=T2=10,a1=1,a2=2)	118
Table 4.4	Experimental Results for weighted predictive scheme (T1=T2=5,a1=2,a2=3)	118
Table 4.5	Experimental Results for weighted predictive scheme (T1=T2=8,a1=1,a2=3)	118
Table 4.6	Experimental Results by including pixel a in the prediction scheme (T1=T2=10)	119
Table 4.7	Experimental Results by including pixel a in the prediction scheme (T1=T2=5)	119
Table 4.8	Experimental Results by including pixel a in the prediction scheme (T1=T2=8)	119
Table 5.1	Bit rates produced by the proposed scheme versus MPEG-2 (loc. act. est.)	136
Table 5.2	Bit rates produced by the proposed scheme versus MPEG-2 (exp. mod)	144
Table 5.3	Bit savings in transmission of the changes of the final modulation factors (exp. mod)	144
Table 5.4	Comparison of the final number of bits produced (std dev/SAD)	152
Table 5.5	Bit savings in transmission of the changes of the quantization parameter (mquant) in SAD case (std dev/SAD)	152
Table 5.6	Bit savings in transmission of the changes of the quantization parameter (mquant) in standard deviation case (std dev/SAD)	152
Table 5.7	Comparison of the final number of bytes produced (MSE/Q. step R-D imp)	182

CHAPTER 1 - INTRODUCTION

1.1 Introduction to image and video coding

The field of image and video coding has seen considerable advancements in the last few years. It is a multi-disciplinary field, spanning electrical engineering, computer graphics, networks and data communications, neural networks and human computer interaction. Furthermore, image and video coding will be very important in the future for two reasons: the need for storage savings and the need for bandwidth optimization.

The need for storage savings mostly affects the disciplines of computer science and consumer electronics. In computer science, storage mostly relates to multimedia databases stored in servers where the true size of the database changes dynamically and is affected profoundly by the compression rates of multimedia elements. In consumer electronics, storage is important in any digital device such as a camera or digital video disks where the compression rate determines the quality of the stored medium (voice, images, home video etc).

The need for bandwidth optimization is evident in any sort of information transfer. Video and audio streaming, voice mail, multimedia applications over the web are just some examples where bandwidth is an important factor. This is likely to become an increasing problem due to the exponential growth of demand for multimedia based services. Furthermore, bandwidth optimization is more important than storage conservation since storage is relatively cheap while network capacity is expensive.

In image and video coding there are two conflicting requirements: compression and quality (both objective and subjective). Although there is no exact mathematical relationship between them, we can say that when compression increases, quality decreases

and vice versa. Any compression scheme also has to take into account the computational overhead. Compression of images and videos is computationally expensive and *low computational cost schemes* could provide better solutions for real time situations.

However there is a strong relation between image and video coding. While in the case of image coding spatial redundancy is exploited for improving compression rates, the extra temporal dimension gives more opportunities for exploitation of redundancy in video coding. Quality issues (both in statistical terms and in visual quality terms) are common to both image and video coding. In this perspective, any improvements in image coding are either directly applicable to video coding or are applicable with minor modifications.

This thesis is focused upon the development of novel low computational cost algorithms for image and video coding based on the JPEG-LS, MPEG-2 and MPEG-4 standards. Through these algorithms, new ideas will be explored for potentially improving the standards and attempts will be made to reconcile the conflicting requirements of compression and quality.

A detailed description of the standards is beyond the scope of any PhD thesis. Image and video coding standards have been developed over a period of years from a large number of people and after a strong collaboration between companies and academics. However, the scope of this research spans more than one coding standard, seeking a balance between compression rates, quality and complexity.

1.2 Research Objectives

The general research objective is to develop low cost algorithms for image/video compression and for the rate control problem.

The specific research objectives can be summarized as:

1. To develop an HVS based approach for JPEG-LS and subsequently to add rate control to the standard based on this HVS approach.
2. To utilize pixel trend variation for improving the padding scheme of MPEG-4 in terms of compression performance and for performing low cost diagonal edge detection for JPEG-LS.
3. To devise low cost estimates for "on-the-fly" improvements of the R-D performance of MPEG-2 and to use Lagrangian theory for local optimization of the buffer based only rate control scheme of the standard.

1.3 An Overview of the Thesis

Chapter 2 represents the "Literature review" part of this thesis, where essential background and state of the art techniques about image/video coding will be presented. Since some of the proposed algorithms in this thesis are based on properties of the Human Visual System (HVS), the corresponding section refers to current research on this topic. Subsequently, in the "Image and Video Coding standards" section, "the big picture" of the most important image and video coding standards along with potential applications and trade-offs involved will be presented. In the section about "Wavelet based image/video coding", issues and algorithms about the state of the art wavelet based codecs will be discussed. The section about "Motion estimation and segmentation" will present some recent research efforts for these two computationally intensive problems. The section about "Adaptive quantization" will examine the problems of scalar and vector quantization as a more general case, and many theoretical issues relating quantization and adaptivity will be investigated. This section is very relevant to this thesis since many of the proposed algorithms use adaptive quantization to improve R-D and visual performance. In the section entitled "Lossless

image compression", adaptivity and modeling issues in the context of lossless coding will be addressed through the description of the design rationale of the JPEG-LS standard for lossless/near lossless image compression. The section entitled "Empirical versus model based R-D approaches", will present and critically evaluate previous work in the R-D optimization area, relating to the proposed algorithms for low cost R-D improvements. The literature review will conclude with a section entitled "Rate Distortion and complexity" which will address the issue of complexity in a rate distortion framework. This is relevant to the presented algorithms in this thesis, since all of them are low computational cost schemes. In Chapters 3-5, existing approaches relating to the investigated problems will be examined *on individual problem basis and research contributions* will be presented in the following order:

a) Proposed algorithms for the investigated problems.

b) Experimental results by testing the proposed algorithms against the standards.

c) Critical evaluation of the proposed algorithms along with conclusions.

Finally, Chapter 6 will conclude this thesis by summarizing the main research contributions and proposing further research directions.

1.4 Research contributions

This thesis has resulted in a variety of contributions in refereed journals and conferences which are represented by the following list:

Journal papers

1. Grecos C. Jiang J. 'Achieving a better balance between image compression and image quality' IEE Electronic Letters, Vol. 35, No 23, pp2019-2020, 1999.
2. Edirisinghe E.A. Jiang J. and Grecos C. 'Object boundary padding technique for improving MPEG-4 video compression efficiency' IEE Electronic Letters, Vol. 35, No 17, 1999, pp1453-1455.
3. E.A.Edirisinghe, J.Jiang, C.Grecos, "Shape Adaptive Padding for MPEG-4", IEEE Transactions on Consumer Electronics, August 2000, Vol. 46, No 3, pp. 514-520, ISSN 0098-3063
4. J.Jiang, C.Grecos' A Low Cost Design of Rate Controlled JPEG-LS Near Lossless Image Compression', Image and Vision Computing, Vol.19, Issue 3,pp 153-164,ISSN 0262-8856, January 2001.
5. J.Jiang, C. Grecos " Adding rate control to JPEG-LS ", to appear in SPIE Journal of Electronic Imaging, Volume 10, no 3, July 2001. (Paper No JEI 20047).

Conference Papers

1. E.A.Edirisinghe, J.Jiang, C.Grecos, "Shape Adaptive Padding for MPEG-4", IEEE International Conference on Consumer Electronics (ICCE 2000), Los Angeles, USA, June 2000.
2. Edirisinghe E.A., Grecos C. and Jiang J. 'A modified padding technique for MPEG-4 video object planes', Proceedings of IWSNHC3DI'99: International Workshop on Synthetic-Natural Hybrid Coding and 3D Imaging, Santorini, Greece, 1999, pp. 45-49.

3. C Grecos. Jiang J. 'Rate control - a low complexity approach' Proceedings of International Conference on Information, Communications and Signal Processing, 7-10 Dec 1999, Singapore, ISBN: 981-04-2108-7.
4. C.Grecos, Jiang J. and Reddy M. 'Near lossless image compression using local texture adaptive information loss distribution', Proceedings of International Conference on Information, Communications and Signal Processing, 7-10 Dec 1999, Singapore, ISBN: 981-04-2108-7.
5. C.Grecos, J.Jiang "Improved estimation of quantifier moderators in MPEG-2 using a novel robust estimate and a family of exponential modulators", SPIE Photonics East, Boston, November 2000,Vol 4296.
6. C.Grecos, J.Jiang, E.Edirisinghe "An HVS based rate control algorithm using JPEG-LS with applications to wound imagery", SPIE Medical Imaging 2001, Vol. 4324, San Diego, CA.
7. C.Grecos, J.Jiang "Low cost improved activity estimation in MPEG-2 rate control", SIP 2000, Las Vegas, NV, pp. 186-191, ISBN 0-88986-308-3,ISSN 1482-7921
8. C.Grecos, J.Jiang "On improving the rate distortion performance in MPEG-2 rate control", IMSA 2000, Las Vegas, NV, pp. 381-387, ISBN 0-88986-314-8
9. C.Grecos, J.Jiang "Two low cost algorithms for improved diagonal edge detection in JPEG-LS", IEEE International Conference on Consumer Electronics (ICCE 2001), Los Angeles, USA, June 2001. (Accepted)

Journal submission

Online improvements of the Rate Distortion Performance in MPEG-2 Rate Control using the Lagrange Multiplier Method, submitted to CSVT, January 2001.

CHAPTER 2 - AN OVERVIEW OF IMAGE/VIDEO COMPRESSION ALGORITHMS

2.1 The Human Visual System

The study of HVS has been covered within the field of psychophysics and it usually involves intensive experiments and visual tests. A very useful model from this research is the Multi-Channel model [1] according to which HVS is modeled as a bank of filters, with each filter tuned to a specific band of spatial frequency and orientation. Two key concepts, the contrast sensitivity and the masking effect govern the perception of the signal in each band. The contrast sensitivity accounts for the perception of a single band and the masking effect quantises the interactions between several bands. Contrast sensitivity is defined for a given spatial frequency as the minimum amplitude of the signal required in order to be detected. The Human Visual System perceives the output of each band with different sensitivity. For example it is more sensitive to lower spatial frequencies than to higher frequencies and is more sensitive to horizontal and vertical patterns than to diagonal ones. The masking effect describes the fact that if there are more than one signal (in different bands) present in the same area and the energy of the largest signal is higher than any others by some threshold, all other signals will be masked. There are two types of masking effects for still images. The first is due to the DC band of the signal. Because the DC band corresponds to background luminance, it is also known as *background luminance masking*. On the other hand, if the masking is caused by other higher frequency bands, it is usually called *texture masking*. For video or motion pictures there is another type of masking known as *temporal masking*. This is due to the fact that human eyes have to be focused on an object long enough (e.g. 0.1 seconds) in order to clearly see the details of that object.

Hence, a scene with fast moving objects or frames just after a scene change is usually masked. More details of HVS related studies can be found in [1-4, 26-30]. To distinguish statistical from visual issues, two kinds of quality are currently used in image and video coding research, namely the objective and the subjective quality. *Objective quality* is the statistical measure of the distance between the original and the reconstructed image/video frame and the usual metrics are the Peak Signal to Noise Ratio (PSNR) or the Mean Square Error (MSE). On the other hand, there is no reliable statistical metric *for subjective quality*, it can only be evaluated by running experiments with users or with reference to models of HVS. In general, it seems that the requirement is that the tolerance of HVS to distortion is frequency dependent in images, while constant or near constant distortion is desired for video sequences due to extra sensitivity of HVS to luminance changes. Comparing the objective and subjective measures of quality, we can say that PSNR or MSE can show the average amount of information loss, while the subjective quality can show where the information loss occurred.

2.2 Image and Video Coding standards

2.2.1 Image coding

The research efforts have centered around the development of compression standards such as JPEG lossy, JPEG-LS and JPEG2000 [5-6, 17-19].

JPEG lossy [31,111] can achieve high compression rates (> 80% typically) of arbitrary size grey scale and colour images [32] at the expense of image quality loss. The image is split into 8*8 blocks of pixels which are individually processed in a raster scan order from left to right and from top to bottom. First, each 8*8 pixel block is transformed into the

frequency domain by using the Forward Discrete Cosine Transform (FDCT) [20]. This transformation effectively packs the signal into 64 bands and the packed signal is represented after transformation with 64 coefficients. FDCT and its inverse transform, namely Inverse Discrete Cosine Transform or IDCT, are very important in the compression pipeline since most of the compression is achieved due to these transforms. They are still an active research topic with the majority of research centered around fast algorithms of implementing them [32-35] or theoretical lower bounds for the minimum number of operations required in implementations [36-42]. The DCTed coefficients produced by the FDCT transform are quantized using frequency weighted quantization in the signal domain. After quantization, the DCTed coefficients are processed in a zigzag order and are finally entropy coded, based either on Huffman coding [21,110,112] or binary arithmetic coding [110,113-115].

JPEG-LS is the latest standard for lossless/near lossless coding. The image pixels are processed separately (i.e the 8*8 block structure is not used) and each pixel is predicted based on a template of neighboring pixels. The errors (or the quantized errors in the near lossless case) are entropy coded. The decoder follows the reverse procedure by using the same prediction mechanism for reconstruction. More about JPEG-LS in Chapters 3 and 4.

JPEG2000 [6] is the newest standard for coding still colour images. It offers a variety of important features such as:

- Very low bit rates (<= 0.25 bits/pixel) using wavelet based sub-band coding [43-49]
- Ability to compress/decompress both continuous tone and bi-level images
- Both lossless and lossy compression mechanisms
- Progressive transmission

- Robustness to bit errors
- Image security using labelling [50], stamping or encryption

2.2.2 Video coding.

In the field of video coding, the bandwidth is the determinant factor for the classification of standards.

There have been several major initiatives in video coding such as :

- Video coding for video teleconferencing, which has led to the ITU standards called H261 for ISDN videoconferencing [22] . H263 for Plain Old Telephone Service (POTS) [23] and H262 for ATM/broadband videoconferencing.
- Video coding for storing movies on CD-ROM, in the order of 1.2Mbits/sec allocated to video coding and 256kbits/sec allocated to audio coding which led to the initial MPEG-1 standard.
- Video coding for broadcast and for storing video on DVD (digital video disks) with on the order of 2-15 Mbits/sec allocated to video and audio coding which led to the MPEG-2 standard [51].
- Video coding for low bit rate telephony over POTS networks, with as little as 10kbits/sec allocated to video and as little as 5.3kbits/sec allocated to voice coding, which led to H324 standard [52].
- Coding of separate audio-visual objects, both natural and synthetic, which lead to ISO-MPEG-4 standard [17,54,55].
- Coding of multimedia meta-data (i.e data describing the features of the multimedia data) which lead to MPEG-7 standard.

Px64 and the H2x (x=61,63) family [22-25] are used for low bandwidth multimedia applications. The H261 video codec, initially intended for ISDN teleconferencing is the baseline video mode for most multimedia conferencing systems. The H262 video codec is essentially the high bit rate MPEG-2 standard and will be described later in this Chapter. The H263 low bit rate video codec is intended for use in POTS teleconferencing at modem rates from 14.6 to 56kbits/sec where the modem rate includes video coding, speech coding, control information etc.

The *H261 codec* encodes video frames using a Discrete Cosine Transform (DCT) on blocks of size 8*8 pixels, much the same as used for the JPEG lossy codec described previously. An initial frame (called intra frame) is coded and transmitted as an independent frame. Subsequent frames, which are modeled as changing slowly due to small motions of objects in a scene, are coded efficiently in the inter mode using motion compensation (MC)[53] on 16*16 pixel macroblocks (integer pixel displacement). The produced motion vectors are transmitted together with the quantized DCT coded difference between the predicted and original macroblocks. Quantization is performed using an adaptive quantizer and entropy coding using a Huffman coder .

The *H263 video codec* is based on the same DCT and motion compensation techniques as used in H261 but also provides several incremental improvements such as:

- Half pixel motion compensation
- Unrestricted motion vectors
- Arithmetic coding instead of Huffman coding

MPEG-4: Most recently, the focus has shifted to object-based coding at rates as low as 8kbits/sec or lower or as high as 1Mbits/sec or higher. The MPEG-4[17,54-55] standard is the first audio-visual compression standard that follows the object based coding instead of block based coding approach. The main advantages of the standard can be summarized as:

- Reduction of blocking artifacts due to the non block based coding mechanism
- Audio and video stream synchronization which is important for multimedia presentations
- Supports user interactivity necessary for multimedia authoring through scene composition from arbitrary audio-visual objects
- Ability to easily edit parts of the compressed bit-stream without requiring full decompression

More about MPEG-4 in Chapter 4.

The *MPEG-1 Video Coding Standard* [7,8,97,98] is a true multimedia standard with specifications for coding, compression and transmission of audio, video and data streams in a series of synchronized multiplexed packets. The driving focus of the standard was storage of multimedia content on a standard CD-ROM, which supported data transfer rates of 1.4Mbits/sec and a total storage capacity of about 600Mbytes. The video coding in MPEG-1 is very similar to the video coding of the H.26X series described above. Spatial coding is achieved by taking the 8*8 pixel blocks, quantizing the DCT coefficients based on perceptual weighting criteria, storing the DCT coefficients for each block in a zigzag scan and doing a variable length coding on the resulting DCT coefficient stream. Temporal coding is achieved by using the ideas of uni and bi-directional motion compensated prediction with three types of pictures, namely:

- I or intra pictures which are coded independently of all previous or future frames.
- P or predictive pictures which are coded based on previous I or previous P pictures.
- B or bi-directionally predictive pictures which are coded based on either the next and/or previous pictures.

The *MPEG-2 standard* [7,8,97,98] was designed to provide the capability of compressing, coding and transmitting high quality, multi-channel signals over terrestrial broadcast, satellite distribution and broad-band networks. The MPEG-2 video part of the standard was originally designed for high quality encoding of interlaced video from standard TV with bit rates in the order of 4-9 Mbits /sec. As it evolved, MPEG-2 video was expanded to include high-resolution video, such as HDTV, as well as hierarchical or scalable video coding for a range of applications. The video encoder consists of an inter-frame/field DCT encoder, a frame/field motion estimator and compensator and a variable length encoder (VLE). The frame/field DCT encoder exploits spatial redundancies and the frame/field motion compensator exploits temporal redundancies in the video signal. The standard uses the same frame types as MPEG-1.

2.3 Wavelet based image/video coding

Wavelet based image/video coding is the newest trend in the field and has become a reality mainly due to reductions of the computational complexity of proposed schemes. The benefits of using wavelets for compression can be summarized as *better rate distortion performance (R-D) at lower bit rates* and *scalability in both rate and quality*. Scalability of rate and quality is aided by the wavelet transform itself since the separation between the "base" image/video signal and its details is performed naturally. JPEG 2000 used wavelets for compression and the main algorithm employed is based on Shapiro's contribution [44],

better known as the embedded zerotree wavelet (EZW) algorithm. The central ideas in this algorithm are joint exploitation of *significant redundancy between subbands* and *progressive encoding*. The algorithm can be described as follows:

Step 1: Search all coefficients to find the one with the maximum magnitude, $C_{\max}$. The initial threshold is then determined as: $T_0 = \left\lceil \frac{|C_{\max}|}{2} \right\rceil$.

Step 2 (Dominant pass) : Scan all coefficients into the encoder along the zigzag route as shown in Figure 2.1. For each coefficient, one of the four classifications is assigned: positive symbol (POS), negative symbol (NOS), isolated zero symbol (IZ) and zerotree root symbol (ZTR). The details of such assignment are illustrated in Figure 2.2.

Step 3 (Subordinate pass) : Divide the range $[T_0, |C_{\max}|)$ into two intervals: $[T_0, M), [M, |C_{\max}|)$, where $M=(T_0 + |C_{\max}|)/2$ is the medium value in the range. Examine all significant coefficients in the dominant pass. If each coefficient is greater than M, the coefficient is assigned into the interval $[M, |C_{\max}|)$ and a bit 1 is produced. Otherwise, bit 0 is produced. Details are illustrated in Figure 2.3.

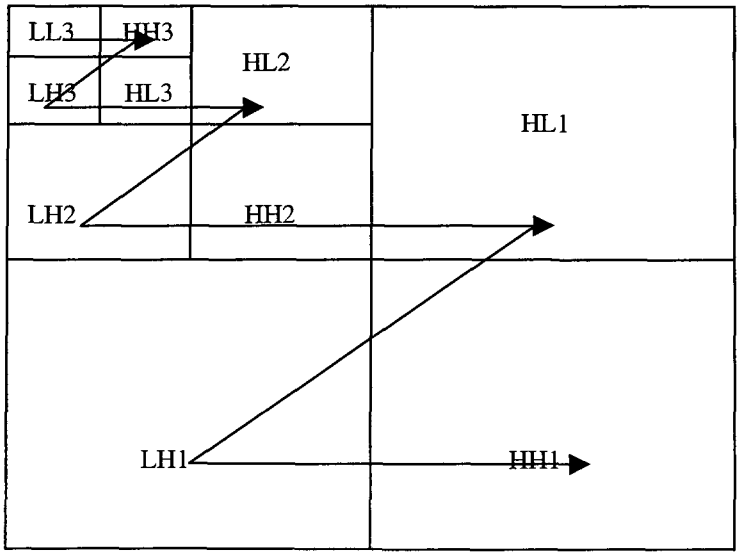

Figure 2.1: Scanning route

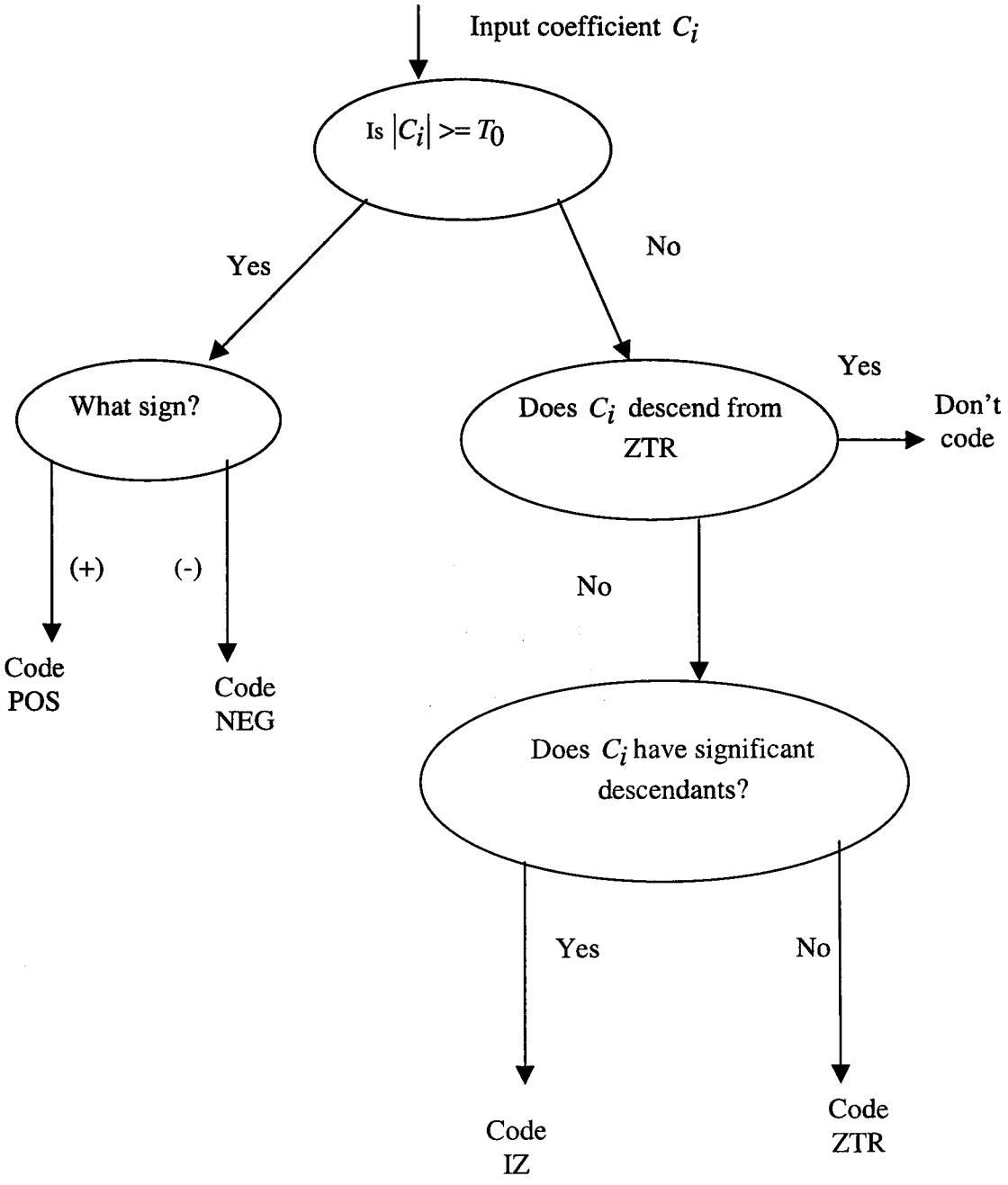

Figure 2.2: Dominant pass

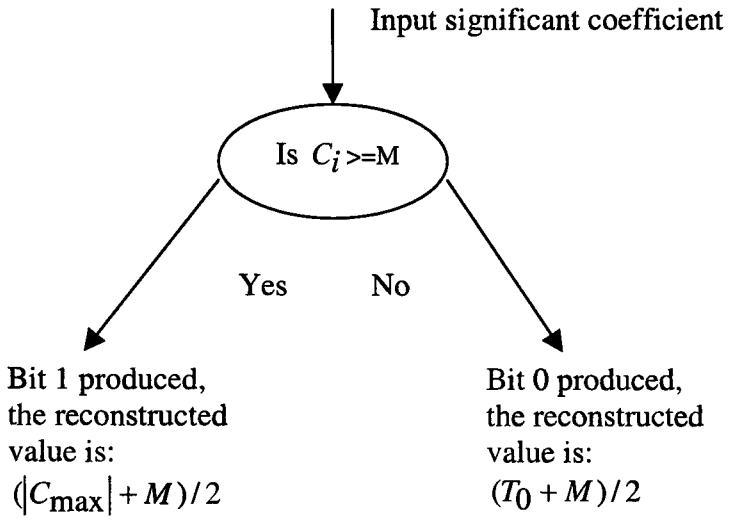

Figure 2.3: Subordinate pass

Step 4: Change the threshold to half of its previous value. Repeat the process from Step 2 for all non significant coefficients until either there are no more non significant coefficients or the threshold has fallen below a critical value.

The efficient exploitation of redundancy between subbands in the above algorithm lies on the fact that once a coefficient in a parent subband is classified as insignificant (i.e. the code Zero Tree Root (ZTR) has been produced), no bits need to be transmitted for its descendant coefficients in a lower subband in case they are also insignificant. The only exception to this rule (in which case an isolated zero code (IZ) code will also be produced) is when an insignificant coefficient comes from a significant parent and has significant descendants. This is a necessary price to pay in transmitting such a coefficient along with the IZ code, in order to avoid losing significant information down the tree and therefore generating large distortions. This scheme obviously improves compression rates since the probability of having insignificant descendant coefficients stemming from insignificant

parent coefficients is very high. It is also interesting to note that an insignificant coefficient in a resolution T, can be classified as significant at a finer resolution T1. This is important since it clearly shows that certain coefficients are only carriers of details in the signal. Progressive encoding is achieved in the subordinate pass, as illustrated in Figure 2.3. For every significant coefficient, an extra degree of detail is added in every subordinate pass (represented by the produced bits 0 or 1) starting from the most significant bits (MSB) and progressively reaching the least significant bits (LSB). In this manner, a bit-plane for significant coefficients is produced in every iteration, signifying the added image detail for the given resolution. Progressive encoding has become an important issue in state of the art codecs due to mainly three reasons. Firstly, the progressive mechanism enables the encoder to achieve a given bit rate pretty accurately at a low computational cost. Secondly, the decoder can stop decoding at any given point, generating an image that is the best possible representation with a given bit budget. This is of practical interest in broadcast applications where multiple decoders of varying computational, display and bandwidth capabilities receive the same bit stream. Such receivers can decode the bit stream according to their particular needs and capabilities. Thirdly, progressive encoding is also very useful for indexing and browsing where only a rough approximation is sufficient for deciding whether an image/video frame needs to be decoded or received in full. The process of screening images/video frames can be sped up considerably if after decoding only a small portion of the compressed data, one can decide if the target image/video frame is present. If not, decoding is aborted and the next image/video frame is requested, making it possible to scan a large amount of image/video frames quickly. Once the desired image/video frame is located, it can be fully decoded. Shapiro's algorithm was enhanced by Said and Pearlman [43] who exploited further redundancy between subbands, thus achieving improvements of 0.3-0.6db for the same bit rates.

2.4 Motion estimation and segmentation

In the context of video coding, a variety of sub-optimal search algorithms for block based motion estimation have been proposed in the literature. All the proposed schemes attempt to find a balance between speed of motion estimation, statistical quality of the reconstructed frames as compared to the originals and bit rate of the transmitted motion information. These algorithms can be broadly classified in two categories. The first category consists of the *traditional search algorithms* such as Three Step Search (TSS) [165], Four Step Search (FSS) [166], Spiral Search (SS) [167], Two Dimensional Logarithmic Search (LS) [168], Orthogonal Search (OS) [169], Cross Search (CS) [170], One at a Time Search (OTM) [171] etc. A common feature of the traditional search techniques is that in terms of speeding up the motion estimation, they either choose to evaluate (in terms of a statistical metric) only a subset of pixels inside the search window or they even use early jump-out techniques in the pixel subset to speed up the computation even further. MPEG-2 (TM5) chose an intermediate solution in order to balance speed and accuracy since it performs a full spiral search inside the search window, sped up by a jump out technique applied every 16 pixels for the macro-block to be motion estimated/compensated. MPEG-4 chose the Diamond Search (DS) [173-174], since it was shown that for small motion, typical in video conferencing sequences, it outperforms all other search methods in terms of computational complexity and reconstructed frame quality [172]. The problem with the traditional search methods is that they do not exploit the correlation of motion vectors of adjacent macro-blocks to the motion vector of the macro-block to be encoded, thus making the choices of the initial point for the search and of the size of the search window ad-hoc. This problem is addressed by the second class of motion estimation methods, namely the *predictive techniques* where the initial search point and the search window size are determined by *a function of the motion vectors* of adjacent

macro-blocks. For example, in H263 the *median* of the motion vectors of adjacent macro-blocks is chosen as initial search point. A wide range of predictive search methods have been proposed. In the Adaptive Spiral Search (ASS), the size of the search window is also adaptively chosen based on a threshold [175]. The median of the Mean Absolute Differences (MAD) between adjacent macro-blocks and their predictors is used as a threshold. The spiral search is stopped when the calculated MAD falls below this threshold. In the Adaptive Window Size Search (AWSS), the motion vectors of the adjacent macro-blocks are classified in three categories, namely small, large and medium [175]. Each category corresponds to a certain window size. The window size that corresponds to the category *containing the majority of the motion vectors* is chosen as the size of the search window. In the absence of a clear winner, a medium window size is chosen. A full search is subsequently performed only in the intersection of this window and the original search space. In the Extended Majority Voting Search (EMV), the motion vectors of the adjacent macro-blocks will both determine the type of the search, TSS for large motion and FSS otherwise, as well as the initial search point [175].

Motion segmentation refers to *labeling pixels/blocks* associated with different coherently moving objects or regions of a frame in a video sequence. The process of segmenting motion can be seen as an extension of pixel/block based motion estimation, since groups of pixels/blocks comprising scene objects or scene regions and having coherent motion are assigned the same label. The estimation of the 2-D dense motion field, which is used for determining coherent motion, can be block based (MPEG-2, MPEG-4), pixel recursive based, optical flow equation based or determined by Bayesian probabilities [176]. Motion segmentation is particularly effective in the case of non-uniform motion of pixels/objects/regions in a scene. Essentially, motion segmentation is an optimization process since pixels/blocks comprising objects/regions have to be clustered one or more

times according to whether they form a locally uniform motion field. As such, motion segmentation algorithms are not appropriate in a real time video coding framework because they are computationally expensive. It is difficult to associate a generic figure of merit with a motion segmentation result according to Altunbasak et. al [177] since the usefulness of segmentation really depends on the application. If motion segmentation is employed to *improve the compression efficiency*, then over-segmentation may not cause a concern provided that it results in reduction of errors between the object/region to be encoded and its predictor. On the other hand, if it is used *for object definition*, as in the MPEG-4 standard, then it is of outmost importance that the resulting motion boundaries align with actual object boundaries. Although, it may not be possible to achieve this in a fully automated manner, elimination of outlier motion vector estimates and imposition of spatio-temporal smoothness constraints improve the chances of obtaining more meaningful segmentation results. Various approaches exist in the literature for motion segmentation [176] which may be grouped as segmentation by affine clustering [178], segmentation by Hough transform analysis [179], segmentation by Markov Random Fields (MRF) modeling [180] which is computationally intensive, segmentation by mixture modeling [181], simultaneous motion estimation and segmentation [182], segmentation by dominant motion estimation [183-184] and segmentation by change-detection-mask analysis with temporal integration [185-186] . Segmentation by dominant motion analysis [183-184] refers to extracting one object (with the dominant motion) from the scene at a time. Multiple object segmentation can be achieved by repeating the procedure on the residual image after each object is extracted. Multiple object segmentation could have some problems when there is no single dominant motion in a scene. Wang and Adelson [178] suggested clustering of affine motion parameters (initialized by dividing the frame into blocks) with some pre- and post- processing. All pixel/block based segmentation methods,

including [178,183], suffer from the drawback that the segmentation map may contain isolated labels (outliers), thus suggesting potential over-segmentation. Spatial continuity constraints in the form of Gibs random field models have been introduced to overcome this problem [187]. The simultaneous Bayesian motion estimation and segmentation approach has also been proposed [182] at considerable computational cost.

2.5 Adaptive Quantization

In scalar quantization, each of the samples (blocks) generated by the input source is quantized separately. Then the set of input blocks S will be some subset of R , the set of real numbers. The code-book design problem consists in selecting a finite number L of values $r_i \in R$ to be used as reproduction levels, as well as the corresponding codewords to be transmitted, c_i . For a sample X_i and its corresponding reconstructed sample X_i', the encoding algorithm will be such that $X_i' = r_j$ where r_j is the reproduction level closest to X_i. Under the assumption of a stationary source with known statistics, well known design techniques can be used to determine the (r_i, c_i) pairs. For instance, the Lloyd-Max quantizer design technique [79,116] provides optimal, i.e distortion minimising r_i's for fixed length c_i's . The model can be either explicit, through knowledge of the probability density function (pdf) of the source, or implicit through the choice of a specific training sequence or set of blocks as being characteristic of the source.

If S is a finite set (as is the case for example with image pixels) then one can use entropy coding techniques to minimise the expected number of bits needed to encode the source without distortion, i.e $X_i' = X_i$. This would be an example of lossless compression. Calling $s_1, s_2, ..., s_N$ the elements of S , assume their probabilities $p(s_1), p(s_2), ...p(s_N)$ are known.Then the first order entropy of the source in bits is:

$$H = -\sum_{k=1}^{N} p(s_k) * \log_2(p(s_k)) \qquad (2.1)$$

The entropy dictates a lower bound in the number of bits per input sample needed to transmit sequences generated by the source assuming that the source follows the model and the samples are to be coded individually. Well known techniques such as Huffman or arithmetic coding can provide performance close to the entropy. Note that given a continuous set S and a set of reproduction levels r_i one can measure the expected probability of the r_i's and then use entropy coding to determine the c_i s. The resulting c_i s will be of variable length.

The main point to note is that both the scalar quantizer and entropy coder rely on having an available model of the input source. In cases where the source is known to be non-stationary one can resort to techniques that adapt the codebook to changing statistics.

When we encode blocks X_i which contain n samples, i.e. for S a subset of R^n, we are considering the more general Vector Quantization (VQ) codebook design problem. Similar properties, although without a simple optimization procedure, can be defined for vector quantization schemes. See [79] for an excellent review of VQ rechniques.

Note that as the dimensions of the vector increase, it becomes increasingly unrealistic to expect to obtain explicit models of the source, hence VQ techniques rely on training sequences to design the codebooks. Obviously the codebook obtained through training will do a good job of representing the blocks *within the training set* , as measured by how well the codebook performs for blocks *outside the training set.* Also increasing the dimension of the vector increases the complexity of both the codebook design and the encoding procedure.

For the above reasons VQ schemes of interest typically rely on relatively small values of n (number of samples). Given the complexity of generating a codebook typical approaches

use a fixed one (JPEG, MPEG) although recent work has also explored different strategies for updating the codebook "on the fly" while encoding the source [79, 117-121].

Due to the complexity of the codebook design and encoding mechanism of the methods described above, all practical image/video coding algorithms rely on the "divide and conquer" approach to make the coding design and encoding algorithm realizable. Discrete cosine transform (DCT) based coding[122] , VQ[79] are examples of algorithms that decompose the input signal into sub-blocks, which are independently quantized (sub-block size codebooks can then be designed). Similarly, sub-band and wavelet coders produce several sets of samples (each of the bands) which can then be quantized independently.

Let's consider the design for a linear transform DCT based coder in more detail, since Chapter 5 of this thesis refers to the MPEG-2 standard, which uses such a coder. A video frame is first decomposed into blocks on which the DCT is computed. Then the resulting set of coefficients (in the transform domain) is quantized. While there is no theoretical justification to encoding independently the transform coefficients (or sub-bands in wavelet based codecs), in practice this approach is used under the generally correct assumption that after the signal decorrelation achieved by the DCT, the gain to be expected by using vector quantization would be limited. Therefore, one can treat the set of all coefficients corresponding to the same frequency as a single source for which a single quantizer has to be designed. The problem of determining how coarsely to quantize each of the coefficients is again one where models are typically used. For example in the case of DCT methods, one can measure the variance of each of the coefficients based on an image or a set of images and then use bit allocation techniques to determine the coarseness of quantization [116]. This results in set of factors (usually denoted as a quantization matrix) which specify the relative coarseness of quantization for each of the coefficients. For simplicity of implementation, *uniform quantizers* are normally used and then the codewords for each of

the possible quantized values are found in order to minimize the entropy using variations of Huffman coding [21,110,112]. It should be pointed out that inter coefficient correlation is exploited to some extent by using techniques such as zigzag scanning and run length coding [123]. Example of this design technique can be found in [97,123,124].

Furthermore, to make the design of these systems more versatile, an additional parameter called quantization parameter (QP) is also available. This determines the coarseness of quantization for a given block (as the MQUANT parameter in MPEG) or for all the blocks in the image (as in JPEG lossy). While the quantization matrix determines the relative coarseness of quantization for each of the coefficients, the QP parameter scales the quantizer step sizes *equally for all the coefficients in the block*, while preserving the relative degrees of coarseness determined by the quantization matrix. Thus, if QP can change on a block by block basis, it allows the encoder to assign different levels of quantization coarseness to each block. Typically, increasing QP results in higher compression at the cost of higher distortion. The role of this parameter is analogous to that of the gain, in gain shape VQ schemes [79]. To transmit the coder corresponding to a given input block it will be necessary to first communicate to the decoder which codebook was selected and then transmit the index of the appropriate codeword. Thus, the QP value can be seen as an overhead information.

Design of sub-band codecs [125,126] resort to similar techniques where quantizers are designed a priori and trained on some representative set of images. Similar training approaches have also been used for wavelet based coding schemes [127] . Only more recent work [128], along with Shapiro's pioneering zerotree wavelet based coding scheme [44] have achieved a higher degree of adaptivity by exploiting dependencies between bands while not requiring training.

Finally, it should be pointed out that choosing the codelengths for the different vectors in block based motion compensated video coding also resorts to training. In this case, a first phase in the design process determines which vectors turn out to be more "popular" and the relative frequencies of occurrence are then used to compute an entropy code for the vectors.

A common thread of all the schemes mentioned above is to operate on smaller coding units (blocks in DCT and VQ, bands in sub-band and wavelet coding, pixels in JPEG-LS, vectors in motion compensation) and define a codebook for such units. The main motivation of this approach is the reduced complexity of all small coding units approaches, as well as the difficulty of achieving good models for larger block sizes. In most cases the codebook does not change after the design stage. In the following discussion it is assumed that the codebook is fixed and our aim is to achieve some adaptivity.

Let's consider two cases according to whether the encoder chooses the codeword corresponding to a block form from a single codebook or from one among several possible codebooks. The latter is the most attractive alternative to implement adaptive encoding algorithms, but good results can be obtained using the former approach as well. As an example, thresholding algorithms perform an adaptive encoding within a single codebook. For instance in [130,131] thresholding is used to remove in an R-D optimal way, coefficients after having quantized the whole image by using a single QP. A similar approach has been proposed to improve the performance of a wavelet based encoder in [132].

Obviously, the simplest encoding algorithm is that which maps each of the input blocks into a codeword regardless of the context. In other words, each block symbol will be considered independently of the others and will be mapped to the nearest codeword (in terms of the distortion measure used). If several code-books are used, then the choice of

the codebooks will also be made independently, so that for instance one can choose the same codebook for all blocks in the source or choose a codebook for each block based on some other factor, e.g. the buffer fullness in a typical buffer controlled scheme. This approach has the advantage of not requiring encoding delay. JPEG lossy is an example where a fixed codebook is used for all blocks in the image, whereas MPEG-2 chooses the codebook on a macroblock basis, depending partially on the buffer fullness (see Chapter 5).

Roughly speaking, we can define adaptivity as the ability to change the choice of codeword for a given block *depending on the context.* More formally, if X_i is the current block and $X^*_i = f(X_i)$ is the codeword nearest to it within the codebook (in the sense of the distortion being minimised) , than an adaptive encoding algorithm selects X'_i which may be different from X^*_i.

Let's denote R(X'_i) and D(X'_i) the rate and distortion for a given codeword X'_i, where R(X'_i) includes any possible overhead needed to specify the choice of codebook C_i.

Adaptivity can be summarized by writing the encoding algorithm for block i as :

$$X'_i = f(X'_i,...,X'_{i-1},X_1,...,X_{i-1},X_i,...,X_N) \qquad (2.2)$$

In the case of :

$$X'_i = f(X'_i,...,X'_{i-1},X_i) \qquad (2.3)$$

we would be considering *backward adaptation.* In some cases, if multiple codebooks are used, the information of which codebook to be used would not necessarily have to be sent as overhead since both encoder and decoder have access to the information needed to adapt the coding rule (except for X_i). A predictive scheme would be an example of this type of adaptation, since past quantized blocks are used to predict the current one and the

predictor defines the codebook to be used. In the context of rate control, memoryless schemes (where the buffer state is fed back to choose the next codebook) would not require overhead, while schemes where the incoming block X_i is analysed before the codebook decision is made, would require overhead. In an R-D framework, the MPEG-2 rate control scheme operating on a macroblock basis would not require overhead since it is based on the buffer estimate from previously encoded macroblocks. In a visual perception framework though, it would require overhead since the activity of the macroblock to be encoded also plays a role in the determination of the quantization step size. To minimise the overhead, the standard only sends the quantization parameter (MQUANT) to the decoder if it has changed. Still the amount of bits consumed in overhead information can be significant and the estimates proposed in the first part of Chapter 5 deal with this problem from the R-D point of view.

Conversely, if the encoding rule was such that:

$$X'_i = = f(X_i,...,X_{i+D+1}) \qquad (2.4)$$

we would have an example of *forward adaptation*. Again, if multiple codebooks are used, the encoder will have to rely on sending its choice of codebook to the decoder, since the decision will be based on information available only at the encoder. Note that in this example, the encoding delay would be D+1 blocks since the encoder has to know the next D+1 blocks in order to quantize block i. All of the empirical approaches for R-D performance optimization in Chapter 5 fall in the category of forward adaptive schemes.

The notion of adaptivity in quantization is a popular area of research. Recent work [133,134] looks at forward adaptive quantization and describes a procedure to optimally obtain the various codebooks from a training set of data. Two different approaches can be mentioned in the case of backward adaptive quantization. In [135-137], the objective is to adjust the support region of a scaler quantizer so that the quantizer can be used in

conjunction with a predictor in DPCM system. The original idea of Jayant's adaptive quantizer [135,116,138] was to change the support region based on the previous quantized sample, while in [136] more than one sample of memory is used. In [137] both the support region and the bin sizes can be adjusted, although the bin sizes are restricted to a finite set of values.

A somewhat different problem is tackled in [120] where an initial tree structured vector quantizer (TSVQ) is first designed with a rate higher than the rate available for transmission. Then the adaptive algorithm chooses which sub-tree of the previously designed tree has to be used for every instant. Both encoder and decoder keep counts of the number of samples that correspond to each of the nodes in the tree and they select the subtree which minimises the expected distortion (under the assumption that future samples will have the same distribution as past ones).

Note that all these systems use (implicitly or explicitly) simple models of the source to determine changes in quantization. For instance [135] assumes that the sources are relatively smooth but have varying dynamic range, so that the role of the adaptation is to estimate the changes in the variance of the source (so the dynamic range of the quantizer is adapted) while a uniform quantizer is used. Similarly, the assumption in [120] is that the initially designed tree structured codebook is sufficiently representative of the expected input signals, so that the adaptive algorithm can find a "good sub-tree" at any time. In the work relating to the Lagrangian framework in Chapter 5, the aim is to explicitly utilise the buffer state model of the MPEG-2 rate control scheme and then adapt the quantization scheme to get the best performance for the given model.

2.6 Lossless data compression

Since lossless coding [139] is gaining popularity due to advances in the communications field, it would be instructive to see the underlying principles in more detail. The state of the art in lossless coding is described by the JPEG-LS standard in its lossless mode of operation and the core of this standard is described by the LOCO-I algorithm (LOw COmplexity Lossless Compression for Images). Lossless data compression schemes often consist of two distinct and independent components: *modelling* and *coding*. The modelling part can be formulated as an inductive inference problem in which the data (i.e. the image) is observed sample by sample in some pre-defined order. At each time instant t, and after having scanned past data $x^t = x_1 x_2 ... x_t$, one wishes to make inferences on the next sample value x_{t+1} by assigning a conditional probability distribution $P(./x^t)$ to it. Ideally, the code length contributed by x_{t+1} is $-\log P(x_{t+1}/x^t)$ bits. In *a sequential formulation* of the problem, the distribution $P(./x^t)$ is learned from the previously encoded pixels in the encoder side and it is available to the decoder as it decodes the past pixels sequentially. The conceptual separation between the modelling and coding operations [114] was made possible by the invention of the arithmetic coders (AC) [115,140,141], which can realise any probability assignment $P(./.)$ dictated by the model to a pre-set precision. In [85], the authors present a process for *universal modelling* which essentially optimizes the sequential probability assignment problem at the expense of high complexity. Rather than pursuing this optimization, the main objective driving the design of LOCO-I is to project the image modelling principles outlined in [85] into a low complexity plane, both from the modelling and coding perspective. This task is formidable, especially from the coding perspective, because generic arithmetic coders, enabling the most general probabilistic coding models, are ruled out in software implementations of many low complexity

applications. This is due to the fact that in the AC algorithm [115,140,141], the encoder has to update the probabilities of incoming symbols, which is a computationally expensive process due to the large number of conditional probabilities that need to be estimated. If the source is stationary and the model is correct then AC can provide a performance very close to the first order entropy. However, in real life environments, where sources need not be stationary, the performance of the algorithm is determined by how well it adapts to the changing statistics of the source. In that sense, the model tracking part of the AC algorithm plays an essential part in the system performance which further adds to the complexity. The problem of tracking the changing source statistics in a practically realisable way in terms of the accuracy/complexity trade-off, is reflected in IBM's implementation of AC [142]. The main problem is to find, for every newly arrived symbol whether the occurrence is normal (i.e. consistent with the current model) or non normal (i.e. unexpected with the current model). The proposed solution is to have different rates of change in the model so that the estimated probability of the most likely symbol will change slowly, while the estimated probability of the least likely symbol will change faster. The basic idea is that unlikely events (such as the occurrence of the least likely symbol) may signal a change in the distribution. These ideas also highlight the main trade-off in defining an adaptive coding algorithm. Because of the need to adapt to changing statistics, the scheme of [142] will perform worse than a static algorithm for an i.i.d source. A similar trade-off can also be seen in the context of adaptive filtering, where in Least Mean Square (LMS) type algorithms fast convergence comes at a price of noisy behaviour if the source is stationary [143].

While [85] represents the best published compression results of significant computational complexity in the modelling process, it can be argued that lower cost modelling approaches such as the ones represented by the Sunset family of algorithms [158-161] are competitive

in terms of the entropy/complexity trade-off. The diminishing returns in terms of entropy of computationally expensive modelling approaches can also be seen in the work relating to the CALIC [162] and TMW [163] compression algorithms.

On the other hand, simplicity driven schemes propose minor variations of traditional DPCM techniques [164] and include Huffman coding of prediction residuals obtained with some fixed predictor. These simpler techniques are fundamentally limited in their compression performance by the first order entropy of the prediction residuals and the compression gap between these schemes and the more complex ones is significant.

As another example of adaptation in the context of lossless coding, it has been shown that the Huffman coding tree can be modified on the fly so that the code would adapt to the changing statistics or learn them starting with no prior knowledge [144-146]. A first approach to generate these statistics would be to choose *the number of samples N* over which symbol occurrences are counted. However, a fully adaptive scheme would also require a procedure *to change N if necessary* during the coding process in order to improve the performance. Recent work [147] presents a solution to this last question at the cost of some complexity by proposing that *the window size N* be updated by choosing, among several possible sizes, the one producing a code with better compression.

It is worth noting that the question of what constitutes a good model for random data is a topic of interest not only for compression but also as a model per se. Indeed, the minimum description length (MDL) technique introduced by Rissanen [148,149] provides a link between these two problems by establishing the asymptotic optimality on describing a distribution with a set of parameters that requires the least total number of bits to be encoded when counting *both* the bits needed to describe the model and the bits needed to encode the occurrences of the different symbols within the model. This criterion has been

shown to also provide an asymptotically optimal universal code for data generated by a stationary source in [85].

Let's examine the JPEG-LS standard in more detail. Initially, the predictive value for the pixel to be encoded is estimated based on a fixed template of neighbouring pixels. The *predictive error* is then calculated as the difference between the actual value of the pixel to be encoded minus its predictive value. It is well known [164] that prediction residuals in continuous tone images are adequately modelled by a Two Sided Geometric Distribution (TSGD). According to this distribution, the probability of an integer value ε of the prediction error is proportional to $\theta^{|\varepsilon|}$, where θ belongs to the interval (0,1) and controls the two sided exponential decay rate. However, in *context conditioned models*, an offset μ is typically present in the prediction error signal [160] due to possible bias in the prediction. If we break this offset μ into an integer part R (bias) and to a fractional part ρ (shift), the TSGD parametric class assumed by JPEG-LS for the fixed prediction error ε at each context is given by:

$$P_{(\theta,\mu)}(\varepsilon) = C(\theta,\rho) * \theta^{|\varepsilon - R + \rho|} \qquad \varepsilon = 0,\pm1,\pm2.... \qquad (2.5)$$

where $C(\theta,\rho) = (1-\theta)/(\theta^{1-\rho} + \vartheta^{\rho})$ is a normalisation factor. After adaptive prediction, resulting in bias cancellation, equation (2.5) reduces to:

$$P_{(\theta,\mu)}(\varepsilon) = C(\theta,\rho) * \theta^{|\varepsilon + \rho|} \qquad \varepsilon = 0,\pm1,\pm2.... \qquad (2.6)$$

where $0 < \theta < 1$ and $0 < \rho < 1$.

Assuming a to be the alphabet size, the error range of the residuals is subsequently reduced to the interval [–a/2,a/2-1] resulting in further improvements in compression efficiency.

The context that conditions the encoding of the current prediction residual is constructed from the local gradients of surrounding pixels, which govern the statistical behaviour of the

prediction error. To reduce the modelling cost, the local gradients are quantized into a smaller number of approximately equiprobable connected regions. The number of contexts is further reduced (context merging) due to the assumption that a context triplet (q1,q2,q3), where qi represents a local gradient, is equiprobable with the context triplet (-q1,-q2,-q3) for the same prediction error. The general formula for the number of contexts after context merging is $(2*T+1)^3/2$, where T is a tailorable parameter for different images.

The standard uses a low cost procedure for *bias cancellation* of the context dependent distribution of the prediction errors. In the following pseudo-code, B and C are model parameters, N represents the occurrences of a given context and ε is the error residual:

```
B = B+ε ; /* accumulate prediction residual */
N= N+1;  /* update occurrence counter */
/* update correction value */
if (B<= -N) {
C=C-1; B=B+N;
If (B <= -N) B=-N+1;
}
else if (B>0) {
C=C+1;B=B-N;
If (B>0) B=0;
}
```

Finally, JPEG-LS chose to use a special variant of Golomb codes (GPO2) to encode the quantised error residuals. Given a positive integer parameter m, the mth order Golomb code G_m encodes an integer y >= 0 in two parts: a *unary representation* $\lfloor y/m \rfloor$ and a *modified binary representation* of y mod m. The modified binary representation uses

$\lfloor \log m \rfloor$ bits if $y < 2^{\lceil \log m \rceil}$-m and $\lceil \log m \rceil$ bits otherwise. The special case of Golomb codes with $m = 2^k$ leads to very simple encoding/decoding procedures: the code for y is constructed by appending the k least significant bits of y to the unary representation of the number formed by the remaining higher order bits of y. The length of the encoding is $k+1+\lfloor y/2^k \rfloor$ and these codes are referred as Golomb-power-of-2 (GPO2) codes.

2.7 Empirical versus model based R-D approaches

In the following discussion, the most common R-D approaches in image and video coding will be reviewed. The "video coding terminology" will be used, although all of the surveyed techniques are also applicable in an image coding framework.

In the empirical approaches for R-D optimization, the entire video sequence or part of the future frames is known in advance. Figure 2.4 shows a typical block diagram of the empirical approaches.

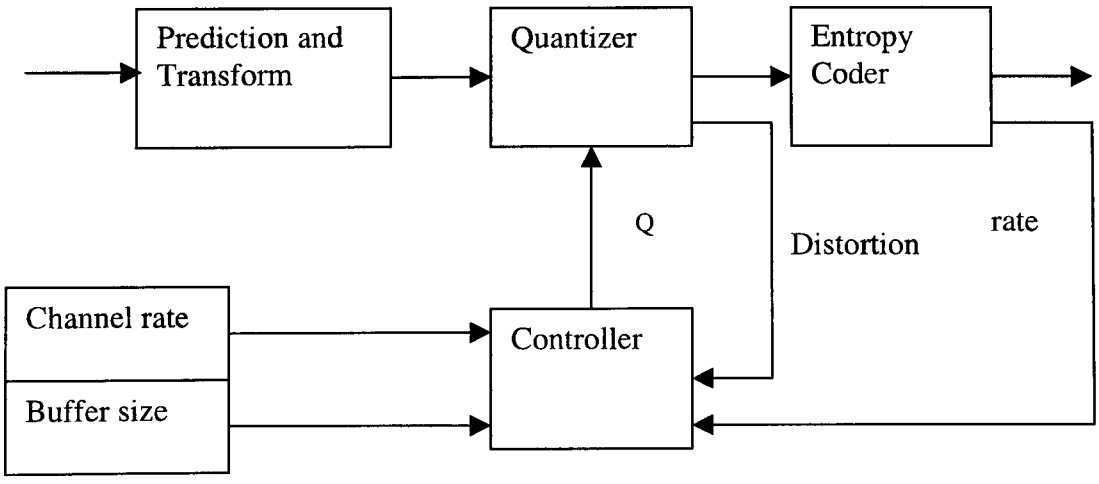

Figure 2.4: Empirical R-D approaches

From the above diagram, it can be clearly seen that empirical approaches are computationally intensive in estimating the R-D performance, since the distortion can only be measured after block reconstruction and the rate after entropy coding. It can also be inferred that, if a number of iterations are needed for the final estimation of the quantizer step size Q, the complexity increases even more. In Chapter 5, a detailed complexity analysis will be presented in terms of the number of operations needed, for a variety of empirical approaches that follow the pattern described in Figure 2.4.

Most of the empirical R-D optimisation approaches are based on the Lagrange multiplier method. Let's consider initially the case where *the units of encoding are independent* and where the buffer size is infinite (no buffer constraints). The independence of quantization means that the quantization setting for a given unit of encoding does not affect any of the other units. The size of a "unit" can be a macroblock in a Local Control Scheme, or a frame in the Global Control case. In this discussion, let's assume that the Control Scheme is local.

The optimisation problem can then be formulated as follows:

Formulation 2.7.1: *Independent macroblock Coding without Buffer Constraints*

Determine q(i), i = 1,2,...M_b in order to minimise $\sum_{i=1}^{M_b} d_i(q_i)$ subject to

$$\sum_{i=1}^{M_b} r_i(q_i) <= B \qquad (2.7)$$

where M_b are the number of macroblocks in the frame to be encoded, d_i (q_i) is the distortion of macroblock i when quantized with quantization step q_i , r_i is the produced rate for macroblock i, and B is the number of bits allocated to the current frame.

The above problem can be solved by using the Lagrange Multiplier method according to the following theorem:

Theorem 2.7.2: *Lagrange Multiplier method*

If a set of q^*_i , i=1,2,..M_b minimises the following set of expressions for a given λ ,

$d_i(q_i)+\lambda * r_i(q_i)$, i=1,2,..M_b , (2.8)

then it is also a solution to Formulation 2.7.1 for a given B equal to

$$B'(\lambda)=\sum_{i=1}^{M_b} r_i(q^*_i) \quad (2.9)$$

In the above theorem, $B'(\lambda)$ is the total bit rate achieved for a given Lagrange multiplier which is used to minimise the set of expressions described by equation (2.8).

Theorem 2.7.2 is valid in both continuous space (where q_i takes a continuous range of values) and discrete space (where q_i is only defined for only some discrete values such as in the MPEG-2 case). A proof of this theorem can be found in Chapter 14 of [100] for the continuous case, and in [101] for the discrete case. To find the multiplier that minimises the set of expressions in equation (2.8), the bisection method [103-104] can be used:

Algorithm 2.7.3: *Lagrange Multiplier Method with Bisection Search*

Step 1. Make an initial guess on $\lambda 1$ and $\lambda 2$, with $\lambda 1 < \lambda 2$.

Step 2. Substitute $\lambda 1$ into (1.6) and minimise the set of expressions to derive q^*_i , i = 1,2 ..... M_b.

Substitute q^*_i into (1.7) to get B'($\lambda 1$).

Step 3. Follow the same procedure as in Step 2 for $\lambda 2$ to get B'($\lambda 2$).

Step 4. If [B'($\lambda 1$) - B]. [B'($\lambda 2$) - B] > 0, *i.e*, the solution does not fall in between the two initial guess values, go to Step 1 and make another guess. Otherwise, continue to the next step.

Step 5. Let λ_m = ($\lambda 1$ + $\lambda 2$)/2.

Step 6. Follow the same procedure as in Step 2 for λ_m to get q^*_i , i = 1, 2,..., M_b and B'(λ_m).

Step 7. If [B'($\lambda 1$) - B]. [B'($\lambda 2$) - B] < 0 , substitute $\lambda 2$ by λ_m , otherwise, substitute $\lambda 1$ by λ_m .

Step 8. Check if

$$\left|\frac{B'(\lambda_m)-B}{B}\right|<\varepsilon$$

Where ε is a pre-set small number. If this condition holds, the optimisation is done and the solution is q^*_i , i = 1, 2,..., M_b . Otherwise, go to Step 5 for another iteration.

In addition to bisection search, other iterative algorithms for solving non-linear equations (see Chapter 6 of [102]) can also be used for searching the solution. For the case where qi's are discrete and finite, an algorithm has been proposed in [61]. Note that in the Lagrange Multiplier Method, all input data have to be collected (for calculating r-q and d-q functions) before any real encoding can take place. A method which used sliding-window to shorten the delay based on *constant slope optimization algorithm* has been proposed in [58,105]. The computational complexity of Algorithm 2.7.3 is lower than the dependent quantization case, because the R-D measurement and the minimisation of equation (2.8) can be done independently for each block. However, this assumption is not met by an MPEG encoding scheme where rate-distortion values for a given frame depend on previously quantized frames. Therefore, the algorithm can not be applied to MPEG directly.

If there are constraints on the buffer size , but the macroblocks are still independently encoded, the Formulation 2.7.1 becomes:

Formulation 2.7.4: *Independent macroblock coding with buffer constraints*

Determine q_i, i=1,2,…,M_b in order to minimise

$$\sum_{i=1}^{M_b} d_i(q_i) \qquad (2.10)$$

subject to $b(i,q_1,q_2, \ldots..q_i)<b_{max}$ i=1,2,..,M_b (2.11)

where b_{max} is the buffer size and b_i is the buffer state when macroblock i is encoded.

The buffer state after macroblock i is coded is given by the following recursion:

$$b(i,q_1,q_2, \ldots..q_i) = \max(b(i-1,q_1,q_2, \ldots..q_{i-1}) + r_i(q_i) - r_b, 0) \qquad (2.12)$$

where r_b is the number of bits output to the channel (constant).

Equation (2.12) implies that the buffer state is updated based on the previous buffer state plus the number of bits when macroblock i is encoded minus the number of bits output to the channel (constant). The *max function* is used to handle the buffer underflow case. Because the value of the buffer occupancy for each macroblock depends on the quantization steps of previous macroblocks, it is no longer possible to optimise each macroblock independently.

There are multiple constraints in the above formulation. It is still possible to solve the problem with multidimensional Lagrange multipliers [106] but the technique proposed becomes very complex in both the formulation and the calculation at a higher dimension. A method based on forward Dynamic Programming, known as Viterbi Algorithm has been proposed [58,107,108] . The first step is to build a special trellis graph. The trellis consists of several stages, with each stage corresponding to a block to be coded. A node in the stage is defined as a particular buffer occupancy, after the block corresponding to that stage is coded. The branches, which connect nodes from stage i to stage i + 1, are grown for every node in stage i and for every possible quantization setting for block i. The cost for each branch is then defined as the distortion produced with the corresponding quantization setting. The problem becomes to find a path in the trellis graph that has smallest total cost, which can be solved by dynamic programming techniques. The buffer constraints are

satisfied by "pruning" all the branches that violate the constraints during the growth of the trellis. This algorithm can find the true global optimum solution. However, the number of nodes could grow rapidly with the number of stages, which contributes the increase of both the computational complexity and the memory requirement. Several techniques have also been proposed to reduce the complexity, including the use of buffer state clustering, sliding window, and an approximation using the Lagrange multiplier method.

In the dependent quantization case, the fact that the R-D characteristics of predicted frames (P and B frames in an MPEG-2 framework) are dependent on their reference frames, has also been considered in the literature [74,106]. By considering the unit of encoding to be a whole frame for ease of description and by considering the buffer unconstrained case, the optimisation becomes:

Formulation 2.7.5: *Dependent frame coding without buffer constraints*

Determine q_i , i=1,2,...N to minimise $\sum_{i=1}^{N} d_i(q_1,q_2,...,q_i)$ subject to

$$\sum_{i=1}^{N} r_i(q_1,q_2,...,q_i) < R \qquad (2.13)$$

Where q_i is now the quantization step for the whole frame i and R is the bit budget for the whole Group of Pictures (GOP).

Two interesting observations can be made regarding Formulation 2.7.5. First, that it is easily parametrised in case joint optimisations are desired. For example, in [155] a joint thresholding and quantizer selection is proposed for transform coding for the JPEG baseline coder but it is easily extended in a video coding framework. Assuming that the thresholding technique is applicable on a frame basis, Formulation 2.7.5 becomes:

Formulation 2.7.6: *Joint optimization of quantizer section and thresholding in dependent frame coding without buffer constraints*

Determine (q_i ,t_i) i=1,2,...N to minimise $\sum_{i=1}^{N} d_i((q_1,t1),(q_2,t2)...,(q_i,ti))$ subject to $\sum_{i=1}^{N} r_i((q_1,t1),(q_2,t2)...,(q_i,ti)) < R$ (2.14)

Where t_i is the thresholding technique chosen for frame i. Formulation 1.10.5 is generic in the sense that it can accommodate any joint optimisation of a number of parameters.

Second, it can be easily seen that the rate $r_i(q1,q2,...,qi)$ for every frame in the Group of Pictures is actually a composite rate:

$$r_i(q1,q2,...,qi) = r_{coefficients}(q1,q2,..qi) + r_{motion}(q1,q2,...,qi) + r_{seg}(q1,q2,..qi) \quad (2.15)$$

where $r_{coefficients}(q1,q2,...qi)$ is the bit rate produced by the quantized transformed coefficients, $r_{motion}(q1,q2,...,qi)$ is the rate allocated to motion information and $r_{seg}(q1,q2,..qi)$ is the rate necessary to convey the segmentation information to the decoder. Equation (2.15) is also generic since the coefficient transformation can be either DCT or wavelet based, the motion information can be either associated with blocks of fixed or variable size (regions) and the segmentation information depends purely on the representation of the frame to be encoded (e.g. block based versus quadtree based schemes).

The minimisation of Formulation 2.7.6 has to be solved in an N dimensional space and unfortunately the cost function described by equation (2.8) can no longer be minimised independently. It is evident that the complexity grows exponentially not only for the operations required in the minimisation but also for the evaluation of the R-D functions which has to be done over all possible quantization settings. In the case of joint optimization schemes, as the one described in Formulation 2.7.6, it is worth mentioning that each extra parameter added to the optimization procedure increases the computational cost exponentially.

The complexity of the minimisation of formulations 2.7.5 and 2.7.6 can be reduced by using the *monotonicity property* [109]:

Definition 2.7.7

For any dependent coding system, for any $\lambda >= 0$, if the quantization step size of q_1 is finer than that of q* implies:

$$J_2(q_1,q_2) < J_2(q^*,q_2) \qquad (2.16)$$

then the coding system is defined to possess the monotonicity property.

In the above definition,

$$J_2(q_1,q_2) = d_2(q_1,q_2) + \lambda * r_2(q_1,q_2) \text{ and } J_2(q^*,q_2) = d_2(q^*,q_2) + \lambda * r_2(q^*,q_2) \qquad (2.17)$$

which are the cost functions of rate and distortion for a coding unit in the dependent case.

The monotonicity property implies that a better quality (finer quantization) in the reference frame will lead to more efficient coding in the R-D sense. Most of the MPEG encoding results in [74] confirm this property. By applying the monotonicity property, many branches and nodes in the trellis can be eliminated (pruned), thus saving computations including the costly evaluation of the rate quantization and distortion quantization functions associated with these nodes and branches. Even after pruning though, the R-D evaluations needed to optimise the quantization settings may still require a significant amount of computation.

Trellis based optimisations are guaranteed to give the optimal R-D performance, while solutions based on pruning, approximations and heuristics will give sub-optimal R-D estimation, compensated by the smaller computational cost.

In most *model based approaches*, the statistical model for Gaussian sources is used because it usually leads to simpler expressions.

Theorem 2.7.8: *Rate-Distortion Function for Gaussian Source*

The rate distortion function for a zero mean Gaussian source with variance σ^2 is:

$$R(d) = \begin{cases} (1/2)*\log(\sigma^2/d) & 0 \le d \le \sigma^2 \\ 0 & d \ge \sigma^2 \end{cases} \qquad (2.18)$$

where the distortion d is measured in terms of squared error and R(d) is measured in bits/pixel..

In model based R-D approaches, there is also the assumption that the distortion and the quantization step are linearly related:

$D(q) = m*q$, m an integer greater than 1 (2.19)

A proof of theorem 2.7.8 can be found in [110]. The above model assumes an explicit relation between rate and distortion so the R-D characteristics of the encoding unit are predicted rather than derived from the actual encoding process with every/some of the quantization settings. Furthermore, no future encoding units are needed so these models are suitable for *online applications requiring low cost and encoding delay.*

The above model has been used in many contexts where a rate distortion function is required [73]. To estimate the model parameters, the variance can be measured directly from source data and the value of m has to be estimated some way. The problem of this general model, when applied to an MPEG framework, is that a general DCT transformed video signal is usually not a Gaussian source and the linear assumption in equation (2.19) does not generally hold. The non-linearity between distortion and quantizer step size is especially evident in P and B frames of a video sequence. As such, the above model is likely to produce significant errors in R-D estimation when used in a realistic encoding scheme.

From all the above discussion we can infer that in order to perform online image/video coding of reasonable computational complexity, *hybrid schemes* that combine the simplicity of model based approaches with the benefits of the optimisation based empirical approaches are necessary. These schemes are expected to reconcile the conflicting requirements of compression rates, quality and complexity. The second part of Chapter 5 is targeted towards such schemes.

2.8 Rate Distortion and complexity

From the above discussion, it can be inferred that in terms of improving the R-D performance in image and video coding, the main research efforts are centered around:

- Better transformations [46,127,150]
- Improved quantizer bit allocation [60,61,74]
- Efficient entropy coding [129]

There are a number of algorithms that provide high efficiency in each of these areas. Examples include using the wavelet transform with progressive quantization and efficient entropy coding [43,44,151-154], DCT with optimal thresholding and quantization [155], DCT with progressive coding [156], variable block size DCT [157], etc. In none of the above works the complexity issue is considered. Typically, encoders with longer memory, more computational power and larger context statistics can perform better than encoders with fewer resources. In a complexity constrained environment, such as in software implementation of real time en/de-coding systems and in battery limited pervasive devices, complexity becomes a major concern in addition to rate distortion performance. Normally, one would prefer to have a system that encodes or decodes with a higher frame rate with a small degradation in picture quality rather than to have a slightly better rate distortion

performance with much more complexity or delay. Thus in order to achieve the best of rate-distortion-complexity performance, all three factors must be explicitly considered together.

With the fast increase in the clock speed and performance of general purpose processors, software only solutions for image and video coding are of great interest. Software solutions result not only in cheaper systems, since no specialised hardware needs to be bought, but also provide extra flexibility as compared to specialised hardware.

Consistent with this trend for low computational complexity algorithms for software only codecs, this thesis will present a variety of such algorithms in the contexts of image and video coding.

CHAPTER 3 - LOW COST RATE CONTROL ALGORITHMS FOR IMAGE CODING IN A JPEG-LS FRAMEWORK

3.1 Introduction to JPEG-LS

JPEG-LS is the latest international standard for lossless/near lossless still image compression. The formal standard was issued in 1998. As with previous JPEG standards, JPEG-LS is based on a combination of optimized coding schemes selected from a number of successful candidate algorithms on a world wide competitive basis.

The operation of JPEG-LS for lossless/near lossless image compression can be divided in the following four parts: i) run-length coding, ii) non-linear prediction, iii) context-based statistics modeling and iv) Golomb coding[88,89]. The information loss in the standard (near lossless mode) is induced by a constant integer value called NEAR. This NEAR value is *user defined* and its range is between 1 and 9. The predictive pattern or template, used for selecting either the run length or the non-run length coding modes and also for context based statistical modeling, consists of four neighboring pixels of the pixel to be encoded (Figure 3.1).

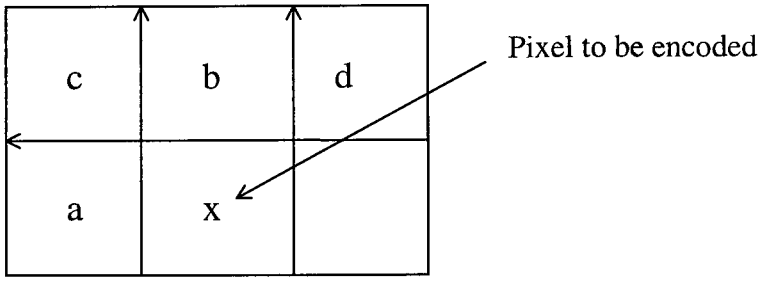

Figure 3.1: Predictive pattern in JPEG-LS

Since the number of contexts produced is large with this arrangement, only three delta values are considered as shown below:

$$\Delta_1 = d - b; \quad \Delta_2 = b - c; \quad \Delta_3 = c - a; \tag{3.1}$$

If the three delta values are less than the NEAR value, this indicates that the local image texture is very smooth and the run length coding mode is chosen. Otherwise the non-run mode will be selected, in which the encoding is done using techniques such as predictive coding, quantization using the NEAR value in the quantization step determination and finally entropy coding.

To maximize the performance of predictive coding, JPEG-LS adopted a simple edge detection scheme involving only three out of the four neighboring pixels in order to analyze the local texture and to determine the predictive value. The predictive value is estimated according to the following rules:

i) If an edge is detected, the pixel *not on the edge* is taken as the predictive value as shown in Figures 3.2(a) and (b). This case reflects that the local texture is rough.

ii) Otherwise, the predictive value is a+b-c. This case reflects that the local texture is smooth.

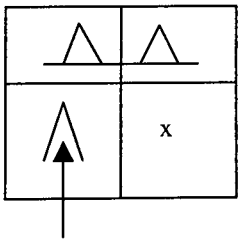

Figure 3.2(a): Predictive value for horizontal edge prediction

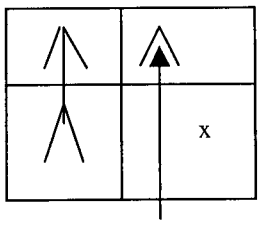

Figure 3.2(b): Predictive value for vertical edge prediction

The important element in the above prediction scheme is that it not only returns a predictive value, *but it also characterizes local texture.*

The predicted errors are then quantized using the single parameter NEAR for the determination of the quantization step, before they are encoded using LGC (Limited length Golomb coding). With such an information loss scheme introduced in JPEG - LS, the major drawback is that the information loss introduced is fixed and predetermined by the value NEAR. This can cause conflict between compression efficiency and quality requirements since smooth areas in the image will incur the same information loss as rougher areas. However, human visual perception is more sensitive to smoother areas in the context of image coding. This discrepancy between the way information loss is distributed in the standard and the way an HVS (Human Visual System) treats information loss, gives rise to the following set of objectives:

1. The need for designing a low cost technique that will distribute information loss according to HVS tolerance among different textures to improve performance in terms of visual quality and rate distortion terms.
2. The need for designing low cost rate control algorithms that utilize such a multilevel information loss distribution for achieving a given compression rate, while optimizing the image quality in HVS terms, regardless of the variety of compressibility of the input images.

The design of a low cost multilevel information loss distribution according to HVS could exploit the simple but effective prediction scheme that JPEG-LS uses for activity analysis. However, the design of a low cost rate control algorithm according to HVS is more challenging since, from the literature, we can see that most of the current research addresses the problem from the rate distortion point of view, which may not be the optimal approach from an HVS point of view. Furthermore, most of the approaches used are

computationally expensive as they treat rate control as an optimization problem. Specifically, in a number of rate distortion approaches [58-60,62-69] it was observed that the R-D (rate-distortion) characteristics of the input data have to be measured before any decision can be made about the quantization step assignment or information loss distribution. Typical work includes dynamic programming [58] and Lagrange multiplier optimization[59-62]. To obtain the R-D characteristics, various techniques have been proposed. These include trellis-based[58], model based[60,66]and piecewise approximated [66] approaches. The situation is further exasperated as some of these techniques require multiple passes over the input data to obtain the R-D curves, and a considerable number of iterations in order the approximation for the quantization step size assignment to converge to the optimal solution.

The high computational complexity of current approaches for the rate control problem in still image coding, coupled with the different sensitivity of HVS towards different textures calls for effective and efficient algorithms. Towards this end, an HVS based multilevel information loss scheme is initially developed and is subsequently used in the design of two low cost rate control algorithms for JPEG-LS. The chapter concludes with potential applications of the second rate control algorithm in the context of medical imaging.

3.2 Multilevel information loss in JPEG-LS image compression

To optimize the information loss distribution, local texture analysis can be exploited by considering the characteristics of human visual perception towards different textures. Specifically, in the case of rough textures, human perception of distortion tends to be more tolerant in comparison with the case of smooth texture (i.e. irregularities in

smooth areas are easily detected, whereas in rougher areas they are much harder to pinpoint). This property gives the opportunity for designing a scheme where the information loss parameter NEAR in JPEG-LS, will vary according to texture properties so that a better balance between compression rate and visual quality of reconstructed images can be achieved. In this chapter, such a scheme is proposed and is based on the prediction mechanism of JPEG-LS (see Section 3.1) but also uses a multilevel information loss distribution, instead of using a single information loss parameter (NEAR). The flexibility of the multilevel information loss distribution combined with the simple but accurate prediction mechanism of the standard are the keys in distributing information loss according to the affordance of the human visual system. In the proposed scheme, three parameters (namely NEAR_H, NEAR_M, NEAR_L) are used, corresponding to the three texture types (namely rough, smooth, very smooth) identified by the JPEG-LS prediction scheme. The information loss is allocated according to the following rules:

i) If the run length coding mode is selected, the minimum amount of information loss is afforded since the texture is very smooth. Parameter NEAR_L reflects this rule.

ii) If an edge is not detected in the prediction phase (Section 3.1), the texture is still smooth but more information can afford to be lost than in the run length mode case. Parameter NEAR_M reflects this rule.

iii) If an edge is detected, more information can afford to be lost than in the previous two cases. Parameter NEAR_H reflects this rule.

The modified (HVS based) information loss distribution of the standard is illustrated in the following figure:

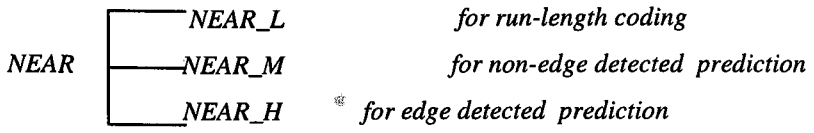

Figure 3.3: Modified information loss distribution in JPEG-LS

The assessment of the proposed scheme was performed by devising two sets of experiments. In these experiments, the JPEG – LS software was enhanced with the necessary modifications, in order to account for the multiple levels of information loss.

In the first set of experiments, the fact that the proposed scheme is competitive even in terms of conventional image quality measurements (PSNR) was established . The results after applying the proposed technique on the typical JPEG – LS test image sample (test8.pgm) can be summarized in Table 3.1. The "test8.pgm" image was specifically recommended from the JPEG committee as a suitable test image for proposed compression algorithms. The three digit NEAR values for the proposed scheme correspond to the triplet (NEAR_L, NEAR_M, NEAR_H).

Table 3.1: Phase 1 of experiments for test8.pgm

JPEG - LS			The proposed Scheme		
NEAR	**CR**	**PSNR(db)**	**NEAR values**	**CR**	**PSNR(db)**
1	2.48:1	50.94	011	2.45:1	51.50
2	2.89:1	46.34	122	2.82:1	47.13
3	3.13:1	42.68	233	3.11:1	43.68
4	3.39:1	40.77	344	3.39:1	41.38
4	3.39:1	40.77	335	3.40:1	40.83

Table 3.1 shows that the proposed scheme *does not lose any ground* even in terms of conventional measurement of image quality (PSNR values) for the same compression rates as the standard, provided a suitable triplet of NEAR values is chosen. While all compression ratios remain similar to JPEG – LS , with the first two digits at least being the same, the PSNR values achieved by the proposed scheme remain very competitive and even slightly better in some cases compared to the ones JPEG – LS produced. This could be important in applications where the PSNR metric really matters (e.g. medical imaging, video aided terrain mapping, etc.) since in these applications the average distance per pixel between original and reconstructed images is more important than visual considerations.

In the second phase of the experiments, which utilized the same three parameter information loss distribution as in the first phase, the fact that the proposed scheme is able to produce higher compression ratios and better visual quality of the reconstructed images compared to JPEG – LS was shown. By better visual quality, we refer to the ability of the algorithm *to retain smooth texture better than the standard*, for the same or higher compression rates, rather than *to enhance smooth texture*. Consequently, the visual effect becomes better but also the visual distance between original and reconstructed smooth textures is kept close. In contrast, in the case of smoothing, the visual effect may become better, but the visual distance between original and reconstructed images *may increase*. All the experiments in Table 3.2 produced reconstructed images with lower PSNR values compared to JPEG – LS but with better visual quality. This is mostly visible on the bottom left quartile where the texture is smooth. The lower PSNR values are expected, since in order to retain smooth texture, we need to compress more on rough textures to achieve higher compression rates than JPEG-LS. A representative table of results follows, along with reconstructed images for visual inspection.

It was also shown that the conventional measurement in terms of PSNR of the image quality does not take into account the human visual system perception of image quality (i.e. you can have reconstructed images of better visual image quality in accordance to HVS with lower PSNR values). This is because the statistical quality, measured in PSNR terms, only shows how much information is lost in the reconstructed image as compared to the original. Where this information is lost is not considered. On the contrary, visual quality based schemes distribute information loss differently to different textures depending on the tolerance of HVS to distortion. In Table 3.2, the triplets of NEAR values were empirically found.

Table 3.2: Phase 2 of experiments for test8.pgm			
JPEG – LS		**Proposed Algorithm**	
Compression Ratio	**NEAR**	**Compression Ratio**	**(NEAR_L, M,H)**
2.49:1	1	2.64:1	(0,1,2)
2.49:1	1	2.79:1	(0,2,2)
2.89:1	2	2.92:1	(1,2,3)
2.89:1	2	3.05:1	(1,2,4)
2.89:1	2	3.19:1	(1,2,5)
3.13:1	3	3.13:1	(1,3,4)
3.13:1	3	3.23:1	(1,4,4)
3.13:1	3	3.39:1	(1,4,5)
3.39:1	4	3.44:1	(1,5,5)

Figure 3.4(a) is the original "test8.pgm" image and Figure 3.4(b) is its bottom left quartile blown up. To see the effect of the algorithm on smooth textures, the bottom left quartile of the reconstructed images (both for JPEG-LS and for the proposed scheme) is blown up in Figures 3.4(c)-3.4(h). From visual inspection, we notice that JPEG-LS produces a variety of artifacts with respect to the original image, while the proposed algorithm retains smooth texture better and produces higher compression rates (Table 3.2).

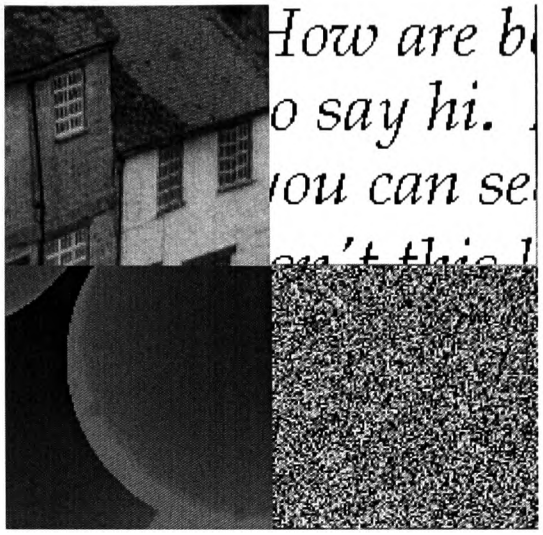

Figure 3.4(a): Original "test8.pgm"

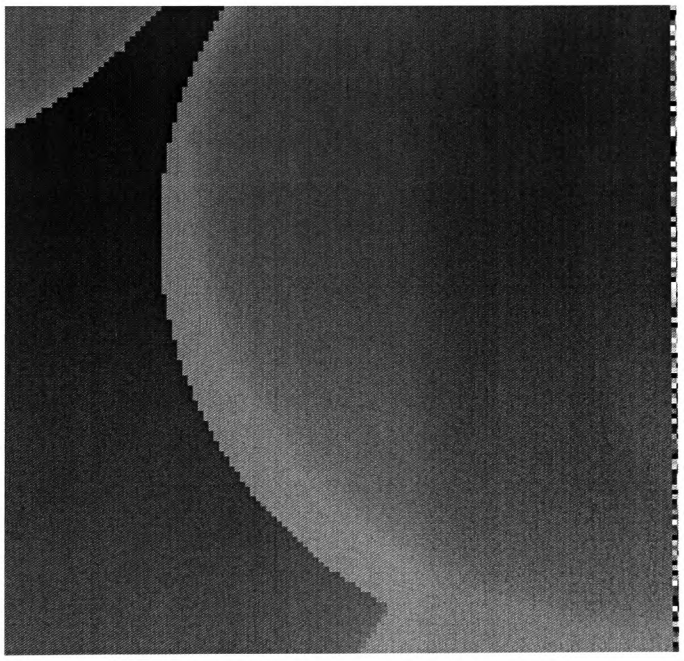

Figure 3.4(b): Smooth part of test8.pgm blown up

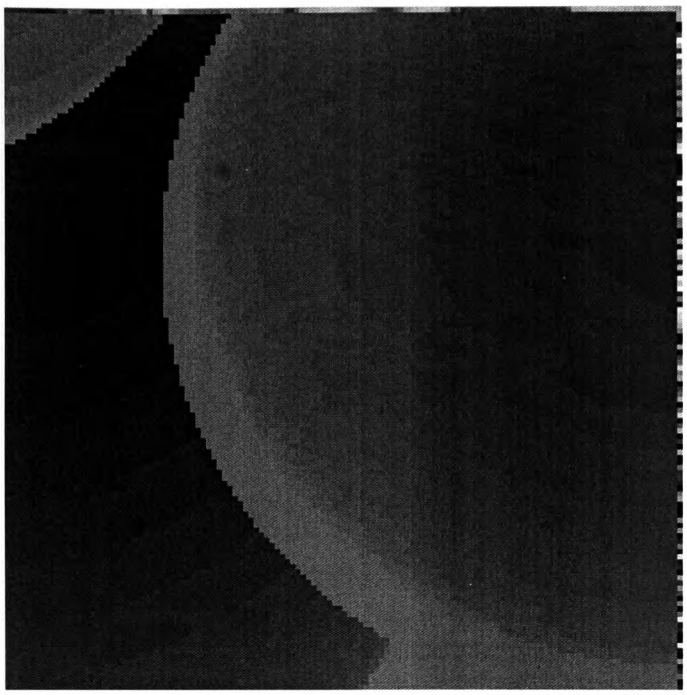

Figure 3.4(c): Reconstructed by JPEG-LS (NEAR=4)

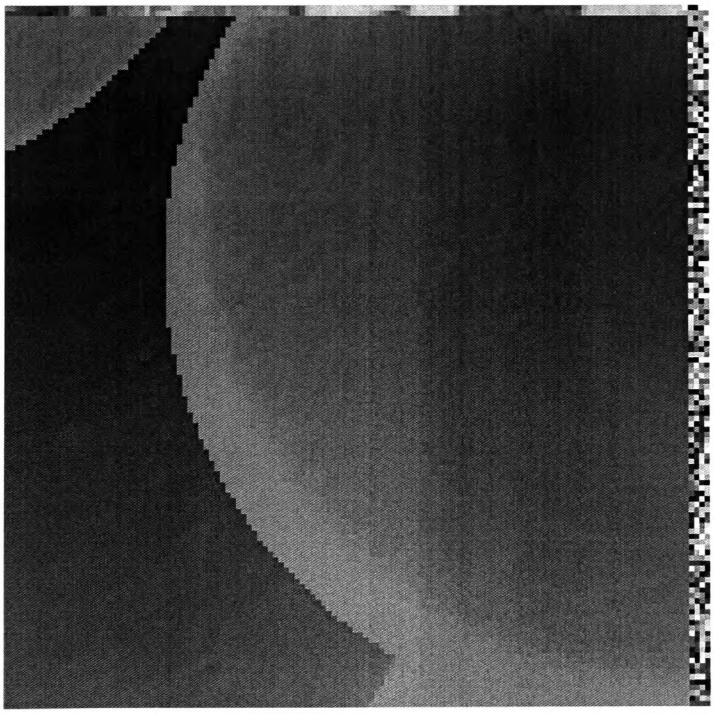

Figure 3.4(d): Reconstructed by the proposed scheme (NEAR_L=1,NEAR_M=5,NEAR_H=5).

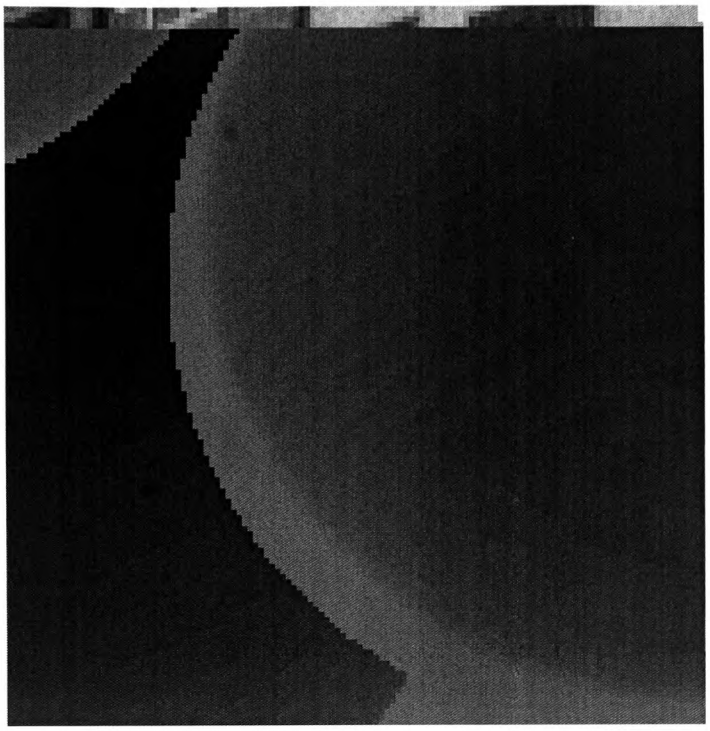

Figure 3.4(e): Reconstructed by JPEG-LS (NEAR=2)

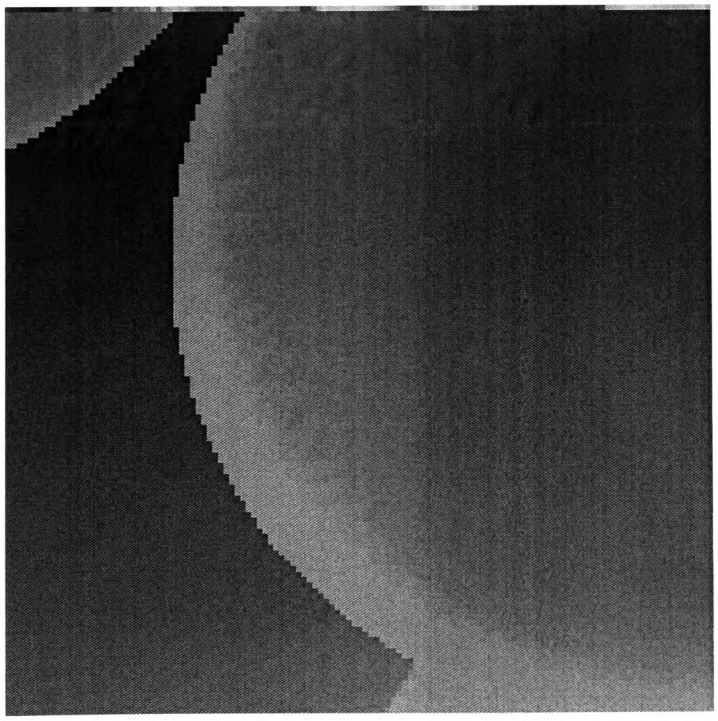

Figure 3.4(f): Reconstructed by the proposed scheme (NEAR_L=1,NEAR_M=2,NEAR_H=5).

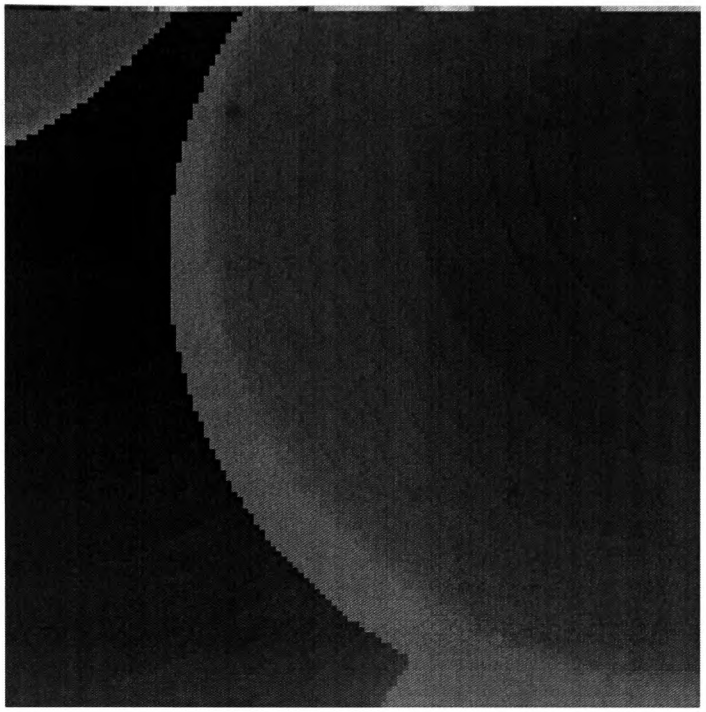

Figure 3.4(g): Reconstructed by JPEG-LS (NEAR=3)

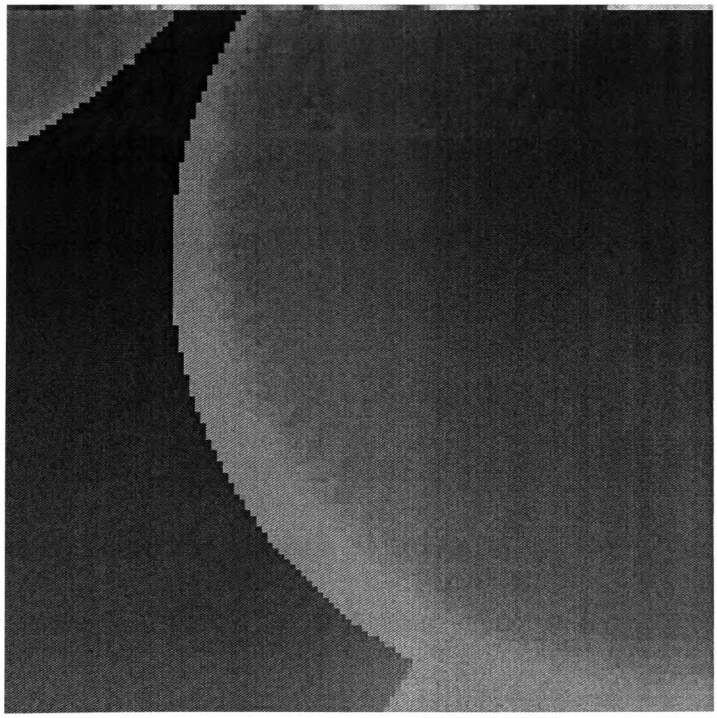

Figure 3.4(h): Reconstructed by the proposed scheme (NEAR_L=1,NEAR_M=4,NEAR_H=5).

3.3 Low cost algorithms for Rate Control in still image compression

In this section, a low cost algorithm based on HVS considerations is initially proposed in order *to add rate control* to JPEG-LS. The standard does not provide this feature, which may be important in applications such as digital cameras where a captured image may be required to fit accurately in the space available of a previously deleted image. Subsequently, an improved second algorithm is proposed which attempts to address jointly the problems of rate control with the visual quality improvement.

Problem formulation: Given a user defined target compression ratio, can we design a rate control algorithm based on JPEG-LS that exploits the multilevel information loss scheme described in the previous section? Can this rate control algorithm achieve bit rates closer to the target compared to the standard? What is the performance of such an algorithm both in terms of statistical (PSNR) and of visual image quality?

3.3.1 1st algorithm proposed

The first algorithm proposed is *designed to assess the feasibility of adding a low cost rate control mechanism* to JPEG-LS. In such a scheme, both the rate and distortion are controlled through changing the three NEAR parameters of the multilevel information loss distribution discussed above. In particular, what is really examined is the range of compression rates in which such a scheme is applicable and the negative effects of such a scheme in terms of PSNR. The negative effects on PSNR are expected since we rather intend to control R-D low cost and online, rather than apply the computationally expensive offline R-D optimization methods .The proposed algorithm proceeds as follows:

To detect the compressibility of each input image, the compression ratio can be computed and compared with *a user defined target compression ratio* as encoding proceeds. Such a comparison would provide a good indication of whether the information loss should be increased or decreased in order to force the compression ratio to be close to or equal to the target. To this end, the compression of an input image can be described as a two dimensional function, the range of which is defined by the size of the image. Hence the overall problem can also be described as an automatic control process through which the achieved compression ratio at the termination point is regulated to be equal or close to a pre-defined target compression ratio.

However, there are two unique features associated with this problem:

(i) To achieve the best possible quality for the reconstructed images at the decoding end, the compression ratio should be allowed to vary according to the local compressibility. The variation of the compression ratio will be controlled by the increment/decrement of the three information loss parameters (NEAR values) described in the previous section. Any excessive adjustments made by the control process will either incur unnecessary information loss and hence jeopardize the decoded image quality or will adversely affect the control over the compression rate. In order to avoid these problems, information loss should only be introduced when it is absolutely necessary and the unit of increment/decrement of the three NEAR parameters should be small.

(ii) When extra information loss is required, it should only be introduced to those regions which tend to tolerate more information loss from the human visual perception point of view.

To exploit the first feature, we convert the compression ratio from a two dimensional function to a one-dimensional function by allowing the compression ratio to be assessed only at the end of each row. By on-line compression ratio, we refer to the compression ratio that is computed at a point before the next pixel is to be encoded. By designating the assessment points *at the end of each row* along the raster scan route, we have the advantage of allowing the compression ratio to adjust itself according to the local compressibility embedded inside each row.

At each compression assessment point, the rate control is implemented according to the simple principle that if the on-line compression ratio is smaller than the target compression ratio, we should introduce extra information loss in order to force the on-line compression ratio to be close to the target. Otherwise, we should decrease the information loss in order not to spoil the image quality.

To exploit the second feature, we design the increase of information loss in a cycle of the three values of NEAR corresponding to the multilevel information loss scheme developed previously. The order of increase is designed as incrementing the NEAR_H parameter first , the NEAR_M parameter subsequently and the NEAR_L parameter finally. The increase of the NEAR values is also controlled by three thresholds (LimitHM, LimitML and LimitL) . LimitHM denotes the maximum distance between NEAR_H and NEAR_M, LimitML denotes the maximum distance between NEAR_M and NEAR_L, and LimitL denotes the maximum increase of NEAR_L respectively. Figure 3.5 shows the three NEAR parameters and their respective limits of increase. The highest value NEAR_H can have is the value 9 and the lowest value NEAR_L can have is 0, which are the highest/lowest allowable NEAR values from the standard.

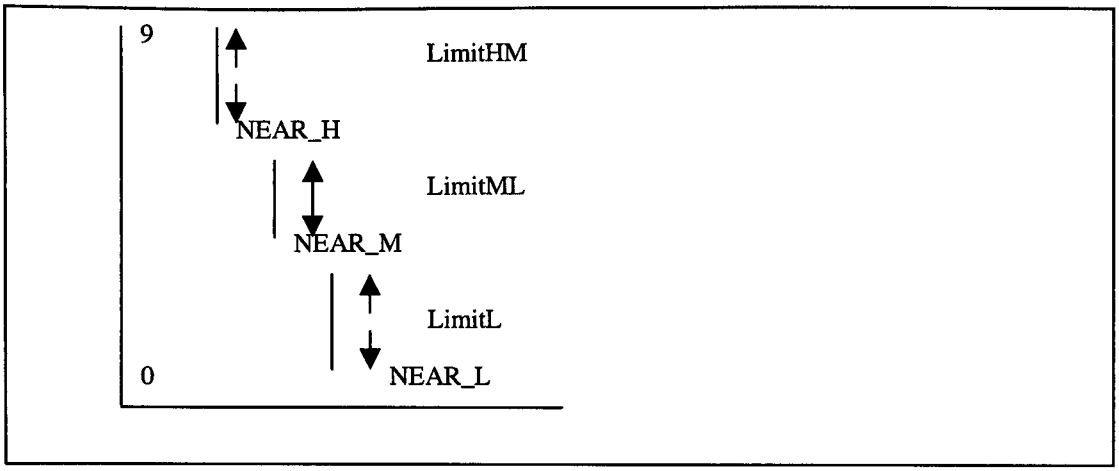

Figure 3.5: The change of the NEAR values along with their thresholds in the proposed rate control scheme

NEAR_H is always incremented first in the cycle as long as its distance from NEAR_M is less than LimitHM.. If NEAR_H has reached its limit, we then start to increase NEAR_M in the same way until it reaches the LimitML. Similarly we proceed for the increase of NEAR_L.

If we do not use the distance thresholds, excessive high value of NEAR_H or NEAR_M will bring extra distortion not only to the local region but also to the local texture which is even more damaging than the simple loss of information.

By considering the prediction scheme adopted by JPEG-LS, it is clear that the neighboring pixels used for prediction are not the originals but the reconstructed ones and are dependent on the NEAR value that the JPEG-LS uses as the information loss parameter. If NEAR_H is excessively high, yet the other two or one parameter is kept low, the pixels reconstructed by NEAR_H may not represent the true texture of the local region because edges may be detected instead of smooth regions. This situation results in distortion introduced to the decoded image and the compression ratio also deteriorates because of the wrong prediction.

Assuming that TCR and OCR represent the target compression ratio and the on-line compression ratio respectively, the proposed rate control algorithm can be summarized as follows:

Step 1: All parameters are initialized as: NEAR_H = NEAR_M = NEAR_H . It was found empirically that such a setting achieves rates closer to the target, while at the same time the PSNR differences between the non rate controlled JPEG-LS and the rate controlled proposed scheme become smaller. Extra variables are added representing the target compression ratio (TCR) and the online compression ratio (OCR). OCR is calculated as the total number of bits produced at each assessment point. LimitHM, LimitML and LimitL are also initialized.

Step 2: At the end of each row, comparison between OCR and TCR is made in order the rate control process to start as shown in Figures 3.6(a) and 3.6(b).

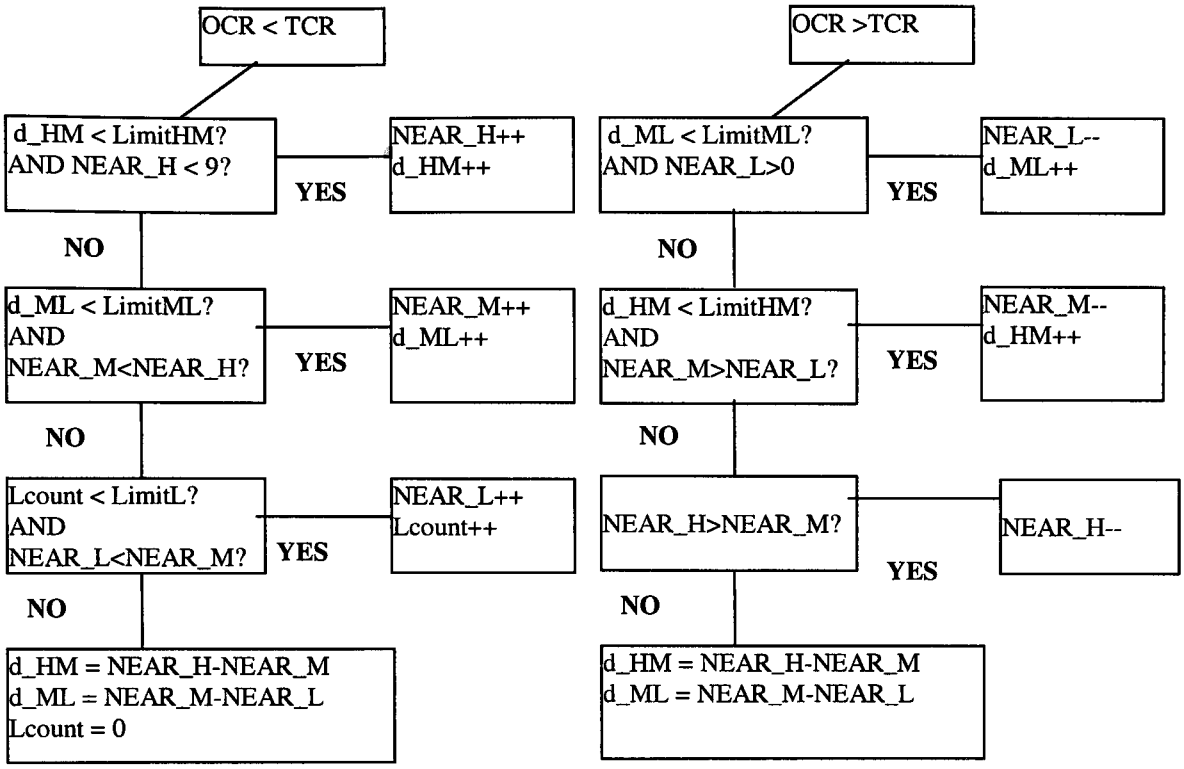

Figure 3.6(a): A flow chart for the rate control algorithm design when OCR < TCR

Figure 3.6(b): A flow chart for the rate control algorithm design when OCR > TCR

The principle adopted in designing the rate control algorithm is that the distances between the three information loss parameters should be kept within reasonable limits defined by LimitHM, LimitML and LimitL. Each time in a cycle of increase the three parameters reach their distance limits, the parameters d_HM, d_ML and Lcount ,which represent the number of increments within the cycle for NEAR_H,NEAR_M and NEAR_L respectively, are reset in order to give more room for increase in the next cycle. A similar path is followed in the decrease cycle with the only exception that the LimitL is not considered.

When OCR < TCR, we need to induce more information loss in order the OCR to increase. The three information loss parameters are increased in the order NEAR_H,NEAR_M,NEAR_ L in this case. Otherwise (OCR > TCR), we need to reduce

the amount of information loss and the information loss parameters are decreased in the order NEAR_L,NEAR_M,NEAR_H. This order follows the principle that we should throw away information where it is least visible in case the compression rate needs to be increased and only when *it is absolutely necessary* in order to control the rate, to consider throwing away information where the local texture is smooth. Conversely we should retain information where it is most visible in case the compression rate needs to be decreased and only when *it is absolutely necessary* in order to control the rate accurately, to consider also retaining information on rough textures.

It should be noted from Figures 3.6(a) and 3.6(b) that Lcount represents the total number of increments made for NEAR_L, *not the maximum value NEAR_L can have.* In other words, NEAR_L can have any value but the number of increments it can have within each cycle is limited by the parameter LimitL. This is to ensure that the distance between the NEAR_L and the NEAR_M parameters is retained for the reasons described above but also for allowing the NEAR_L parameter to take any value in the range 0 to 9 in case the accurate control of the compression rate demands that NEAR_L takes a value greater than Lcount.
For the case that the on-line compression ratio is greater than the target compression ratio (OCR>TCR), the information loss parameters should be decreased until lossless mode is reached. The decrease is designed to follow the reverse order: NEAR_L,NEAR_M and NEAR_H. This is designed on the same ground that we should maximise the reconstructed image quality while the compression ratio is under control. Generally speaking, we should try to decrease NEAR_L first whenever it is possible, i.e the distance d_ML is within its limit. Otherwise, we will try to decrease NEAR_M as long as d_HM is within its limit. Finally, we decrease NEAR_H .

There are some salient features in the design of the proposed algorithm that are explained in detail here:

1. We intend to control the compression rate of the source image inside the same limits as JPEG-LS but utilizing an HVS approach instead. For this reason, the range of the three NEAR parameters is the same as the single parameter NEAR used in the standard. Although the compression rate is source dependent, we will typically achieve compression rates between 2:1 and 5:1. If higher rates are desired, standards like the DCT based JPEG lossy would be more appropriate.
2. A multitude of compression rates are achievable with the proposed scheme which are not reachable with JPEG-LS. This is because we have essentially parametrized the information loss distribution, as opposed to the constant information loss used by the standard, according to the number of different texture types identifiable in the prediction phase of the standard. We could have evaluated *the online compression ratio* multiple times inside each row, thus improving the control over the bit rate but unavoidably this would spoil the quality of the reconstructed image due to excessive control. Furthermore, this would add to the computational complexity of our algorithm due to the multiple comparisons and parameter adjustments shown in Figures 3.6(a) and 3.6(b).
3. The starting values of the three NEAR parameters are also important. If we start too low, looking to achieve a high compression rate, we may never reach this rate because we will run out of image rows to compress. Conversely, if we start too high trying to achieve a low compression rate, we can again fail to reach it if we run out of rows. Furthermore, if we do reach the desired compression rate this will happen only after we have spoiled the image quality unreasonably. In general a balance should be found

empirically between the starting values of the NEAR parameters and the desired compression rate.

4. To reflect the principle of different tolerance of HVS to different textures the condition NEAR_L<=NEAR_M<=NEAR_H is crucial for the proposed algorithm.

3.3.2 Experimental evaluation for the proposed scheme

To assess the performance of the proposed rate control algorithm on a number of image samples, we used a software implementation in C. The objective was to achieve exactly or to be sufficiently close to a user defined compression ratio but also to evaluate how negative the effect of adding rate control to JPEG-LS would be in terms of PSNR values.

The overall experiments are designed in two phases: (i) to test the effectiveness of the rate control algorithm in terms of achieving target compression rates and to get an indication about the range of compression rates achievable with such a scheme; (ii) to assess the reconstructed image quality in terms of PSNR (peak signal to noise ratio) values.

Tables 3.3 and 3.4 illustrate the test results for a group of image samples when the target compression ratio is set at 2:1,3:1 respectively. Table 3.5 illustrates the initial NEAR values we used for both rate controlled and non rate controlled algorithms. It is seen that rate controlled compression ratios for all images are indeed close to their targets. This clearly shows that our rate control algorithm is effective. For a further comparison, the non-rate controlled compression ratios for the same initial settings are also presented in the last column of each table. To illustrate what kind of effect the rate control algorithm could have on the reconstructed image quality, we have used the non-rate controlled JPEG-LS as our benchmark. The experiment is carried out to use the compression ratio achieved by the non-rate controlled JPEG-LS as our target compression ratio. We then compare the two

PSNR values, as the two compression ratios are very close. The test results are illustrated in Table 3.6 for all the tested images. The results show that the rate controlled PSNR is indeed close to the non-controlled one by an average of 2-3 db. It is well expected that rate-control based on a multilevel information loss distribution will inevitably introduce extra information loss in order to achieve the target compression ratio, since TCR is reached through adjustments of the NEAR parameters instead of natural compression.

Table 3.3 Rate Control Experimental Results (TCR = 2:1)

Image Samples	Rate Controlled CR	Non Rate Controlled JPEG-LS
Baboon	2.03:1	1.8:1
Barb	2.00:1	1.69:1
Bridge	1.99:1	1.90:1
Camera	1.98:1	1.85:1
Salad	2.05:1	1.58:1

Table 3.4 Rate Control Experimental Results (TCR = 3:1)

Image Samples	Rate Controlled CR	Non Rate Controlled JPEG-LS
Baboon	2.99:1	3.00:1
Barb	2.96:1	2.52:1
Bridge	3.00:1	2.96:1
Camera	2.83:1	2.80:1
Salad	3.00:1	2.81:1

Table 3.5 Initial NEAR Values

Initial NEAR_L,NEAR_M,NEAR_H	TCR
(0,0,0)	<=2.5
(1,1,1)	<=3.5
(2,2,2)	<=4.0

Table 3.6 Results of Compressed Image Quality (PSNR)

Image Samples	Rate Controlled		Non Rate Controlled JPEG-LS	
	CR	PSNR(db)	CR	PSNR(db)
Baboon	3.73:1	33.79	3.73:1	34.40
Barb	4.63:1	35.17	4.64:1	38.85
Bridge	3.51:1	34.81	3.54:1	36.74
Camera	4.09:1	36.31	4.22:1	42.47
Salad	4.78:1	34.27	4.78:1	35.59

3.3.3 2nd algorithm proposed

The second algorithm proposed is centered around the same features as the first algorithm (i.e exploiting local compressibility, small increments/decrements of the information loss parameters and information loss allocated in accordance to HVS tolerance). The purpose of the scheme is to jointly optimize the control over the compression rate along with low cost visual quality optimization (in the smooth texture retaining sense). Its major differences from the first algorithm are:

1. The notion of *predicted compression* ratio is utilized. A number of on-line compression ratios can be obtained during the process of encoding with JPEG-LS, corresponding to each compression assessment point. These OCRs can be viewed as a history or a record of local compressibility for all those regions that have already been encoded. Hence, the records can be utilized to predict their contribution to the final compression ratio towards the end of encoding, which is also the OCR achieved at the last compression assessment point. This prediction follows the same principle as that of general predictive coding that, given previous statistics, a prediction is made based on a local context for what happens in the future corresponding to the similar type of context. As it is not possible to know what compressibility or local texture could be for the non-encoded part of the image, we can only use the already encoded part to predict the future which has the similar local texture. Since it is difficult to optimize such a prediction scheme, we propose to use linear prediction in order to exploit its simplicity . This can also be viewed as a line-fitting problem, in which, we are trying to use a straight line to characterize as many points as possible. The similarity between the rate control problem using a *predicted*

compression rate and *the line fitting problem* is illustrated in Figure 3.7. Therefore, the predictive line can be constructed in such a way that the distance between the line and all the concerned OCR values is kept minimum. Hence, the remaining issue is to determine how many OCR values should be involved in this line-fitting process and how those values should be selected. Assuming the *i*th row has just been encoded, a simpler predictive line can be constructed by selecting only two points, (*i, OCR[i]*) and (*i-d, OCR[i-d]*), where *d* is an integer representing how far away the second point used in prediction is from the current row *i*, as shown in Figure 3.7.

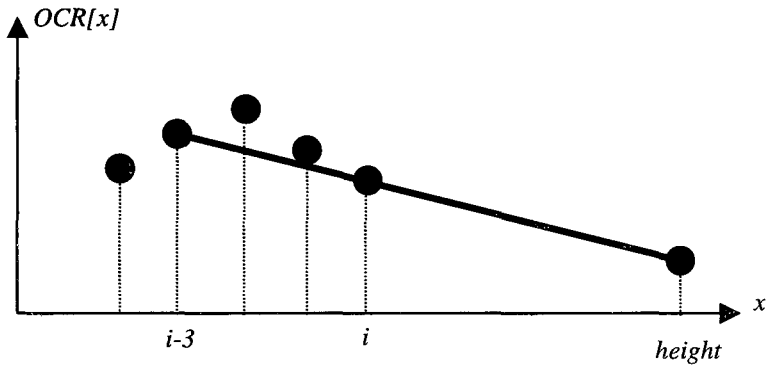

Figure 3.7: Line fitting prediction with two points (d=3)

In our algorithm design, the value of *d* is empirically determined to be 3. As a result, the final compression ratio can be predicted by the following equation corresponding to the point (*height, PCR*):

$$PCR = OCR[i] + (height - i) \times \frac{OCR[i] - OCR[i-d]}{distance} \qquad (3.2)$$

At each compression assessment point, the rate control is implemented on the simple principle that if the predicted compression ratio (PCR) is smaller than the target compression ratio (TCR), we should introduce extra information loss in order to influence the on-line compression ratio as such that the final compression ratio at the end of

encoding could be close to the target. Otherwise, we decrease the information loss to allow better compression quality or to allow opportunities of compensation for any extra information loss introduced earlier.

2.The order of increase/decrease of the three NEAR parameters is not exactly the same as the previous algorithm. A potential limitation of the previous scheme is that if a NEAR parameter needs to be increased in cycle i and cycle (i+1) is a decrease cycle (OCR>TCR), it is not guaranteed that the same NEAR parameter will be decreased. As an example, consider the case where LimitML is equal to 2 and in cycle i, NEAR_M is increased once. This will result in increase of the distance between NEAR_L and NEAR_M by one, so d_ML = 1. If cycle (i+1) is a decrease cycle, according to the previous algorithm, *NEAR_L will be decreased by one and not NEAR_M*, while the distance between the two parameters (d_ML) will be equal to two. In this algorithm design, we explored the potential of guaranteeing that if a NEAR parameter is incremented in a cycle i, it will be the same parameter that will be decremented in the reverse cycle i+1, around a small neighborhood of the target compression rate. This essentially aids in reducing the magnitude of the fluctuations of the compression rate around the target, thus improving the control over the rate.

We used an array implementation for the proposed algorithm. The distance parameters and the constants reflecting the limits of increase/decrease are not utilized since we chose that the maximum distance allowed between NEAR parameters will be equal to unity. This aids in preserving the small distance between NEAR parameters which is crucial both in terms of quality and compression rate, since its inter-linked to the prediction scheme, as explained above. Furthermore, such a scheme guarantees that the minimum information loss will be induced when the PCR needs to be increased thus preserving the image quality.

To simplify the notation in the following discussion, we will denote the three NEAR parameters with their acronyms (i.e L for NEAR_L, M for NEAR_M and H for NEAR_H). To correctly identify the right parameter for the next adjustment, either increase or decrease, we use two arrays of three elements to hold the parameters, which have already been adjusted through the cycle, as well as those remaining parameters. This is illustrated in Figure 3.8, which shows the initial state before rate control is started. Each time a parameter is increased or decreased, it will be moved from its original position across to the corresponding position in the other array, i.e., H on top, M in the middle and L at the bottom. Hence, the rate control algorithm can be described by the movement of the three parameters from one array to the other according to the pre-defined order of adjustment. The order of movement of the information loss parameters can be described as follows:

(i) To increase the information loss parameter, the algorithm will search the I-array in a top-down direction. The first parameter accessed will be increased and moved to the D-array at its corresponding position.

(ii) To decrease the information loss parameter, the algorithm would search the D-array instead in a bottom-up direction and move the first parameter accessed to the I-array at its corresponding position;

(iii) Whenever the parameter being moved is the last one inside the array (either I or D), the array which is full needs to be renamed as an I-array if the next adjustment is to increase, and D-array if the next move is to decrease. In other words, the array full of parameters is always renamed by the name of the next adjustment. This is designed to ensure that the correct order of movement is always maintained even when one of the arrays becomes empty.

The overall rate-control algorithm can also be described by the flow-chart given in Figure 3.9.

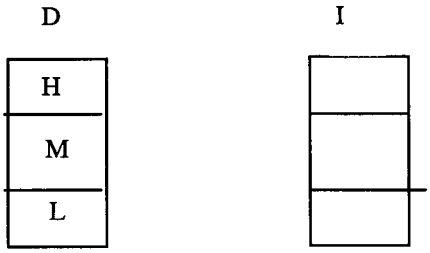

Figure 3.8: Initial state of parameters

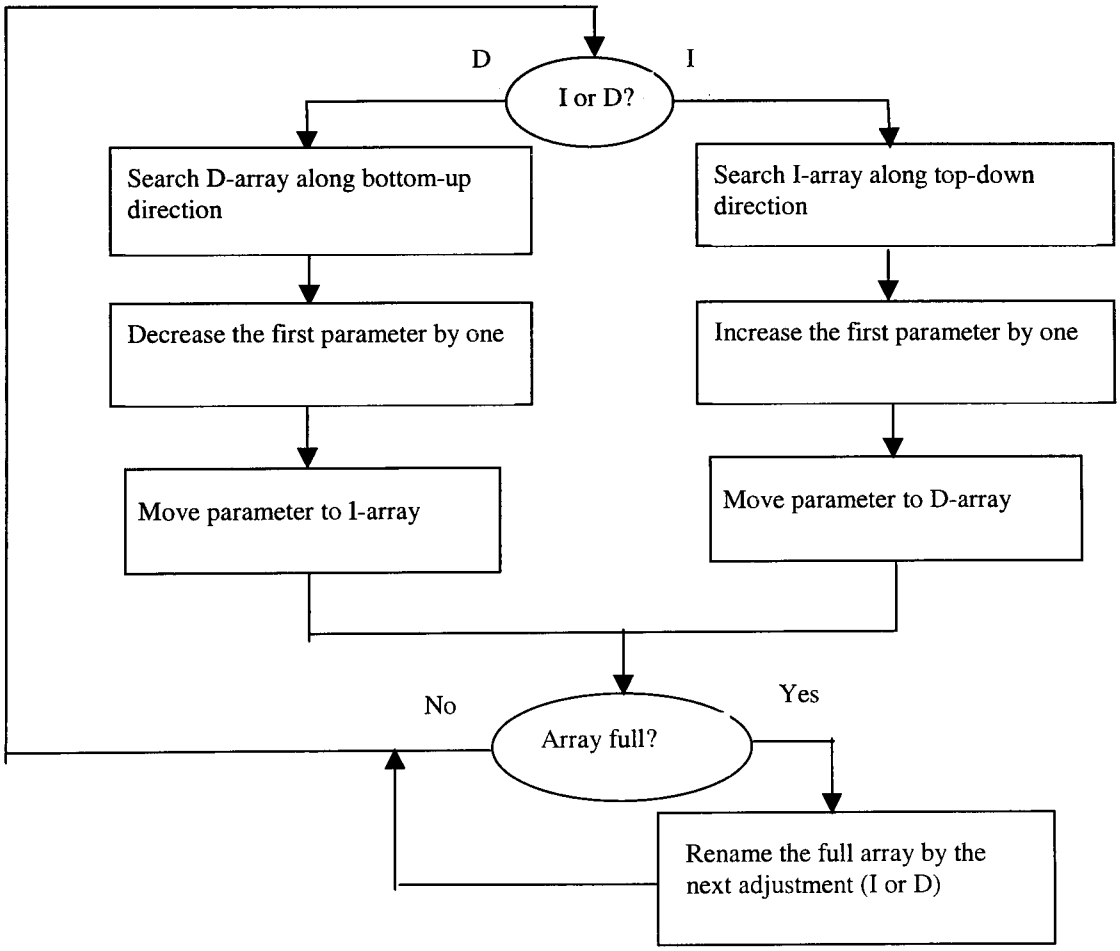

Figure 3.9: Algorithm flow chart

To further illustrate the key operations of the algorithm, we present an example in which it is assumed that the rate control operations for a sequence of nine compression assessment points are given below:

I, I, D, D, D, D, I, I, I

Where *I* stands for increase of parameters and *D* for decrease of parameters.

Further assume that the starting state of the parameters is the same as that illustrated in Figure 3.8 . Hence, the array full of parameters can be named as I-array, since the next adjustment is to increase the parameter. Along the top-down direction, the two parameters, H and M, can be increased by one and moved to the D-array as a result of the two I-operations in the above sequence. After that, the state of parameters can be described by Figure 3.10-(a).

As the next move in the sequence is to decrease the parameter, the search will be conducted instead in the D-array along the bottom-up direction to identify the parameter to be decreased and moved to the I-array. This would give us a state of parameters as shown in Figure 3.10-(b). After the second D operation inside the sequence is completed, it can be seen that the D-array becomes empty and the array full of parameters needs to be renamed, according to the rate control algorithm proposed. The state before the renaming of the array is illustrated in Figure 3.10-(c). Since the next move is another decrease, the original I-array should now be renamed as D, and the parameter L is moved across to the I-array as shown in Figure 3.10-(d). Carrying on with the remaining operations in the sequence, the rest of all corresponding states can be shown in Figure 3.10-(e), (f), (g) and (h) respectively. Note in Figure 3.10-(h), the two arrays are renamed again as a result of the original I-array in Figure 3.10-(g) becomes empty and the next move is I.

As a matter of fact, by varying the size of the two arrays, the algorithm can be designed to have variable steps of increase or decrease to interpret the local textures, if more drastic change of information loss is required. This can be achieved by adding more elements of M, H and L into the two arrays. One example is shown in Figure 3.11, where two arrays of five elements are designed and thus the adjustment of L would not be made until both M and H are adjusted twice. The rest of the algorithm remains the same as already described. Finally, from Figure 3.11, it can also be seen that any form of adjustment on those three parameters can be made by rearranging the size of the array and the position of each parameter.

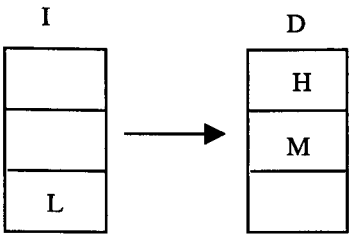

The completed sequence = I. I

(a)

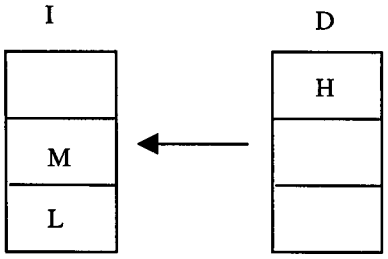

The completed sequence = I, I, D

(b)

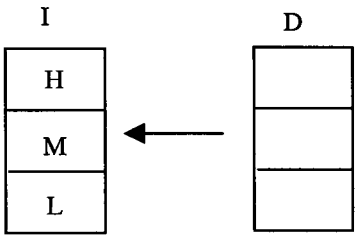

The completed sequence = I. I. D. D

(c)

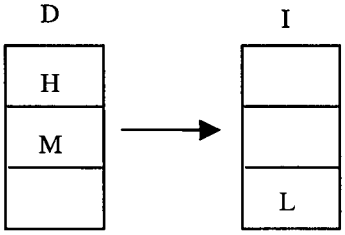

The completed sequence = I. I. D. D. D

(d)

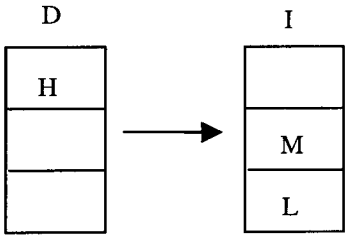

The completed sequence = I. I. D. D. D. D

(e)

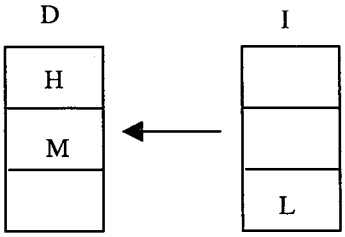

The completed sequence = I. I. D. D. D. D. I

(f)

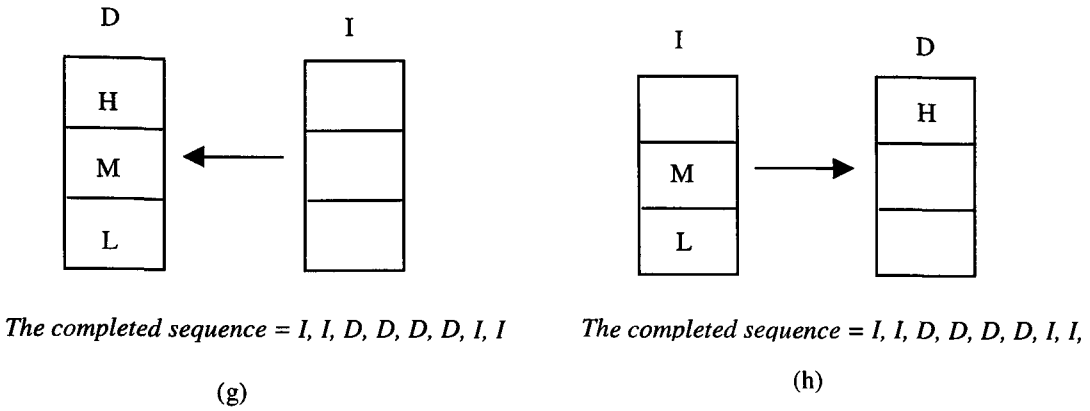

The completed sequence = I, I, D, D, D, D, I, I

(g)

The completed sequence = I, I, D, D, D, D, I, I,

(h)

Figure 3.10: An example of rate control for the sequence: I, I, D, D, D, D, I, I, I

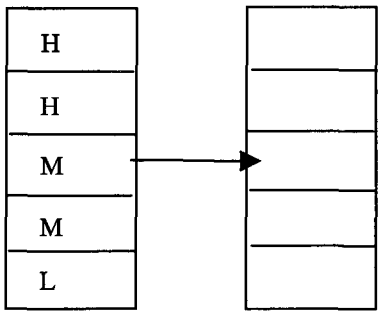

Figure 3.11: Rate control with delayed action for parameter L

3.3.4 Experimental evaluation and analysis of the proposed scheme

We evaluated the proposed scheme in terms of *effectiveness* and *efficiency*. The *effectiveness* refers to the performance of the algorithm in terms of achieving compression rates as close as possible to the target. As in the previous algorithm, the range of compression rates by the proposed scheme is intended to be the same as in JPEG-LS. In this light, this scheme will also be evaluated in terms of achieving rates of 2:1 and 3:1. Any higher compression rates are better served by the JPEG lossy standard. The rate control *efficiency* refers to the assessment of the reconstructed image quality for those image samples measured by both PSNR values and visual inspection. The issue about the balance of the choice of the initial NEAR parameters and the desired target compression rates is also of relevance to the proposed scheme for the reasons outlined in the previous algorithm.

After determining an appropriate initial setting for the three parameters (L,M,H) empirically, we present the experimental results in two phases, i.e., the test of rate control efficiency as the first phase, and the test of rate control effectiveness as the second phase.

To carry out the assessment, we firstly run the JPEG-LS on the same group of image samples to produce a set of variable compression ratios and PSNR values. We then use those compression ratios achieved by JPEG-LS as the target compression ratios (PCR) to test our rate controlled design. In this way, all the compression ratios can be maintained very close, which enables a sensible comparison between PSNR values. However, it must be stressed that this arrangement produces a disadvantage for the proposed algorithm because the results achieved by JPEG-LS use natural compression. Yet the proposed algorithm has to go through the rate control process to redistribute the information loss, in order to achieve the compression ratios similar to those by JPEG-LS. To this end, it is

impossible for any rate controlled algorithm using a multilevel information loss distribution to produce better PSNR values than that of JPEG-LS. Nonetheless, we expect the comparison to give us an indication on how negative our rate control effect is in comparison with the ideal situation where no rate control is added. As a result, we measure the quality performance by a so-called relative difference between the rate-controlled PSNR and the non-rate-controlled PSNR values. This is defined as follows:

$$\mathrm{Re}lative\_diff = \frac{PSNR_{not\_controlled} - PSNR_{rate\_controlled}}{PSNR_{not\_controlled}} \qquad (3.3)$$

All the test results are given in Table 3.7, in which we listed all compression ratios, PSNR values and the relative difference values achieved by the two algorithms. From this table, it can be clearly seen that: (a) the proposed rate control algorithm is very effective since it is able to control the compression ratio very close to the ones achieved by JPEG-LS; (b) when the JPEG-LS compression ratios are used as the target, the PSNR values achieved by the proposed algorithm are indeed very close. This can also be indicated by those relative difference values, which vary from 0.5% to 8.9%.

The test results in Table 3.7 illustrate that the image quality produced by the proposed rate control algorithm is competitive to the one by the non-controlled JPEG-LS, even when the quality is measured by PSNR values.

As stated in the introduction, the proposed algorithm is aiming at jointly optimising the image quality measured *by human visual inspection rather than by PSNR values* and the control over the bit rate, by distributing information loss according to HVS principles. Unless the rate control algorithm is more advanced though (which implies complexity and long encoding delays) , it is impossible to improve the PSNR performance as compared to JPEG-LS. To prove the *efficiency* of the proposed scheme in HVS terms, we further

present the samples of "test8.pgm", the JPEG standard test image, in Figure 3.12 for a visual comparison and inspection. To facilitate a comprehensive visual inspection, Figure 3.12 is arranged as follows:

- Fig.3.12-(a) corresponds to the original test8; Fig. 3.12-(b) corresponds to the blown up bottom left quartile (smooth part) of Fig. 3.12(a).
- Fig.3.12-(c) and (d) present the blown up smooth part of the reconstructed test8 by the non-controlled JPEG-LS and the proposed algorithm respectively, when the distortion level is set to *NEAR=3*;
- Fig.3.12-(e) and (f) present the blown up smooth part of the reconstructed test8 by JPEG-LS and the proposed algorithm, when the distortion level for JPEG-LS is set to *NEAR=4*;
- Fig.3.12-(g) and (h) present the blown up smooth part of the reconstructed test8 by JPEG-LS and the proposed algorithm, when the distortion level for JPEG-LS is set to *NEAR=5*.

From all images in Figure 3.12, it can be seen that the reconstructed test8 by the proposed algorithm clearly show better visual quality than those by JPEG-LS, especially in the region at the bottom left where smooth texture dominates. This is because that the proposed rate control is able to distribute the distortion to those noisy textured areas, while the distortion level is kept low in the smooth ones. In the case of JPEG-LS, the same distortion level has to be applied throughout the whole image without any difference.

To further prove the testing results, we also asked a group of 10 people to view all the reconstructed images and make their options without knowing which image reconstructed by what algorithm. To carry out such a test, five options are established. They are: (1) no difference between A and B; (2) A is better than B; (3) B is better than A;

(4) A is closer to the original; (5) B is closer to the original. To ensure a fair rating, those images reconstructed by the proposed algorithm are labelled as A, and those reconstructed by JPEG-LS are labelled as B. The overall test results are given in Table 3.8.

In the second phase of the experiments we ran the rate control algorithm on the same group of six image samples and tested *the effectiveness* of the proposed algorithm, in which the target compression ratios are set to be 2:1 and 3:1, which is well within the range of near lossless compression. The experimental results are given in Table 3.9-(a) and (b) respectively. Consistent with the above discussion concerning the importance of the balance between the initial settings and the target rate, we empirically chose (0,0,2) as the starting point for target compression ratio 2:1 and (1,8,9) as the starting point for target compression ratio 3:1.

To further facilitate comparison of the proposed algorithm with the non rate-controlled JPEG-LS, the compression rates produced by the standard along with their respective PSNRs are also shown in Tables 3.9-(a) and (b). The JPEG-LS results are obtained by varying the value of *NEAR* and picking up the nearest one to each target compression ratio. In fact, it is not practically possible to manually adjust the parameter *NEAR* for each input image to achieve a compression ratio close to the target. This is because we do not know the compressibility of each input image before the compression can be done, and it is not allowed in practice to compress each image with various NEAR values first and then choose the closest one.

From all the results presented in Table 3.9, it can be summarized that: (i) all compression ratios achieved by our algorithm are indeed controlled at the target compression ratio; (ii) without rate control, the nearest compression ratio achieved by JPEG-LS is still not close enough to the target, even after the parameter *NEAR* is adjusted manually.

Finally, we also tested the proposed algorithm with 5 elements as shown in Figure 3.11. It is discovered that there is no significant difference between the arrays with 3 elements and 5 elements. This is expected since the effect of delaying increment of the parameter L can be achieved by initial settings with larger distance between L and other parameters.

Table 3.7: Phase-1 Rate Control Experimental Results (Initial L, M, H = 1,8,9)

Image samples	*Proposed Algorithm* CR	PSNR(db)	*Non Rate Controlled JPEG-LS* *CR*	*PSNR(db)*	*NEAR*	*Relative-diff*
Baboon.pgm	3.445:1	35.248	3.488:1	35.478	7	0.6%
Barb.pgm	4.161:1	38.131	4.158:1	40.101	4	4.9%
Bridge.pgm	4.002:1	34.265	4.104:1	34.453	8	0.5%
Camera.pgm	4.752:1	36.831	4.907:1	40.447	4	8.9%
Salad.pgm	4.731:1	35.198	4.783:1	35.586	7	1%
Test8g.pgm	3.133:1	39.89	3.127:1	42.677	3	6.5%

Table 3.8: Visual Perception Quality Rating Test Results

Image Samples	*Option-1*	*Option-2*	*Option-3*	*Option-4*	*Option-5*
Baboon	10	0	0	0	0
Barb	8	2	0	0	0
Bridge	10	0	0	0	0
Camera	6	4	0	0	0
Salad	10	0	0	0	0
Test8	0	0	0	10	0

Table 3.9-(a) Phase-2 Rate Control Experimental Results (Initial L, M, H = 0,0,2 and Target-Compression-Ratio = 2:1)

Image Samples	**The Proposed Algorithm**		**The Non-rate-controlled JPEG-LS**		
	C. Ratio	**PSNR(dB)**	**Closest C. Ratio**	**PSNR(dB)**	**NEAR Values**
Baboon	1.997:1	44.891	1.800:1	49.685	1
Barb	2.01:1	51.672	1.690:1	INF	0
Bridge	2.001:1	45.999	1.899:1	49.899	1
Camera	2.039:1	53.961	1.849:1	INF	0
Salad	1.999:1	50.07	1.578:1	INF	0
Test8	2.091:1	51.802	1.915:1	INF	0

Table 3.9-(b) Rate Control Experimental Results
(Initial L, M, H = 1,8,9 and Target-Compression-Ratio = 3:1)

Image Samples	The Proposed Algorithm		The Non-rate-controlled JPEG-LS		
	C. Ratio	PSNR(dB)	Closest C. Ratio	PSNR(dB)	NEAR Values
Baboon	2.994:1	37.444	2.998:1	38.153	5
Barb	3.002:1	42.507	2.524:1	49.893	1
Bridge	3.005:1	38.077	2.956:1	39.950	4
Camera	3.013:1	44.144	2.802:1	49.927	1
Salad	2.999:1	41.58	2.810:1	45.143	2
Test8	3.01:1	40.745	3.127:1	42.677	3

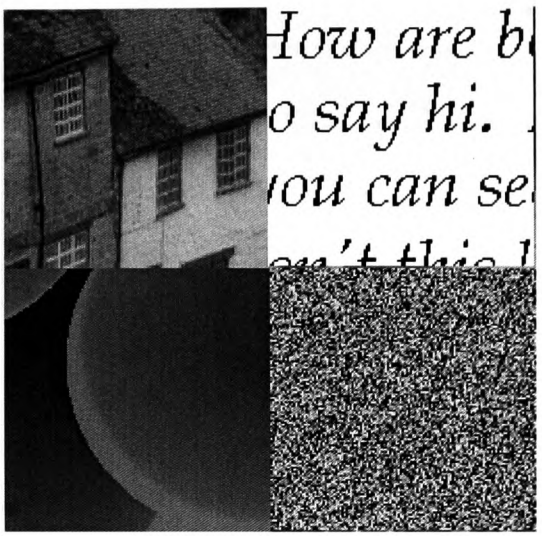

Figure 3.12(a): Original "test8.pgm"

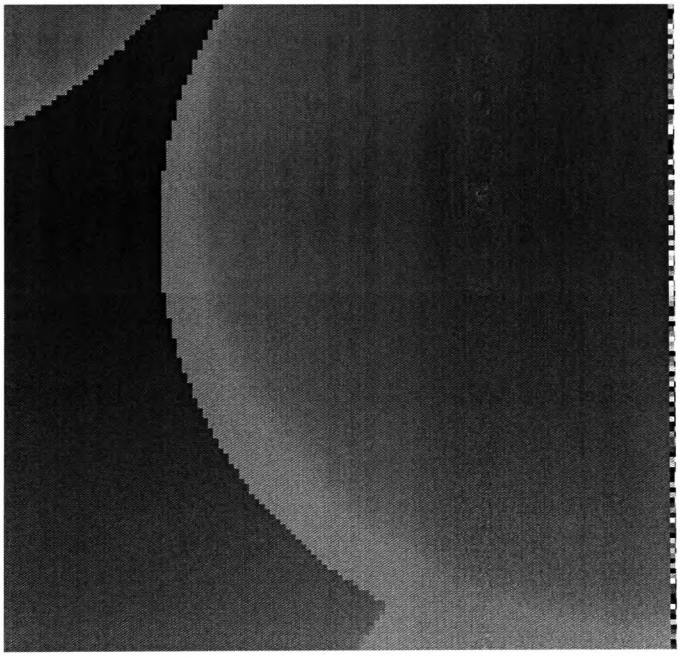

Figure 3.12(b): Smooth part of test8.pgm blown up

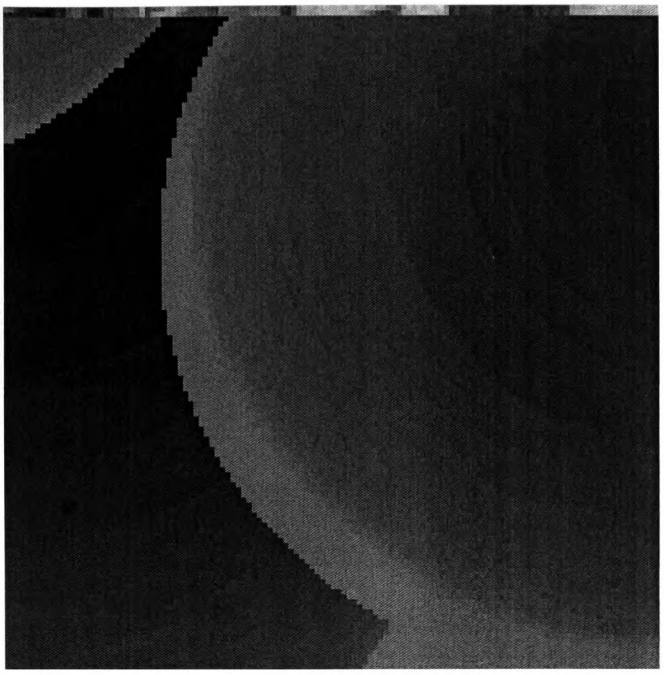

Figure 3.12(c): Reconstructed test8 by JPEG-LS with NEAR parameter equal to 3

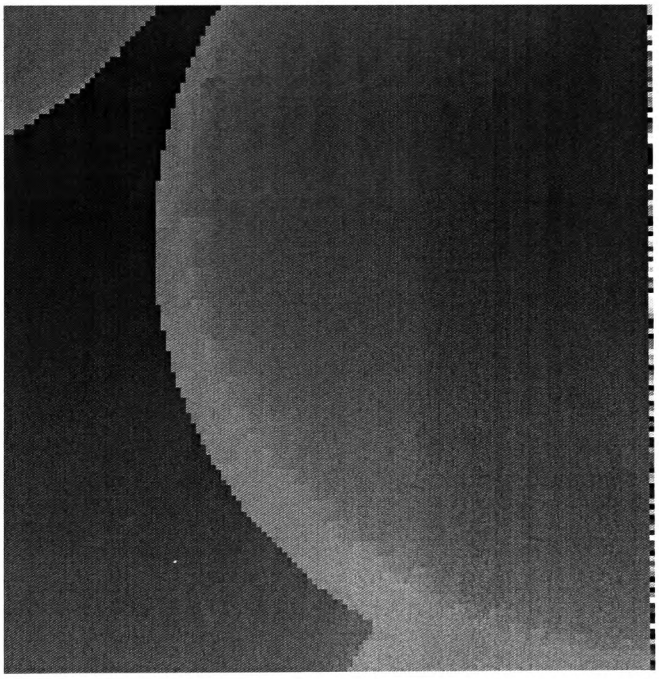

Figure 3.12(d): Reconstructed test8 by the proposed algorithm

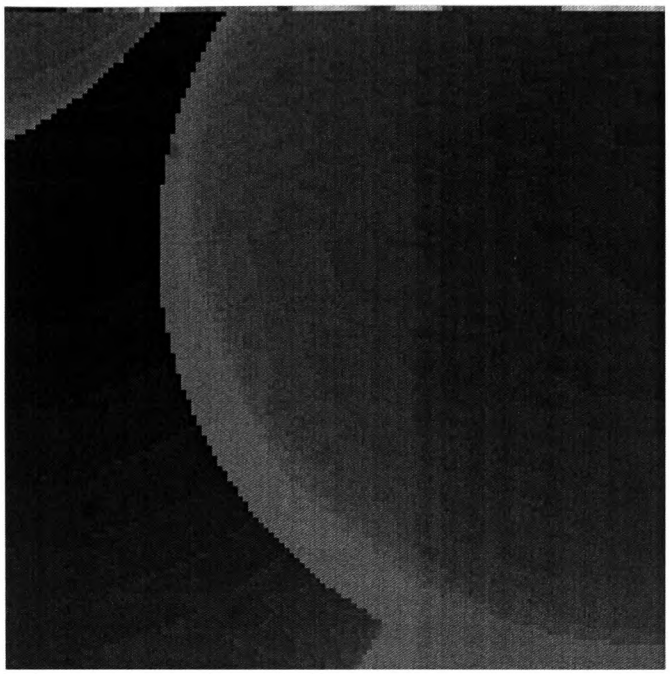

Figure 3.12(e): Reconstructed test8 by JPEG-LS with NEAR parameter equal to 4

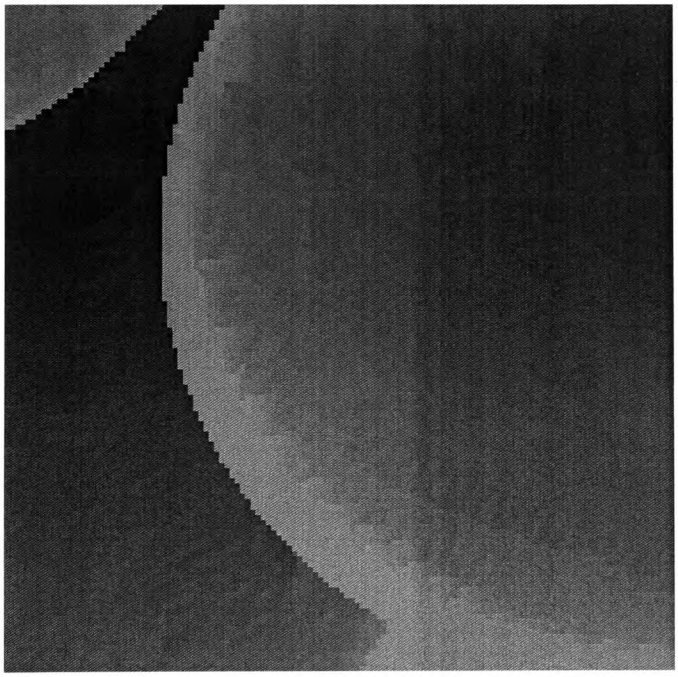

Figure 3.12(f): Reconstructed test8 by the proposed algorithm with the same compression ratio as in (e)

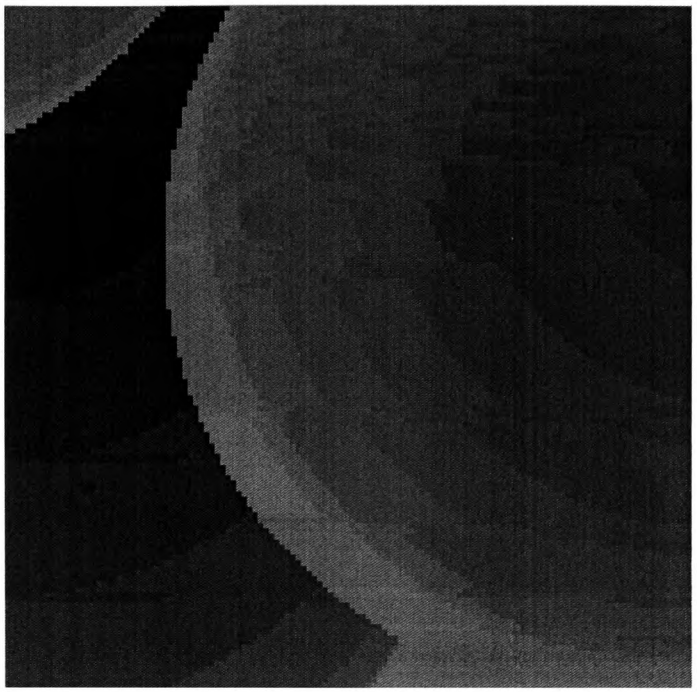

Figure 3.12(g): Reconstructed test8 by JPEG-LS with NEAR parameter equal to 5

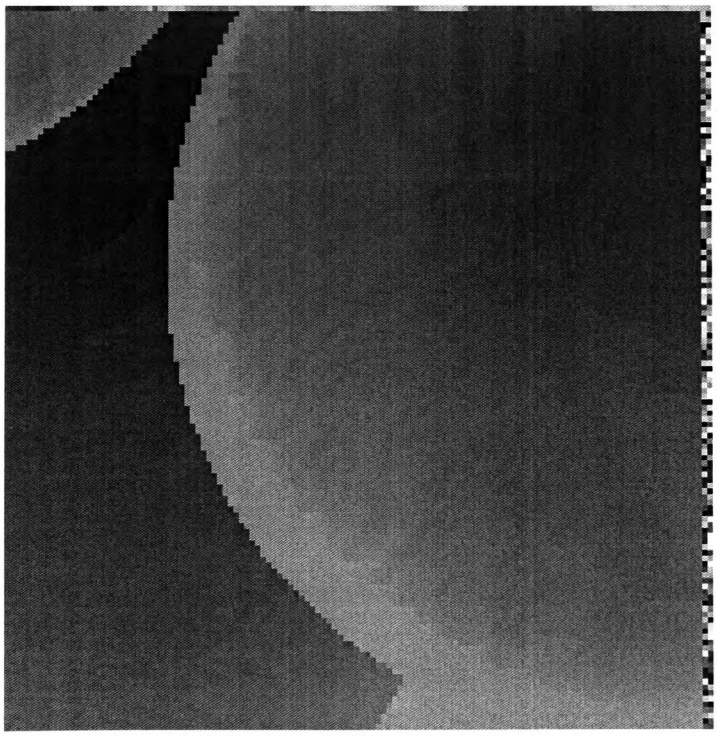

Figure 3.12(h): Reconstructed test8 by the proposed algorithm with the same compression ratio as in (g)

Figure 3.12: Visual comparison of test8 between JPEG-LS and the proposed rate-controlled JPEG-LS

3.4 Applications in Medical Imaging

We also tested the second proposed algorithm in medical images. Such kind of images have unique features since both the texture smoothness should be preserved but also excessive information loss in edges should be avoided. This requirement is tighter *than just retaining texture smoothness* but it is justifiable since the importance of retaining edge detail in medical applications is more critical than in the entertainment industry. We wanted to assess if in this particular kind of images, our algorithm is still effective and if it can preserve texture smoothness for the same bit rates as the standard. Potential uses of the scheme could include tracking progress in wound/rash healing or just providing the physician with a bigger gamut of image qualities than the JPEG-LS standard. Tables 3.10(a) and (b) show the performance of our algorithm in terms of effectiveness for a variety of compression rates as compared to JPEG-LS. It is evident that in the range of compression rates between 2:1-4:1 we can achieve rates closer to the TCR than JPEG-LS. Finally, Figures 3.13(a)-3.13(d) and 3.14(a)-3.14(d) are presented for a visual comparison between the proposed scheme and the non-rate controlled JPEG-LS , for two typical wound and rash images. Figure 3.13(a) is the original wound image and Figure 3.13(b) is the blown up smooth part of the wound. Figure 3.14(a) and 3.14(b) correspond to the original and to the blown up smooth part of the rash image. By comparing Figures 3.13(c) and 3.13(d) to Figure 3.13(b), we can see that the proposed algorithm retains smooth texture better even in wound images for the same bit rates as the standard. This happens due to the HVS based information loss scheme used. The same point is shown by comparing Figures 3.14(c) and 3.14(d) to Figure 3.14(b) for rash images. In particular, it can be seen that JPEG-LS has induced artifacts in Figures 3.13(c) and 3.14(c) represented as lines in the smooth regions, whereas our scheme (shown in Figures 3.13(d) and 3.14(d)) has

preserved the texture smoothness better, thus providing reconstructed images closer to the original image . In order to compare fairly our technique with *the non-rate controlled JPEG-LS,* we used the rate produced by the standard as the target rate in our scheme for the visual part of the experiments. Furthermore, the starting points for our algorithm are the ones shown in Tables 3.10(a) and 3.10(b). From the visual comparison experiments, we can finally infer that the proposed scheme performs better in the medical imaging context when both the requirements for high compression rates (high NEAR values) and for retaining smooth texture are critical.

Table 3.10(a) Rate Control Experimental Results for Figure 3.13(a) (Initial L, M, H = 1,5,5)

Target Compression Rates	JPEG-LS Closest Compression Ratio	Proposed Algorithm Compression Ratio
2:1	1.97:1	2.03:1
3:1	2.917:1	3.05:1
4:1	3.774:1	3.83:1

Table 3.10(b) Rate Control Experimental Results for Figure 3.14(a) (Initial L, M, H = 2,3,6)

Target Compression Rates	JPEG-LS Closest Compression Ratio	Proposed Algorithm Compression Ratio
2:1	1.908:1	2.090:1
3:1	2.918:1	3.013:1
4:1	3.706:1	4.032:1

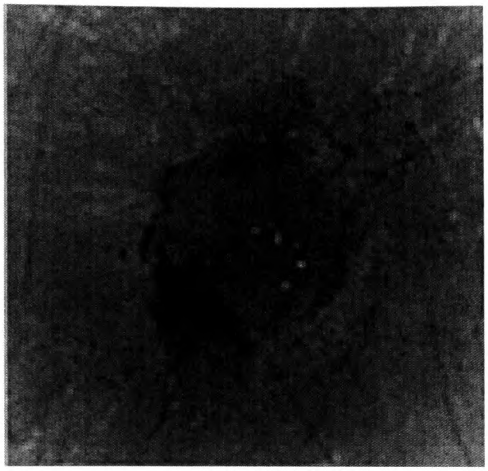

Figure 3.13(a): Original wound image

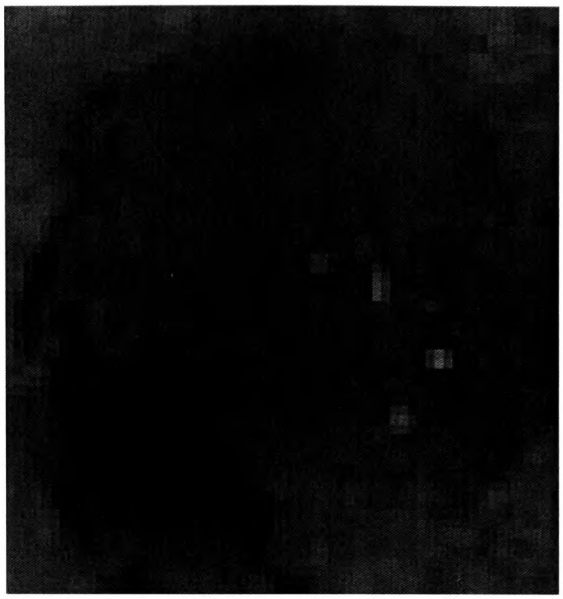

Figure 3.13(b): Blown up part of original wound image

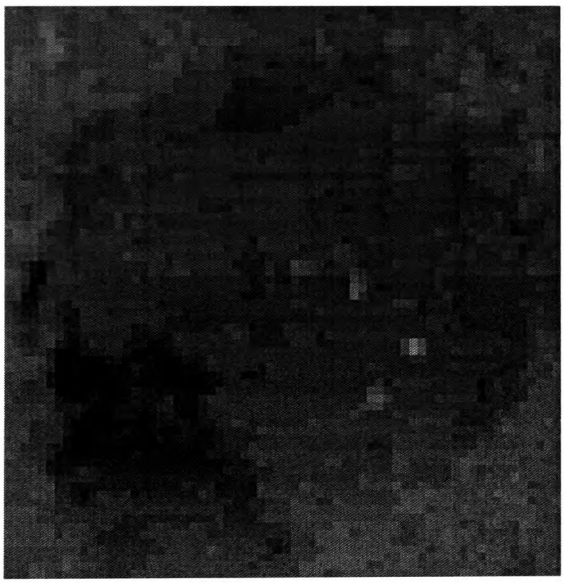

Figure 3.13(c): Blown up part of reconstructed wound image by JPEG-LS with NEAR=7

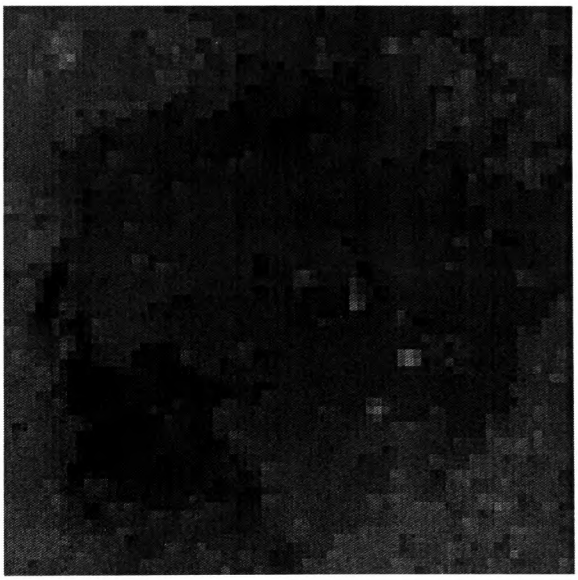

Figure 3.13(d): Reconstructed wound image by the proposed scheme. (L,M,H) = (1,5,5) , TCR= Rate produced by JPEG-LS with NEAR=7

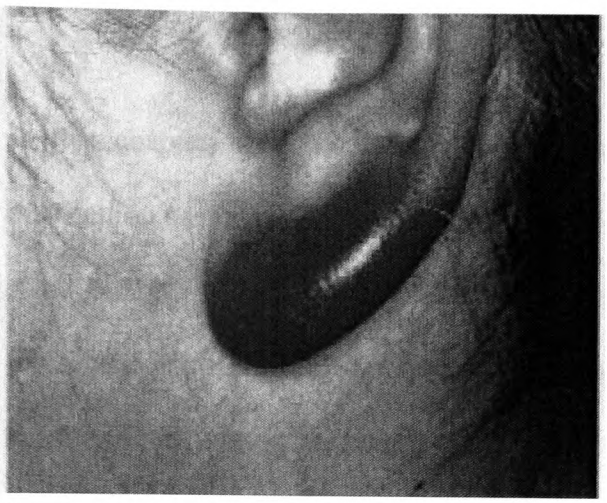

Figure 3.14(a): Original rash image

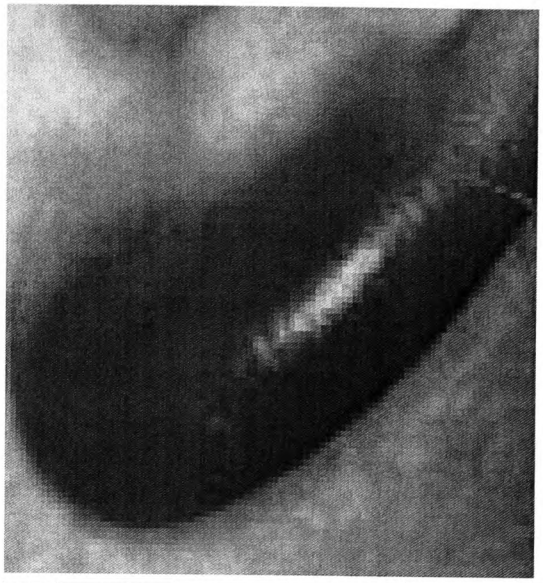

Figure 3.14(b): Blown up part of the original rash image

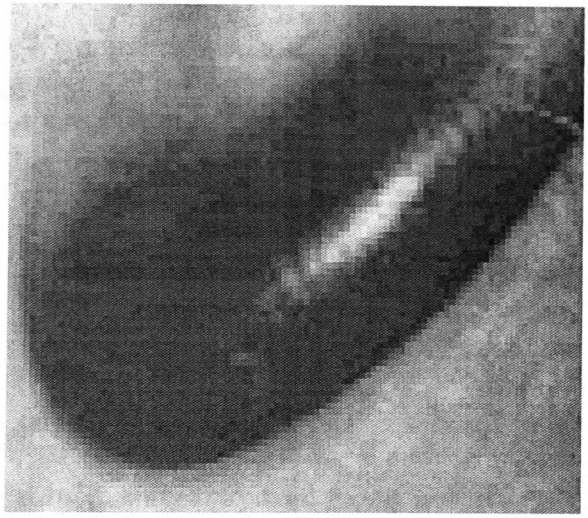

Figure 3.14 (c) : Blown up part of the rash image, reconstructed by JPEG-LS with NEAR=6

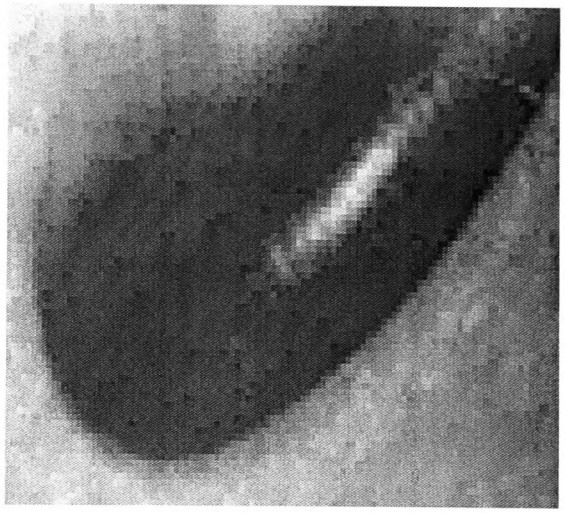

Figure 3.14(d): Blown up part of the rash image reconstructed by the proposed scheme. (L,M,H) = (2,3,6) , TCR= Rate produced by JPEG-LS with NEAR=6

3.5 Conclusions

In this chapter, we initially presented a prediction driven multilevel information loss distribution scheme in order to optimize the visual quality of the JPEG-LS standard for the same bit rates. The proposed information loss distribution scheme was based on HVS principles and achieved better visual quality and higher compression rates than the standard. It was also very competitive even in terms of PSNR performance as compared to JPEG-LS for the same compression rates as the standard, provided a suitable triplet of information loss parameters was chosen. The purpose of the multilevel information loss distribution was to resolve the conflict in visual terms of assigning constant information loss to all textures in an image regardless of smoothness characteristics. Subsequently, we used the multilevel information loss distribution in order *to add rate control* in JPEG-LS. We presented two algorithms to achieve this. The first algorithm proposed was shown to be more effective than JPEG-LS in achieving rates close to the user defined compression rates. The negative impact of the addition of the rate control process was measured to be in the range 2-3db. This impact was expected since any rate control algorithm has to go through adjustments of the quantization parameters (NEAR values) in order to achieve the target rates, whereas the standard achieves them through natural compression. We subsequently improved the rate control algorithm design by using a more adaptive scheme for the change of the information loss parameters (NEAR values) and by using *predictive* instead of *online* measures to control the bit rate. The second algorithm proposed was shown to be more effective than JPEG-LS in producing bit rates closer to user defined target compression rates . It was also shown to be more efficient than the standard in retaining smooth texture closer to the original image for the same bit rates. Finally, we examined the potential usefulness of the second algorithm proposed in the context of

applying rate control in JPEG-LS for medical images. The quality requirements for medical imaging are more stringent compared to the requirements of digital photography since we can not afford to lose too much information on edges. We showed that our algorithm is retaining texture smoothness better than JPEG-LS even for medical images for the same bit rates and is also more effective than the standard in achieving target rates in the range 2.1 to 3:1. For this specific type of images, our second algorithm performs best in visual terms when both the requirements for high compression rates and for smooth texture retaining are critical. Potential uses in medicine could include tracking the progress of wound/rash healing.

CHAPTER 4 - LOW COST, PIXEL TREND BASED IMPROVEMENTS OF COMPRESSION RATES AND QUALITY IN IMAGE/VIDEO CODING

4.1 Introduction

Pixel trend estimation is very important in improving compression rates and quality in the context of image and video coding. In the case of MPEG-4 for example, pixel trend variations in boundary macroblocks can be efficiently utilised to improve compression rates for boundary macroblocks for the same quality as the standard. In the case of diagonal edge detection in JPEG-LS, the Mean Square Error (MSE) can be reduced for the same bit rates as the standard, if pixel correlation is appropriately exploited. This chapter will initially present *two low cost padding techniques* for boundary macroblocks that are used to improve the coding efficiency of arbitrary shaped objects in MPEG-4 for the same quality as the standard. Subsequently, two *low cost edge detection schemes* will be proposed for JPEG-LS which also cater for the accurate prediction of *diagonal edges* along with horizontal and vertical ones. It will be shown that the proposed edge detection schemes outperform the standard in MSE terms for the same bit rates.

4.2 Overview of the MPEG-4 standard

MPEG-4 [9-10] is the first audio-visual standard that represents a scene as a composition of *audio-visual objects* (AVOs) with a certain spatial and temporal behavior. Consequently, an image frame is represented as a composition of AVOs with a number of intrinsic properties which includes shape, motion and texture [70]. The separate encoding of these individual AVOs is a powerful tool that can remove a number of limitations

inherent to other systems and standards such as MPEG-1 and MPEG2. First, it enables interaction with meaningful objects within the same scene. It also enables the re-use of data if the possibility exists to separately store and access objects, rather than frames. It gives the user the ability to create his/her own content by combining several of these stored objects in the same or different places. Excluding the audio component, an image frame is represented in MPEG-4 as a composition of *video objects* (VOs). Each video object is divided into a number of *object layers,* to allow for spatial and temporal scalability. For example, in a scene comprising of a person and some furniture, the person and the furniture can be defined as two separate object layers. Under each object layer there is an ordered sequence of snapshots in time, which are referred to as *video object planes* (VOPs). In the previous example, the person taken as a separate entity from the rest of the frame, in a sequence of frames, forms a VOP. These VOPs are the basic unit where MPEG-4 video compression is applied. A VOP is essentially a rectangular area that completely contains a video object but with the minimum number of macro-blocks contained within it.

The macro-blocks within a VOP are categorized into three groups and are treated differently according to the group they belong to. Those that belong to the interior of the video object are motion-compensated and predicted in a way identical to that of MPEG-2 and h26x (x=1,2,3). Subsequently, the prediction errors along with motion information are encoded. Those macro-blocks that are completely outside the video object but belong to the VOP are not coded as they belong to a different object or the background. A *special shape adaptive motion compensation and prediction scheme* is used for coding the macro-blocks that straddle the boundaries of an object. Figure 4.1 shows an example of the macroblock classification scheme used in MPEG-4.

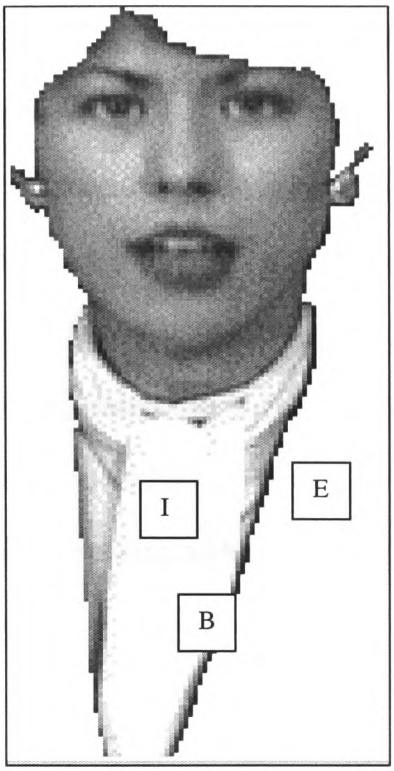

Figure 4.1: Macroblock classification scheme in a VOP. I denotes internal macroblocks, E external macroblocks, B boundary macroblocks

4.3 Reference VOP Padding

In MPEG-4's object based motion compensation / prediction scheme, after the reference VOP has been identified, a three-stage process pads the pixels that are outside the VO. The boundary macro-blocks are first padded using *horizontal repetitive padding* [hor_pad in Figure 4.2]. Under this scheme, each sample at the boundary of the VO is replicated horizontally to the left and/or to the right direction in order to fill the transparent region outside the VO. If there are two boundary sample values for filling a sample outside of a VO, the two boundary samples are averaged.

The remaining unfilled transparent horizontal samples are padded using vertical repetitive padding [hv_pad in Figure 4.2], which is essentially the horizontal padding technique, performed in a vertical direction

After all the boundary macroblocks have been padded, the exterior macroblocks immediately next to them are filled by replicating the samples at the border of the boundary macroblock (Extended Padding [Epad in Figure 4.2]) that has the highest priority number The remaining exterior macroblocks which are not located next to any boundary macroblock are filled with the value 128.

Figure 4.2 depicts the MPEG-4 padding technique, while Figure 4.3 depicts the priority of boundary macroblocks.

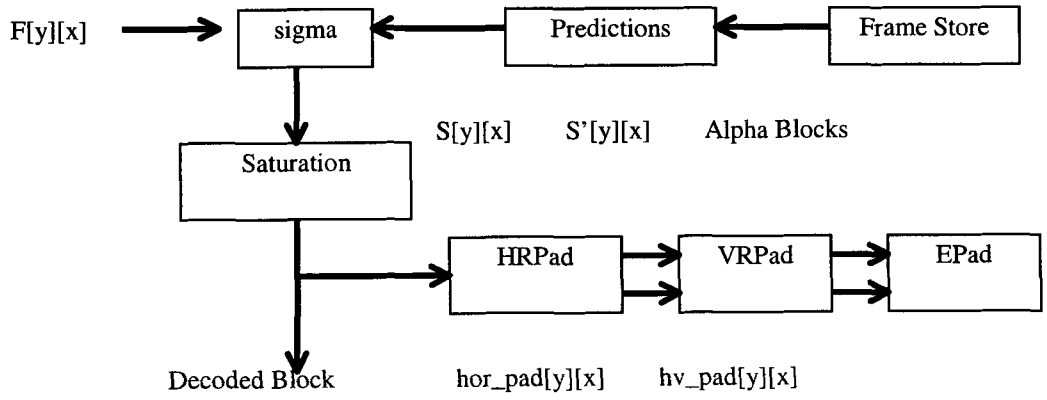

Figure 4.2: MPEG-4 padding technique

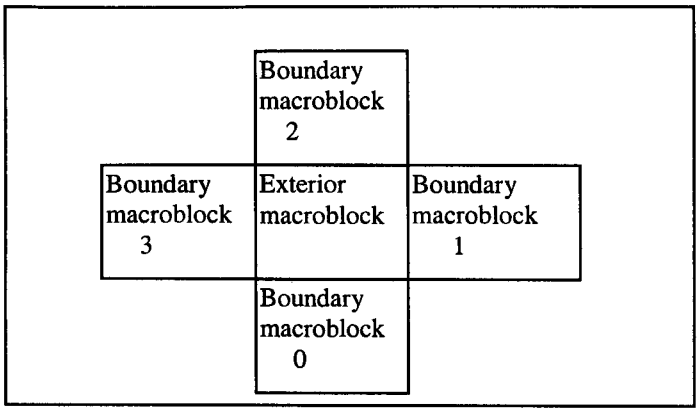

Figure 4.3: Priority of boundary macroblocks

The padded VOP is then used as a reference for motion compensation and prediction of arbitrary shaped boundary macroblocks of the VO to be encoded. During this process the exterior pixels (pixels that are outside the video object) of the boundary macro-block to be encoded are made inactive. After the error blocks are calculated, they are transformed into the frequency domain with a special *shape adaptive discrete cosine transform* (SADCT) [11,13]. This transformation only codes the pixels belonging to the VO in the error blocks, thus reducing the actual amount of bits which would be needed to code the DCT coefficients. SADCT essentially aids in increasing the quality for the same bit rate at a slightly increased implementation complexity.

4.4 Drawback of the MPEG-4 Padding technique and Proposed Linear Extrapolated Padding Technique (LEP)

The main drawback of the above padding technique lies in the fact that it does not make use of the trend of pixel value variation often present near object boundaries for the

boundary macroblock to be encoded. Extensive experiments carried out by us indicated that within arbitrary shaped boundary macro-blocks certain trends exist, with respect to pixel value variation. Thus, replicating the external pixel values of the reference VO without taking this fact into account is not optimal.

Initially, it would be helpful to identify *the geometric conditions* under which improvements of the MPEG-4 padding technique for boundary macroblocks would be possible. Figures 4.4 and 4.5 aid in clarifying these geometric conditions.

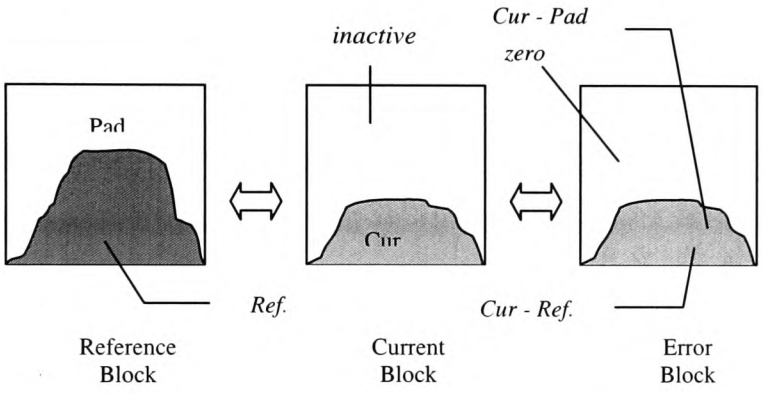

Figure 4.4: Error block formation in boundary blocks when the shape of the block to be encoded is inside the shape of the reference block

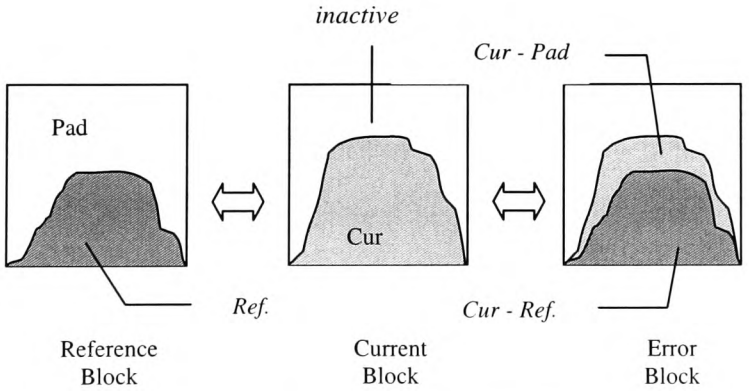

Figure 4.5: Error block formation in boundary blocks when the shape of the block to be encoded encompasses the shape of the boundary block

From Figure 4.4 it can be inferred that only the pixels inside the shape of the boundary macroblock to be encoded are considered active in the motion compensation process. Under this geometrical condition, it can be seen that the padding values of the reference macroblock have no effect on the produced error macroblock. Thus, the coding efficiency of such macroblocks *can not be improved by modifying the padding technique.*

From Figure 4.5 it can be inferred that some of the produced errors to be encoded *will depend on the padding pixel values* (*Cur - Pad area*). This implies that if the padding scheme of the reference macroblock is modified appropriately, potential coding gains could be achieved for the same quality.

As a simple solution to the geometrical condition shown in Figure 4.5, we propose the use of a single iteration of a row-based *linear extrapolation padding* [LEP] step, to predict those exterior pixels adjacent to the boundary pixels of the reference VO. These projected pixel values would then be predicted by the proposed linear extrapolation scheme as follows:

Assume that 'n' ($1 < n < N$) consecutive pixels in a row, immediately either to the left or to the right of a projected pixel, are within the video object. Let these 'n' pixel values be represented by P_n. Let X_n represent the column numbers of these pixels relative to the column number of the projected pixel. We use a linear equation of the form $P_n = A \times X_n + B$ to fit all the internal pixel values denoted by P_n, in least squared error terms, as follows:

Prediction error for a single pixel P_i is given by:

$$E_i = P_i - (AX_i + B) \qquad (4.1)$$

For least, total squared error,

$$\frac{\partial}{\partial B}\sum_{i=1}^{N}[P_i-(AX_i+B)]^2=0 \qquad (4.2)$$

and

$$\frac{\partial}{\partial A}\sum_{i=1}^{N}[P_i-(AX_i+B)]^2=0 \qquad (4.3)$$

By simplifying equation 4.2 and equation 4.3 above, we arrive at the following matrix equation.

$$\begin{bmatrix} N & \sum_{i=1}^{N} X_i \\ \sum_{i=1}^{N} X_i & \sum_{i=1}^{N} X_i^2 \end{bmatrix}\begin{bmatrix} B \\ A \end{bmatrix}=\begin{bmatrix} \sum_{i=1}^{N} P_i \\ \sum_{i=1}^{N} X_i P_i \end{bmatrix} \qquad (4.4)$$

After constants A and B are found from the matrix equation 4.4, equation $P_i = A\times X_i + B$ is used to do the extrapolation and find the projected pixel value. Pixel A in Figure 4.6, illustrates a projected pixel that would be found following a similar procedure. In this way all the projected pixels will be determined by the variation trend of those interior pixel values of the VO, close to the boundary.

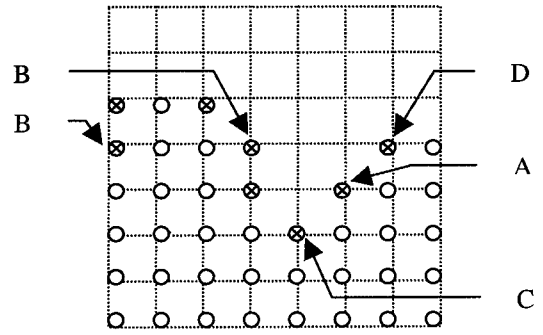

Figure 4.6 : ◯Interior pixels, ⊗ Projected pixels

However, projected pixels that satisfy certain specific neighbourhood conditions need special attention as described below.

- In cases where P_n are bounded by two projected pixels [e.g., pixels denoted by B in Figure 4.6], both projected pixels are determined using the same linear equation.
- If a projected pixel is flanked by interior pixels both on the left and right [e.g., pixel C of Figure 4.6], the above process is performed in both directions and the average of the two resulting extrapolated pixel values are taken as the value of the projected pixel.
- In cases where $n = 1$ [e.g., pixel D of Figure 4.6], the projected pixel value is taken as equal to the single interior pixel value.

After all the projected pixels are padded, the MPEG-4 horizontal and vertical padding steps are performed to pad the rest of the exterior pixels within the macro-block. Note that the projected pixels that were padded using linear extrapolation now act as the new boundary pixels. After all boundary macro-blocks are padded similarly, extended padding is used to pad the remaining exterior macro-blocks within the VOP bounding rectangle.

Figure 4.7 shows the proposed modification to the MPEG-4 padding procedure in schematic form.

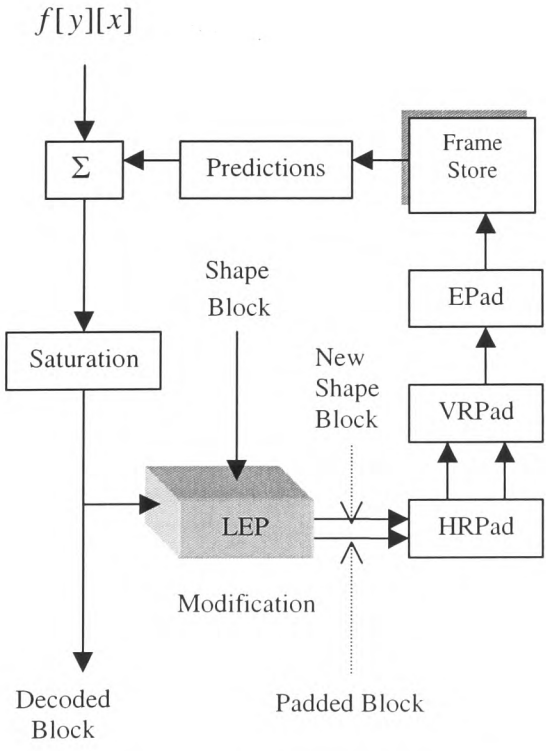

Figure 4.7: Modified padding

4.5 Experimental Results for LEP

Experiments were carried out to calculate the coding gains obtainable with the proposed technique. The test results taken at various temporal locations for five test sequences are shown in Table 4.1. The *Extended Compression Ratio* (ECR) represents the percentage improvement obtainable over MPEG-4 for coding all boundary blocks of video objects in the frame denoted by a higher index, taking the frame with the lower index as the reference. ECR% is defined as follows:

$$ECR=\frac{Bou\_bits_{mpeg4}-Bou\_bits_{proposed}}{Bou\_bits_{mpeg4}}\times 100$$

Results in Table 4.1 clearly indicate that the proposed modification enhances the performance of the MPEG-4 padding technique.

Sequence Nos.	ECR% in Comparison with MPEG-4				
	Miss Ameriica	Salesmen	Car phone	Tennis	Susie
000-001	6.8	4.1	2.1	6.6	3.6
001-002	5.6	4.7	1.8	3.6	2.0
002-003	6.1	3.2	2.8	3.4	1.4
003-004	5.8	3.8	2.3	6.9	2.4
010-011	5.5	1.0	3.1	5.8	4.6
011-012	3.8	3.6	3.6	6.6	4.5
012-013	6.4	5.0	3.5	6.6	4.1
013-014	6.5	2.0	2.5	4.1	4.2
020-021	6.9	6.2	3.9	4.9	2.7
021-022	5.6	1.8	3.1	5.1	2.1
022-023	6.0	1.1	3.5	5.5	3.5
023-024	4.8	4.6	2.8	3.7	4.4
030-031	4.9	4.6	2.6	3.5	1.2
031-032	6.2	5.9	1.9	6.1	1.8
032-033	6.8	2.2	1.1	6.6	1.6
033-034	6.6	2.8	2.7	6.2	3.9
Average ECR% improvement	5.8	3.7	2.7	5.3	3

Table 4.1: Experimental Results

Further experiments indicated that with linear extrapolation, the optimal results in terms of compression gain, are obtained when the number of iterations is limited to one. This is justifiable as further padding steps, which follow a linear variation towards the exterior, may result in larger prediction errors for pixels further away from the boundary.

Note that this additional LEP stage would not modify the prediction error blocks of arbitrary shaped current blocks that find predictors which are completely enclosed within the reference VO. For constant luminance boundary blocks of the reference VO, the additional LEP step will result in an identical padding, to that of MPEG-4. The coding gains are achieved in boundary blocks where the shape of the current block extends beyond the reference VO shape, thus making the padded pixel values active, in the calculation of the prediction error.

Experiments were also performed to check the feasibility of using the proposed technique in the vertical direction as well, i.e. before MPEG-4, vertical padding is done. The results indicated that the extra coding gains obtainable are insignificant and are not worthy of the added complexity.

4.6 Extrapolated Average Padding

Further experiments performed using the MPEG-4 padding technique and the proposed LEP technique indicated that they did not perform well in encoding arbitrary shaped MPEG-4 video objects that have been severely distorted (or have changed shape severely) between consecutive video frames.

Figure 4.8 illustrates the reason for this failure.

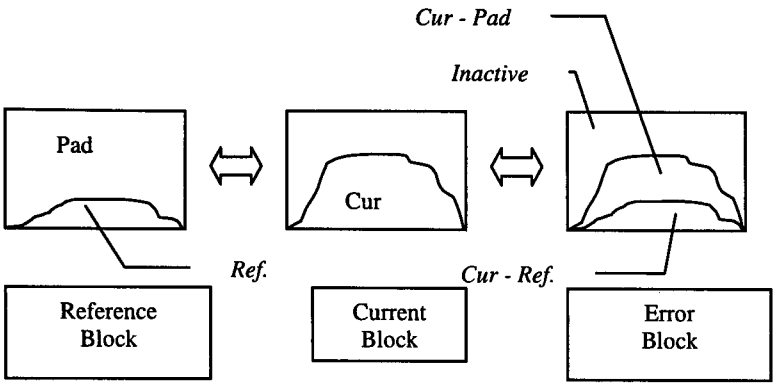

Figure 4.8: Error block formation in severely distorted boundary blocks

In the case of the MPEG-4 padding technique, the area *(Cur - Pad)* consists of errors which are the difference between the corresponding boundary pixel values of the reference VOP (*Pad*) and the interior pixels of the boundary macro-block (*Cur*) to be encoded.

In the case of the Linear Extrapolated Padding Technique (LEP) , the area *(Cur - Pad)* consists of errors which are the difference between the corresponding extrapolated boundary pixel values of the reference VOP (*Pad*) and the interior pixels of the boundary macro-block (*Cur*) to be encoded.

In both cases, if the non-overlapping area is large, the boundary pixel values of the reference VOP (or the linear extrapolated boundary pixel values in the LEP technique) may not be a good approximation for the interior pixels of the arbitrarily shaped boundary macroblock to be encoded. This is mostly evident for interior pixels that that are further away from the shape boundary in the current macroblock to be encoded. Thus, the methods discussed above (i.e. MPEG-4 method and the LEP technique) would fail to produce lower magnitude error blocks.

As a solution to this, we propose an Extrapolated Average Padding (EAP) technique for severely distorted reference VOPs. Here, the horizontal and vertical repetitive padding steps discussed in Section 4.3 are replaced by the EAP technique as illustrated in Figure 4.9.

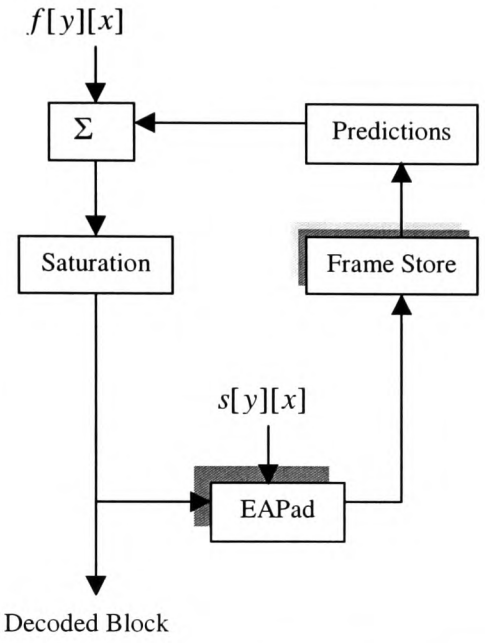

Figure 4.9: Extrapolated Average Padding

A mathematical approach to the padding technique is described as follows. Firstly, the arithmetic mean value *A* of all the pixels *p (i,j)* of the boundary macro-block situated in the interior of the reference VOP is calculated using the following formula:

$$A = \frac{1}{N} \sum_{(i,j) \in L} p(i, j) \qquad (4.6)$$

where, $(1 \leq i, j \leq 8)$, N is the number of pixels situated within the reference VOP. The division by N is done by rounding to the nearest integer. The next step is to assign A to each block pixel situated outside the object region L, i.e.

$$p(i, j) = A \quad for\ all \quad (i, j) \notin L \qquad (4.7)$$

After the boundary macro-blocks are padded according to the above technique,

Extended Padding (see Section 4.3) is used to pad the exterior macro-blocks. Any exterior macro-block that does not get padded at the end of this stage would be padded using the value 128.

4.7 A Hybrid Padding Scheme combining LEP and EAP

Experimental investigations showed that the LEP technique works best when the matching shapes are close, thus performing well, especially in sequences where objects change shape at a slower pace. In contrast, the EAP technique was found to perform best when the shape changes are large. Most video sequences fall into the first category. However, the importance of dealing with large shape mismatches between consecutive VOPs cannot be ignored, especially due to the fact that most video objects would consist of both types. Thus, a hybrid approach that identifies the areas in an object that are 'distorted' and 'undistorted' and apply the appropriate technique to pad the reference frame boundary blocks of such areas, would increase the compression efficiency. Due to the importance of keeping this classification process computationally inexpensive, we use a simple criteria described below, for this purpose.

Firstly, the LEP technique is used to pad the reference frame VOP. Motion compensation for all the arbitrary shaped boundary blocks in the current frame VOP is now performed taking this padded VOP as the reference. Subsequently, for each matching pair a measure of mismatch is calculated by averaging the three largest 'mismatch distances', *H1*, *H2* and *H3*. (see Figure 4.10). If this average is greater than a threshold, T (2.0 for our experiments) a decision is made to re-pad the pixels that are within the best matching block, but are outside the shape of the reference video object, using the EAP technique. i.e.,

If

$$H = \left(\frac{H1 + H2 + H3}{3} \right) > T \quad use \quad EAP \quad else \quad LEP$$

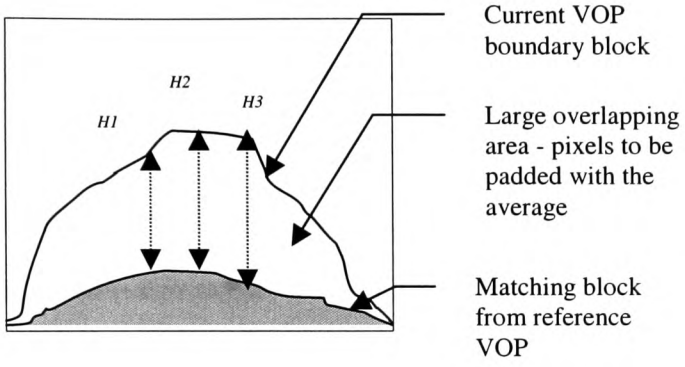

Figure 4.10: Matching geometry under which EAP would be more efficient than LEP.

The prediction errors are calculated based on these new padding values. For the remaining blocks the prediction values are calculated using the original padding values [i.e. padded using LEP] of the reference frame VOP.

4.8 Experimental results and analysis of the hybrid scheme

Experiments were carried out to calculate the coding gains obtainable with the proposed hybrid technique. The test results taken at various temporal locations for seven, standard test sequences are shown in Table 4.2.

Results in Table 4.2 indicate that the proposed technique produces better compression results as compared to the standard MPEG-4 padding technique. Extra compression gains of up to 9% over the MPEG-4 padding technique have been obtained for coding boundary blocks of video objects in such sequences.

Results show that the proposed technique also improves the performance of the LEP technique applied as a stand-alone system as described in our previous work in [71] particularly in sequences such as 'football', 'tennis' and 'parachute'. These sequences contain objects that are distorted severely in certain parts of the objects. Thus, it could be deduced that the proposed scheme adequately identifies, in a low complexity framework, the boundary blocks that are 'distorted' and uses the EAP technique in padding the appropriate reference VOP blocks. Thus, this technique is best used in coding video sequences with objects that are severely distorted.

Sequence Nos.	ECR% in Comparison with MPEG-4						
	Miss Ame.	Salesmen	Car phone	Tennis	Susie	Football	Parachute
000-001	6.6	3.7	2.5	6.8	3.6	4.1	7.7
001-002	5.4	4.8	1.1	3.5	2.1	5.0	7.6
002-003	6.2	3.2	2.6	3.4	1.2	6.7	6.9
003-004	5.9	3.8	2.7	6.7	2.4	4.1	5.1
010-011	5.7	1.1	3.5	5.8	4.6	6.6	1.3
011-012	3.6	3.8	3.7	6.9	4.4	7.2	3.8
012-013	6.7	5.0	3.5	6.9	4.1	3.1	3.2
013-014	6.2	2.1	2.6	4.8	4.6	2.0	2.9
020-021	7.1	6.2	3.7	4.9	3.0	4.2	4.4
021-022	5.8	1.8	3.9	5.2	1.9	5.7	5.6
022-023	6.3	1.0	3.5	5.1	3.5	5.6	5.9
023-024	4.9	4.6	2.7	3.9	4.4	5.9	6.1
030-031	5.0	4.6	2.9	3.7	1.1	7.6	9.1
031-032	6.0	5.9	2.2	6.3	1.8	8.2	8.7
032-033	6.5	2.3	1.9	7.1	2.1	8.7	8.4
033-034	6.6	2.8	2.9	6.7	3.9	8.2	7.3
Average ECR% improvement	5.9	3.7	2.8	5.4	3	5.8	5.8

Table 4.2. Experimental Results

4.9 The edge detection scheme of JPEG-LS and its assessment

Although the predictive template was shown in the introduction section of Chapter 3, it will be shown again in this chapter (Figure 4.11) for clarity reasons. In fact *the*

geographical location of the pixel values inside the template is critical to the proposed algorithms, so its re-use is further justified.

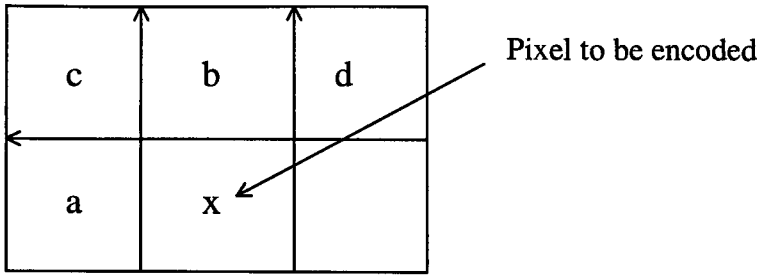

Figure 4.11: Predictive pattern in JPEG-LS

From the standard document of JPEG-LS it can be seen that predictive value of the pixel to be encoded is calculated according to the following pseudo-code:

```
if (c>= max(a, b)) P = min(a, b);
else{
if (c <= min(a, b)) P = max(a, b);                    (4.8)
            else P = a+b-c;
 }
```

where a,b,c are pixels in the template and *max(a, b)* and *min(a, b)* stands for the maximum value and the minimum value among the two pixels, *a* and *b*, in the predictive template. To assess the existing prediction scheme in JPEG-LS, further analysis of the above pseudo-codes can be made to reveal the following facts:

- An edge would be detected among the three pixels when either $c >= max(a, b)$ or $c <= min(a, b)$ is satisfied. Whether the edge is horizontal or vertical depends on which pixel is the maximum or minimum value between *a* and *b*. When $c >= max(a, b)$ is satisfied,

as an example, *max(a, b)=a* give us a vertical edge and *max(a, b)=b* a horizontal edge. Similarly, the condition, *c <= min(a, b)*, would give us a vertical edge if *min(a, b)=a* and a horizontal edge if *min(a,b)=b*. Figures 4.12(a) and 4.12(b) show such an edge detection process. From the geographical arrangement shown in Figures 4.12(a) and 4.12(b), it can be seen that a logical selection of the predictive value would be the pixel, which is not on the detected edge.

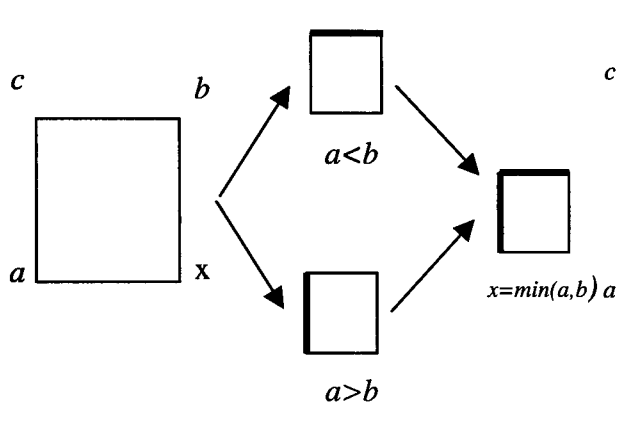

Figure 4.12(a): Edge detection for c>=max(a,b)

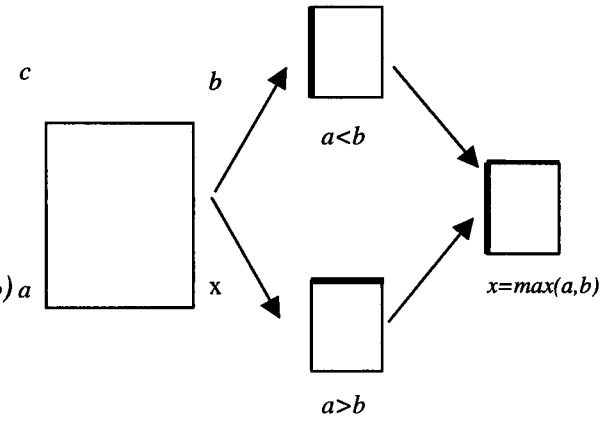

Figure4.12(b):Edge detection for c<=min(a,b)

- All other cases are represented by the condition: *min(a, b) < c < max(a, b)*. Under this condition, it is difficult to construct a predictive value to cover all possibilities in the local texture. This is because there is no clear justification to determine whether there is an edge or not. Even if there is an edge, it is difficult to classify appropriately. This is due to the fact that any prediction has to be dependent on the unknown pixel value *x*. For instance, a horizontal edge may be detected only when *x* is found to be closer to *a*, or a vertical edge be detected if *x* is closer to *b*. In fact, the choice of *a+b-c* is an excellent balance among all possible situations.
- From the above analysis, it can be verified that the prediction scheme adopted in JPEG-LS only considers the detection of a horizontal edge or a vertical edge among the

predictive template to produce a predictive value. This is logical in the sense that the variety of intensity values around a neighbourhood area can always be described by the two types of edges, when the viewing angle is limited to the local predictive template. In other words, combinations of many vertical and horizontal edges can produce a line with arbitrary shape or edges in any image. However, what matters here is whether the description by the two edges will be accurate enough to minimise the predictive errors. In cases where a diagonal edge exists inside the predictive template, it can be expected that the errors produced can be unnecessarily high.

4.10 Two algorithms for low cost diagonal edge detection in JPEG-LS

Therefore, to further improve the prediction scheme, one of the possibilities is to consider the diagonal edge detection among the three pixels inside the predictive template. Due to the fact that the diagonal distance between a and b is larger than any other ones inside the template, and the diagonal edge detected can also be interpreted as either a vertical or a horizontal edge in most cases, it can be anticipated that the occurrence of a true diagonal edge would be much less frequent compared with that of vertical and horizontal edges. Consequently, the possible improvement would be dependent on the number of cases where a true diagonal edge does exist inside the local areas of the input image. Essentially, the possibility of improvement can be explored along two directions: (i) to accurately detect those true diagonal edges; (ii) to correctly construct the predictive value, based on the diagonal edge detected.

In order to detect a diagonal edge, only two possibilities exists among the three pixels, a, b and c, which are $45°$ and $135°$. It can also be assumed that there is no edge with one pixel wide inside the predictive pattern, or if any, such edge can be ignored by our

scheme since it is hardly possible to produce any meaningful prediction out of this type of edge.

Considering all the possibilities in the light of the existing prediction scheme designed in JPEG-LS, a detailed analysis of the diagonal edge detection and prediction can be carried out for each of the predictive contexts given in the pseudo-codes, i.e., *(i)* $min(a, b) \leq c \leq max(a, b)$; *(ii)* $c \geq max(a, b)$; and *(iii)* $c \leq min(a, b)$.

Firstly, when the condition $min(a, b) \leq c \leq max(a, b)$ is satisfied, it can be seen that any prediction for the pixel value x can only be determined by the unknown pixel x. This is reflected in the Figure 4.13(b). If x is close to a we would get a horizontal edge, if x is close to b a vertical edge and if x is close to c a diagonal edge, respectively. Hence, it is unlikely to have any further improvement with this predictive context without jeopardising the good predictive results already achieved by JPEG-LS.

Secondly, with the condition $c \geq max(a, b)$, it is not difficult to see that we would get the case described in Figure 4.13(a), if there exists one diagonal edge. The principle is that we need to detect the diagonal edge with the best possible accuracy from the information given by the available pixels at both encoding and decoding ends, not by the unknown pixel x. Furthermore, since $c \geq max(a, b)$ we could anticipate that the pixel value c although it could be used for detecting diagonal edges, *it would not necessarily influence* the predictive value of x since the distance between x and a, b is expected to be smaller than the distance between x and c (refer to the predictive template in Figure 4.11). We also expect that x would be more correlated to the pixel a than to the pixel b since x and a are on the current scan-line while b is on the previous scan-line. So in both the proposed schemes we initially test for horizontal edges, followed by diagonal edges, followed by vertical edges. By testing through *threshold bounded gradients* for the existence of diagonal edges before resorting to vertical edges, we could potentially reduce the

prediction error. If a diagonal edge is detected, this is indication that the pixel value of d in the template *tends to be smaller* than pixels a and b and could be potentially used for compensating for the large error that a predicted value such as pixel b would produce. Following this reasoning, *a weighted predictive value* of the pixels b and d would be more appropriate. This is illustrated in Figure 4.14(a). The analysis for the condition $c \leq \min(a,b)$ is exactly the same. This is illustrated in Figure 4.14(b).

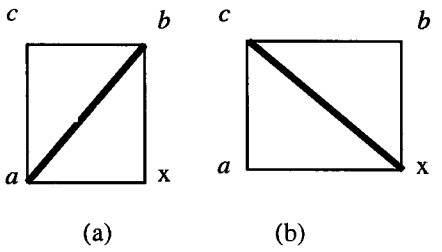

Figure 4.13: Possible forms of diagonal edges

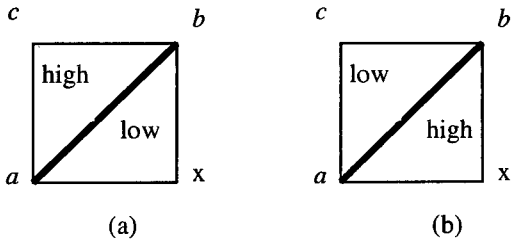

Figure 4.14: Possible forms of pixel intensities in diagonal edges

Based on the above observations we design our first algorithm as follows:

4.10.1 Weight based diagonal edge detection

We propose that the predictive value of x in the case of a diagonal edge being detected can be estimated based on a weighted average of the pixels b and d using the following equation:

$$P = \frac{a1*d + a2*b}{a1+a2} \qquad a1, a2 > 1 \tag{4.9}$$

where *a1,a2* are weights relative to the pixels *b* and *d*. Equation (4.9) would bring the predictive value down to be closer to the unknown pixel *x*.

So the edge detection scheme that JPEG-LS uses and is described in equation (4.8) can be enhanced for also predicting diagonal edges as follows:

if (c>= max(a, b))

{

if (a<=b) P = a;

else if ((b-d)>=T1 and (c-a)>=T2)

$P=\frac{a1*d+a2*b}{a1+a2}$ *(diagonal edge detection)* (4.10)

else P = b;

}

else{

if (c <= min(a, b))

{

if (a>=b) P = a;

else if ((d-b)>=T1 and (a-c)>=T2)

$P=\frac{a1*d+a2*b}{a1+a2}$ *(diagonal edge detection)*

else P = b;}

else P=a+b-c; (condition min(a, b)≤c≤max(a, b);)

}

where a, b, c, d are pixels on the predictive template (Figure 4.11) and P is the predictive value of the pixel to be encoded (*x* on the template). Also *T1,T2* are empirically defined thresholds used to detect diagonal edges based on pixel gradients. The reason for using only two thresholds in our prediction scheme is that we also want our scheme to be of low computational cost. A more elaborate treatment of detecting diagonal edges using more thresholds could also be used for minimising the predictive error[87].

It's worth noticing that the proposed edge detection scheme performs better if the weights *a1,a2* in equation (4.9) are not equal. In fact it performs best if a2>a1. This can be expected since the pixel *x* on the predictive template is more correlated to pixel *b* than to pixel *d*.

4.10.2 Including pixel a in the prediction

In this algorithm, we intend to exploit the effect of the pixel *a* (see template in Figure 4.11) in the determination of the predictive value of pixel x in the case of a diagonal edge being detected. The proposed algorithm, like the one described in 4.10.1, also pertains to the cases of Figures 4.14(a) and 4.14(b). The reasoning here is that since pixel a *is the most correlated* to the pixel x inside the predictive template (see Figure 4.10), it could potentially improve the predictive value of pixel x in the presence of diagonal edges. So instead of predicting using only a weighted average of pixels b and d in the template, we can include pixel a in the prediction as follows:

```
if (c>= max(a, b))
{
if (a<=b) P = a;
```

else if((b-d)>=T1 and (c-a)>=T2)

$$P=\frac{a+d+b}{3} \quad \textit{(diagonal edge detection)} \tag{4.11}$$

else P = b;

}

else{

if(c <= min(a, b))

{

if(a>=b) P = a;

else if((d-b)>=T1 and (a-c)>=T2)

$$P=\frac{a+d+b}{3} \quad \textit{(diagonal edge detection)}$$

else P = b;

}

else P=a+b-c; (condition min(a, b)≤c≤max(a, b);)

}

where a, b, c, d are pixels on the predictive template (Figure 4.11) and P is the predictive value of the pixel to be encoded (*x* on the template). Also *T1,T2* are empirically defined thresholds used to detect diagonal edges based on pixel gradients. The reason for using only two thresholds is that we intend our algorithm to be of low computational cost.

4.10.3 Experiments for the two proposed algorithms

To test the proposed algorithms, we implemented both the prediction schemes and run the programmes on a group of four commonly used testing images: *Lena, Boat, Camera,*

Bridge and *Clown*. In order to ensure a fair comparison with the existing JPEG-LS scheme, we assessed the performance of the proposed prediction schemes in two measurements: (i) the mean-square-error between each pixel to be encoded and its predictive value; (ii) the compression ratio. The first measurement is designed to assess the accuracy of the proposed prediction schemes benchmarked by the existing state of the art prediction adopted in JPEG-LS, the latest JPEG standard for lossless/near lossless image compression. The second measurement is designed to see if the proposed schemes have any impact upon the compression performance without any change to the entire coding scheme, including statistics modelling and Golomb entropy coding. To ensure such a fair comparison, all three algorithms have exactly the same number of operations including coding-mode selection, statistics modelling and entropy coding, apart from the prediction being different.

The experimental results for the weight based diagonal edge detection can be summarised in Tables 4.3-4.5 while the results after including pixel a in the prediction mechanism can be summarised in Tables 4.6-4.8. In the Tables of the weighted scheme, a1 and a2 represent weights while in all Tables of results T1 and T2 represent empirically found thresholds. The percentage predictive Mean Square Error improvement (PMSE) for the same compression rate can also be calculated as follows:

$$\text{PMSE} = \frac{MSE_{JPEG-LS} - MSE_{proposed\ scheme}}{MSE_{JPEG-LS}} \times 100 \qquad (4.12)$$

This value is represented by the third column in all Tables of results.

From these tables, it can be seen that, for all image samples tested, the proposed schemes outperform JPEG-LS in terms of predictive MSE values for the same compression

rates as the standard. As analysed earlier, the extent of improvement depends on the image content, i.e., the number of true diagonal edges, which may exist inside the input image.

Another interesting aspect, which can be observed from Table 4.3-4.8, is that, although the prediction schemes are improved in terms of accuracy measured by predictive MSE values, the compression ratios stay the same. This is expected due to the fact that the entropy coding length is determined by statistical modelling [85],yet this part of operation is not revised in the light of the proposed diagonal edge detection. In this sense, smaller predictive error may not necessarily produce higher compression efficiency. The decisive factor for compression efficiency is how accurate could the statistical modelling produce statistical information to drive the entropy coding [86].However, when predictive error is minimised, the direct and positive effect upon statistical modelling would be significant, since the statistical distribution of those errors would become more focused around its mean value as opposed to being scattered [85].With JPEG-LS, the specific advantage can be illustrated in that the number of context quantization regions could be reduced and more probabilities could be assigned around the centre of the statistical distribution. Another impact upon compression efficiency by smaller predictive errors can be seen with the near lossless compression mode in JPEG-LS. The near lossless mode requires a small quantization of those predictive errors in order to produce higher compression ratios. To this end, the reconstructed image quality could benefit by introducing smaller quantization step corresponding to the smaller predictive errors [83,84].

Samples	JPEG-LS MSE	Weighted predictive MSE	PMSE improvement	JPEG-LS CR	Weighted predictive CR
Lena	37.435	36.599	2.23%	1.991:1	1.991:1
Boat	80.571	80.152	0.52%	2.09:1	2.09:1
Camera	215.664	213.59	0.96%	1.849:1	1.849:1
Clown	94.19	92.712	1.56%	1.702:1	1.702:1
Salad	128.895	127.97	0.71%	1.578:1	1.579:1
Jet	44.978	44.641	0.74%	2.096:1	2.096:1

Table 4.3: Experimental Results for weighted predictive scheme (T1=T2=10,a1=1,a2=2)

Samples	JPEG-LS MSE	Weighted predictive MSE	PMSE improvement	JPEG-LS CR	Weighted predictive CR
Lena	37.435	36.327	2.95%	1.991:1	1.991:1
Boat	80.571	80.394	0.21%	2.09:1	2.09:1
Camera	215.664	213.996	0.77%	1.849:1	1.849:1
Clown	94.19	92.624	1.66%	1.702:1	1.702:1
Salad	128.895	127.826	0.82%	1.578:1	1.578:1
Jet	44.978	44.477	1.11%	2.096:1	2.095:1

Table 4.4: Experimental Results for weighted predictive scheme (T1=T2=5,a1=2,a2=3)

Samples	JPEG-LS MSE	Weighted predictive MSE	PMSE improvement	JPEG-LS CR	Weighted predictive CR
Lena	37.435	36.713	1.92%	1.991:1	1.991:1
Boat	80.571	80.184	0.48%	2.09:1	2.09:1
Camera	215.664	213.944	0.79%	1.849:1	1.849:1
Clown	94.19	92.857	1.41%	1.702:1	1.702:1
Salad	128.895	127.958	0.72%	1.578:1	1.579:1
Jet	44.978	44.749	0.50%	2.096:1	2.096:1

Table 4.5: Experimental Results for weighted predictive scheme (T1=T2=8,a1=1,a2=3)

Samples	JPEG-LS MSE	Proposed MSE	PMSE % improvement	JPEG-LS CR	Proposed CR
Lena	37.435	36.853	1.55%	1.991:1	1.991:1
Boat	80.571	80.206	0.45%	2.09:1	2.09:1
Camera	215.664	213.958	0.79%	1.849:1	1.849:1
Clown	94.19	93.37	0.87%	1.702:1	1.702:1
Salad	128.895	128.125	0.59%	1.578:1	1.579:1
Jet	44.978	44.906	0.16%	2.096:1	2.096:1

Table 4.6: Experimental Results by including pixel a in the prediction scheme (T1=T2=10)

Samples	JPEG-LS MSE	Proposed MSE	PMSE % improvement	JPEG-LS CR	Proposed CR
Lena	37.435	36.763	1.79%	1.991:1	1.991:1
Boat	80.571	80.298	0.33%	2.09:1	2.09:1
Camera	215.664	214.159	0.69%	1.849:1	1.849:1
Clown	94.19	93.476	0.75%	1.702:1	1.702:1
Salad	128.895	127.86	0.80%	1.578:1	1.578:1
Jet	44.978	44.904	0.16%	2.096:1	2.095:1

Table 4.7: Experimental Results by including pixel a in the prediction scheme (T1=T2=5)

Samples	JPEG-LS MSE	Proposed MSE	PMSE improvement	JPEG-LS CR	Proposed CR
Lena	37.435	36.797	1.70%	1.991:1	1.991:1
Boat	80.571	80.239	0.41%	2.09:1	2.09:1
Camera	215.664	214.155	0.69%	1.849:1	1.849:1
Clown	94.19	93.391	0.84%	1.702:1	1.702:1
Salad	128.895	128.015	0.68%	1.578:1	1.579:1
Jet	44.978	44.92	0.12%	2.096:1	2.096:1

Table 4.8: Experimental Results by including pixel a in the prediction scheme

4.11 Conclusions

In this chapter, we initially proposed a simple Linear Extrapolated Padding technique (LEP) to improve the compression efficiency for the reference VOP padding problem in MPEG-4. Compression improvements of up to 6.9% were observed as compared to the MPEG-4 padding scheme. Subsequently, we proposed a shape distortion adaptive hybrid padding technique to minimise prediction errors in coding arbitrary shaped video objects in MPEG-4 video sequences. The proposed hybrid technique is particularly effective in coding video sequences with objects, having a quick pace of shape change. Compression gains of up to 9% over the MPEG-4 padding technique have been obtained for coding boundary blocks of video objects in such sequences, for the same quality as the standard.

Further experimental analysis indicated that the selection of the threshold value, T, plays a major role in the performance of the hybrid algorithm. At present, we have used a fixed threshold (see Section 4.7). It is expected that a dynamic approach in setting this threshold value would enhance the performance and the flexibility of the present version of the algorithm.

We can conclude that if low computational complexity is at premium, the LEP scheme for the reference VOP padding problem is sufficient for improving the compression rate over MPEG-4 for the same quality. On the other hand if compression rate is at premium, the hybrid scheme is a better choice.

In the second part of the chapter, two algorithms were presented for adding diagonal edge detection to JPEG-LS, in addition to the horizontal and vertical edges detected by the standard . Both algorithms utilised pixel correlation inside the predictive template in order to improve the prediction in the presence of diagonal edges, thus reducing the produced predictive MSE. It is worth noting, that both the proposed schemes improve the predictive

MSE only, for the same bit rates as the standard, but this is expected since no changes on the compression mechanism of JPEG-LS are applied. The observed predictive MSE improvements are up to 2.9% for the first scheme and up to 1.9% for the second scheme in predictive Mean Square Error (MSE) values for the same bit rates as the standard. The extend of improvement depends of course on the percentage of the diagonal edges in the image.

CHAPTER 5 - LOW COMPUTATIONAL COST R-D IMPROVEMENTS IN MPEG-2 VIDEO CODING

5.1 Introduction

The rate distortion approaches in the context of video coding can be broadly classified into two major categories. The first category contains the analytic approaches whose objective is to derive a set of mathematical formulas for the R-D curves based on the statistical properties of the source data. In these approaches, the coding system and the video frames are first decomposed into components whose statistical models are already known. Then they are combined together to form a complete analytic model. Typical work can be found in Hang and Chen [72] and in Ding and Liu [73] .The problem with these models is that they show relatively large errors in the estimation of the rate distortion characteristics [60] and that their accuracy depends on the number of control points used to fit the R-D data. Given that the best results from data fitting are obtained when all the data points are used, the complexity of these approaches can still be high when improved accuracy is desired.

The second category of R-D optimisations contains empirical approaches. The observed R-D performance data of the encoding system is mathematically processed first and its output serves as an estimate of the R-D curves for the encoding system. Typical work includes dynamic programming [58] and Lagrange multiplier optimisation [59,62,74-76] which generally involve multiple iterations over the R-D data. Considering the fact that the best results from those observed data are obtained when most, if not all, the data is used, these approaches are also of high computational complexity. The complexity is even more increased in empirical approaches by the overhead required in order to enable the

optimal trellis path being determined in the optimisation stage. To reduce the number of control points, interpolation functions are also proposed to improve the complexity in the process of estimating the R-D data [60]. This work aims to trade complexity to accuracy, producing sub-optimal R-D estimates for rate control design. In general, empirical approaches are not suitable for low encoding delay video coding because of the high overhead in CPU cycles associated with the optimisation of the rate-distortion performance.

The MPEG-2 standard [7,8,97,98] was developed for low end-to-end delay video compression of broadcasting quality. It can not afford high complexity due to optimisation overheads in the encoding stage. In fact, it is evident from the test document that its performance along with visual quality measurements were very seriously considered in every part of the compression pipeline. In particular, the MPEG-2 rate control scheme follows a different approach than the ones outlined above, namely it is a "direct buffer state feedback scheme". These schemes do not measure and monitor the distortion by using multiple-pass coding. Instead the buffer occupancy and the activity analysis determines the quantization settings. Consequently, decisions about quantization step size assignments on a macroblock basis (*mquant parameter*) are made online, which can only become possible when information about the current macroblock or previously encoded macroblocks is primarily used in the decision-making process.

The work presented in this chapter consists of two parts. In the first part, four novel activity estimates for improving *on the fly* the rate distortion performance of the MPEG-2 rate control scheme (TM5) are presented. This part of the work initially identifies the drawbacks in R-D terms of *the normalisation scheme* used in the standard for activity estimation and subsequently improves the R-D performance by proposing new activity estimates. In the second part of the chapter, two low cost rate control algorithms for

MPEG-2 are presented which are based on Lagrange theory. Unlike *the offline approaches* based on Lagrange multipliers, the proposed rate control schemes are applicable *online* since they still fall into the "direct buffer state feedback schemes". Furthermore, they also improve the estimation of the R-D characteristics as compared to MPEG-2 by explicitly including distortion in the calculation of the quantization step size per macroblock through a Lagrangian formulation.

5.2 Review of the MPEG-2 rate control algorithm

The rate control scheme adopted in MPEG-2 can be formulated as, given a group of N frames and a range of quantization parameters, $\text{mquant} \in [\text{mquant}_{\min}, \text{mquant}_{\max}]$, find $q^* = (q_1\ q_2 \ldots q_N)$ with $q_i \in [mquant_{\min}, mquant_{\max}]$, such that:

$$q^* = \arg\left(\min_{q \in [\text{mquant}_{\min}\ \text{mquant}_{\max}]^N} \frac{1}{N} \sum_{i=1}^{N} d_i(q) \right) \qquad (5.1)$$

subject to the condition that the overall bit rate is not greater than a pre-set target. In equation (5.1), the distortion measurement, $d_i(q)$, can be quantitative such as PSNR (peak-signal-to-noise-ratio) or subjective such as visual perception characteristics.

To reduce the level of complexity and the cost of computing, MPEG pursued the issue along the subjective distortion measurement, which allocates the value of *mquant* according to two factors. One factor is the buffer fullness and the other is the activity measurement within each macroblock. Therefore, to encode the *j*th macroblock inside each frame, its *mquant* is determined by the following equation:

$$mquant_j = Q_j \times N\_act_j \qquad (5.2)$$

where Q_j is a modulation parameter, which indicates the contribution from the buffer-fullness, and N_act_j is a normalised activity indicating the contribution from the activity analysis on the jth macro-block.

The activity analysis in MPEG-2 is mainly carried out by calculating the variance of original pixel values within each macro-block in connection to an average activity derived from the preceding frame. Specifically, MPEG determines the value of N_act_j as given below:

$$N\_act_j = \frac{2 \times act_j + avg\_act}{act_j + 2 \times avg\_act} \tag{5.3}$$

where, $act_j = 1 + \min(\text{var}_{blk1}, \text{var}_{blk2}, \text{var}_{blk3}, \text{var}_{blk4})$ and avg_act is the average of all local activities used to encode its preceding frame. Since each macro-block consists of four 8×8 blocks, its activity is seen to be determined by the minimum variance value out of those of four 8×8 blocks. For all the 64 original pixel values, P_k ($k \in [1, 64]$), the variance can be calculated as follows:

$$\text{var}_{blk} = 1/64 \, x \sum_{k=1}^{64} (P_k - P\_mean)^2 \tag{5.4}$$

where $P\_mean = \frac{1}{64} \times \sum_{i=1}^{64} p_i$ represents a mean value of the block.

Essentially, the contribution to the rate control from activity analysis is described by equation (5.3), from which, it is seen that the value of normalised activity, N_act_j, is not only determined by the activity of the jth macro-block, act_j, but also by the average activity, *avg_act.* of the previously encoded frame. The latter can be viewed as a stabilising factor to ensure that any temporary drastic change incurred at the current macroblock will not dominate the role of activity analysis for rate control. This is also seen as the

contribution from the history of activity analysis, which is very important in light of the fact that neighbouring frames and blocks are highly correlated due to the nature of the video sequence data. If we take the average activity as a constant for the time being, we can convert equation (5.3) into:

$$N\_act = \frac{2x+c}{x+2c} \tag{5.5}$$

where c is a constant value determined by the history of activity analysis.

If we ignore Q_j, in equation (5.2), it can be revealed that MPEG-2 relies on the normalised activity to optimise the picture quality while rate control is achieved by distributing the information loss according to the visual perception characteristics. By further examining equations (5.3) and (5.5) it can be seen that the increase or decrease of the normalised activity estimate (N_act_j,) depends on the relation between the two parameters, act_j and c *(avg_act)*. If we let act_j, the local activity inside the jth macro-block vary at: $act_j=0$, $act_j=c$, $act_j=2c$, $act_j=k\times c$ (k is an integer), the change of N_act_j can be illustrated in Figure 5.1(a).

Figure 5.1 (a): Normalised activity as a function of average activity of previous frame

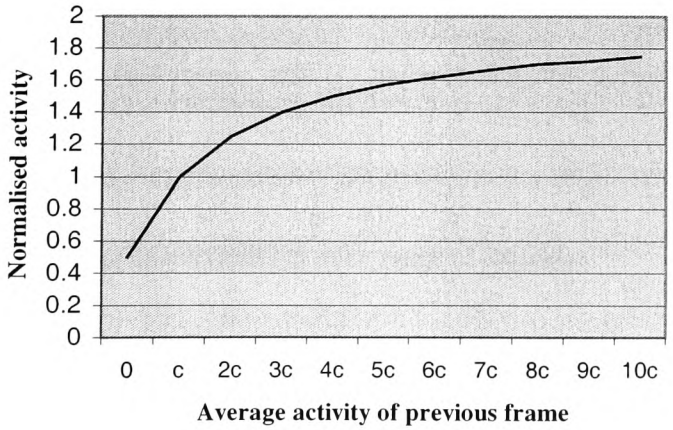

The curve in Figure 5.1(a) shows that the range of N_act_j varies from 0.5 to an upper-bound value of 2 .Therefore, the principle of activity estimation in MPEG-2 can be explained as that the higher activity macroblocks in relation to the average activity of the previously encoded frame provide a favourable environment for more information loss (higher distortion) and lower activity for less information loss (lower distortion).

The contribution to rate control from buffer fullness is relatively straightforward in MPEG-2, in which three virtual buffers are allocated to accommodate the encoding process for I-frames, P-frames and B-frames respectively. To encode a x-type frame, the virtual buffer fullness is determined at macro-block level, which is then used to determine the modulation parameter, Q_j, for the jth macro-block. This operation can be described by the following equation:

$$Q_j = \left(\frac{d_j^x \times 31}{r} \right) \tag{5.6}$$

where $r = \frac{2 \times bit\_rate}{picture\_rate}$ is a so-called reaction parameter determined by the channel bit-rate and the picture-rate; d_j^x is the virtual buffer fullness for the jth macro-block inside the x-type frame, which is determined according to: (a) the target bit rate allocated to this frame to be encoded; (b) the number of bits generated by encoding the previous (j-1) macro-blocks inside this frame; and (c) the initial buffer fullness before encoding of this frame starts.

5.2.1 Drawbacks of the MPEG-2 rate control scheme

Implicitly, the rate control model of MPEG-2 assumes that the distribution of bits among macroblocks for the frame to be encoded is uniform, which is not accurate due to the

variability of the bit rates produced on a macroblock basis. Although neighbouring macroblocks tend to produce similar amount of bits due to pixel correlation, this is definitely not accurate for macroblocks that are further apart in a frame. It can also be observed that any attempt to alter the uniform distribution of bits per macroblock that the standard uses for rate control is unlikely to succeed since we can not know the exact amount of bits that the macroblock will produce when encoded *a priori*. The standard also uses *a variance based normalisation scheme* for activity estimation which is very sensitive to small changes in activity characteristics and as such not optimal in rate distortion terms since it produces a non-uniform information loss distribution [14,15]. To make the rate control algorithm even more sub-optimal in R-D terms, the activity of the macroblock to be encoded is assumed to be close to the average activity of the previously encoded frame (avg_act) *which may not always be the case*. The combined effect of the inaccurate bit allocation per macroblock, of the extra sensitive normalisation scheme and on the incorrect assumption about similarity in activities leads to unnecessary fluctuations in the quantization step assignment phase which is not optimal in rate distortion terms [14,15]. Finally, the standard does not consider distortion explicitly in the estimation of the quantizer step size per macroblock which also aids in R-D sub-optimality.

5.3 Improving the rate distortion performance by using a local activity estimate

As evidenced by equation (5.3), the normalised activity estimate for the macro-block to be encoded depends on the relation between the macro-block activity and the average activity of the previously encoded frame. In the case when the activity of the current macro-block is smaller than the average activity of the previously encoded frame, the normalised activity value is less than one and conversely it is greater than one. On the average, it is assumed that the activity of the macro-block to be encoded is similar to the activity of the

previous frame which will give a value for the normalised estimate close to one. The problem here is that the average activity of the previous frame is a global estimate and as such it does not utilise local activity information.

To illustrate the point, consider a scenario where the previous frame is smooth texture wise while the current frame is rough. According to equation (5.3), all the macro-blocks of the current frame will be over-normalised since the value of the normalisation estimate will be greater than one. Then, the estimation of the quantizer moderator *mquant, for* every macro-block of the current frame, will depend on the discrepancy of the buffer bit residue from the uniform distribution model and the assumption is that by over-normalising the macro-blocks of the current frame, this distance from the uniform model will decrease. While more information loss in rough areas can be afforded, the distance between the buffer estimate and the uniform distribution model is not guaranteed to decrease in a predictable manner since there is a lot of variability in the bit rate production of different macro-blocks. As a result, unnecessary over-normalisation could occur which would lead to PSNR degradation for a given target frame rate. This over-normalisation occurs because the average activity of the previous frame is used as part of the normalisation function.

The point for non-optimal normalisation because of the globality of the activity estimate used, can also be demonstrated by the converse example in which the current frame is smooth but the previous frame is rough. In this case, according to equation (5.3), every macro-block in the current frame will be under-normalised since the value of the normalisation estimate will be less than one. This may be in accordance to the principle of minimal information loss towards smooth textures but its repercussions on the buffers can be realised by observing that the buffer estimate Qj in equation (5.2) assumes a uniform distribution of bits in the frame. In other words every macro-block is expected to produce approximately (Target number of bits per frame/number of macro-blocks per frame) bits.

In a frame where the percentage of smooth macro-blocks is larger than the percentage of rough macro-blocks (as the one we use in this example) this may not be the case and as a result, as encoding proceeds in the frame the straying from the uniform distribution model will increase. In terms of the quantization parameter *mquant* described in equation (5.2), it is assumed that although the buffer estimate increases, it will be moderated by the under-normalisation. Again because of the variability of the bit rates of different macro-blocks, this assumption may not be true. If this is the case, we will have degradation of the rate distortion performance after a point, in order buffer overflows to be avoided. The undesirable effects of over and under normalisation because of the globality of the average activity estimate of the previous frame can be remedied by utilising local activity information described in the following scheme.

Step 1: Compare the absolute value of the distance between the activity of the macro-block to be encoded and the activity of the macro-block just preceding it, to the absolute value of the distance between the activity of the macro-block to be encoded and the average activity of the previously encoded frame. If the former is smaller, this implies that the current macro-block is more correlated to the one preceding it with respect to activity, than it is with the previously encoded frame. If the latter is smaller, it implies that the macro-block to be encoded is more correlated to the previous frame, activity wise.

Step 2: Choosing the smallest of the two distances (in absolute value terms) will also give us the best estimate (activity of the previous macro-block or average activity of the previously encoded frame) to be used for the normalisation. The normalisation will be performed using this best estimate in the place of *avg_act* in equation (5.3).

The principle behind this scheme is that similar activity macro-blocks should be normalised similarly while at the same time over and under normalisation should be avoided as described above. Formally, suppose that macro-block j is the one to be encoded

and it's not the first macro-block in the frame. Then, the following relation best describes the proposed scheme:

$$\begin{aligned} &\textit{if} \quad abs\_d(act_j - act_{j-1}) < abs\_d(act_j - avg\_act) \\ &\textit{use} \quad act_{j-1} \quad \textit{instead} \quad \textit{of} \quad avg\_act \quad \textit{for} \quad \textit{normalisation} \\ &\textit{else} \quad \textit{use} \quad avg\_act \quad \textit{for} \quad \textit{normalisation} \end{aligned} \tag{5.7}$$

where act_j and act_{j-1} are the activities of macro-block j and of the one preceding it, *abs_d* denotes the absolute value of the distance between activities and *avg_act* is the average activity of the previously encoded frame.

As can seen from equation (5.7), the proposed scheme is a low complexity one and as such suitable for real time applications. We tested extensively this technique versus MPEG-2 in terms of rate distortion, for the same final number of bits. Improvements up to 2.5 db along the luminance (Y) and the two chrominance components (U,V) are reported. It is worth noticing that more than 98% of the frames tested showed improvements in both luminance and chrominance components. Figures [5.1-5.5] summarise the performance results for the luminance component and Figures [5.6-5.9] for the chrominance components for a set of commonly used test sequences. Finally Table 5.1 compares the final number of bits produced for the two schemes.

Figure 5.1: Luma Component of miss america sequence

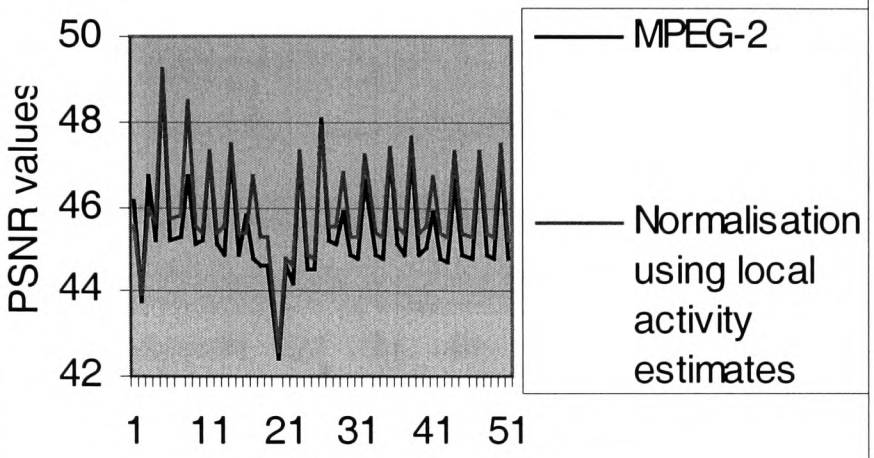

Figure 5.2: Luma Component of calendar sequence

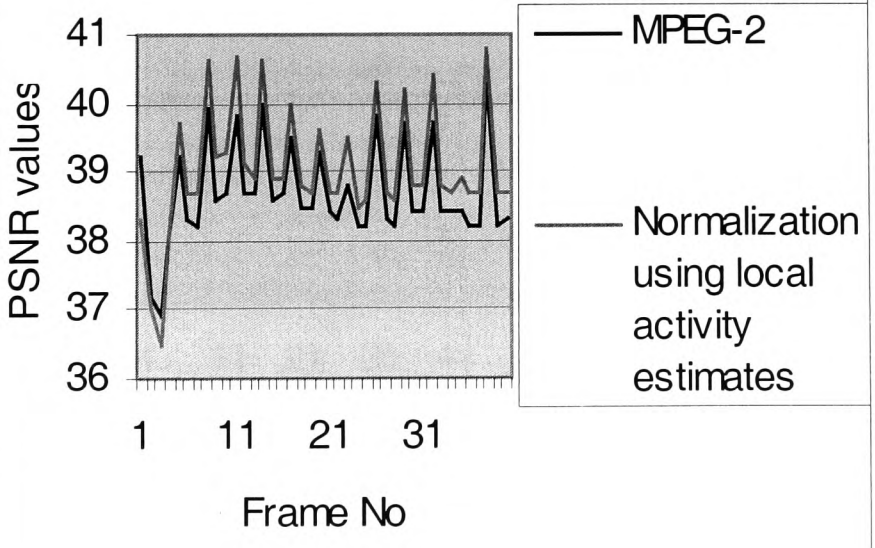

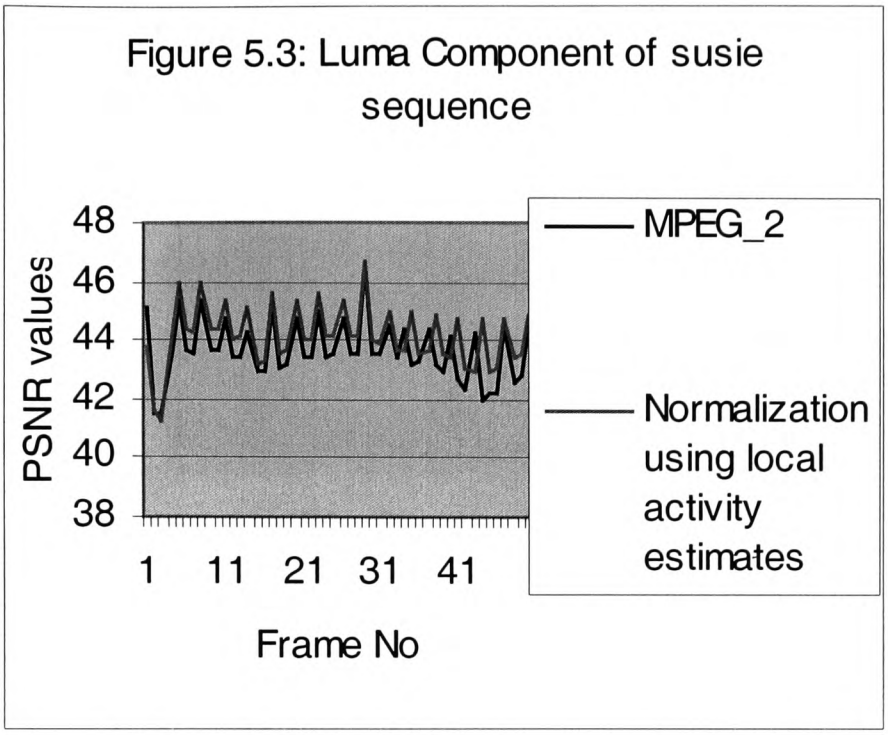

Figure 5.3: Luma Component of susie sequence

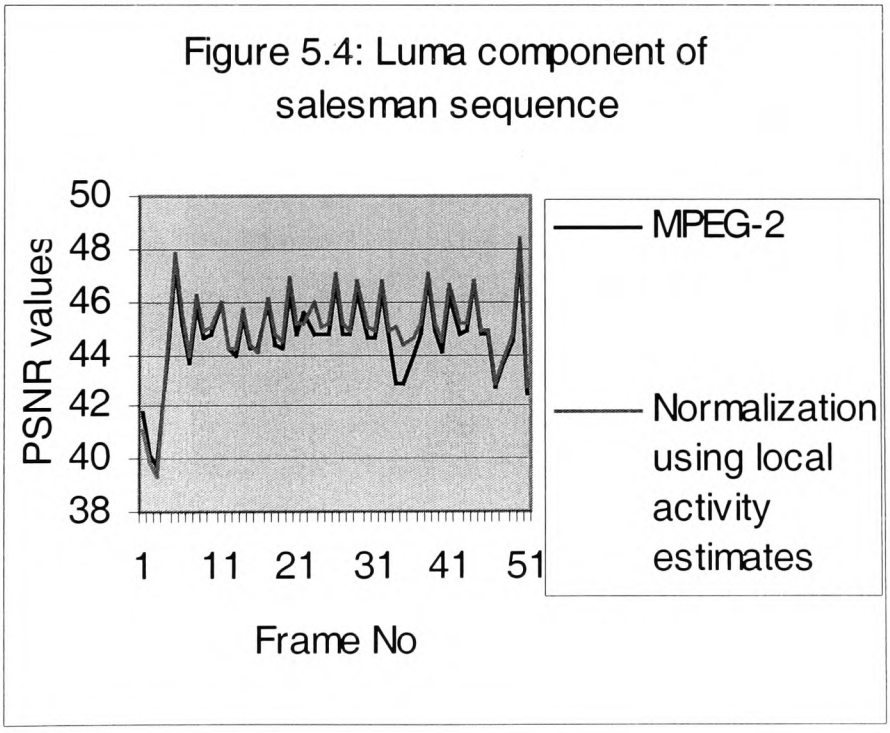

Figure 5.4: Luma component of salesman sequence

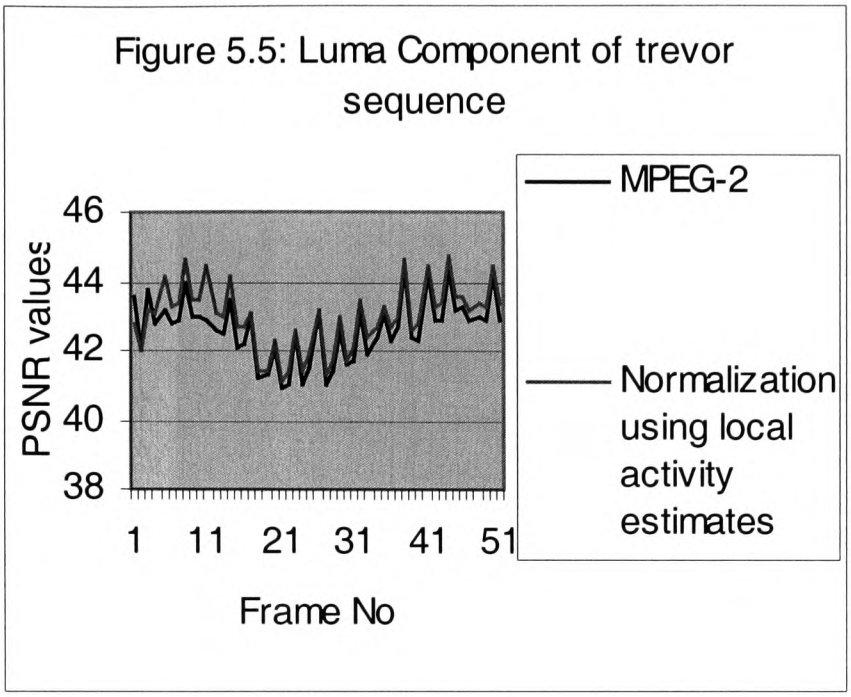
Figure 5.5: Luma Component of trevor sequence
PSNR values
46
44
42
40
38
1
11
21
31
41
51
Frame No
MPEG-2
Normalization using local activity estimates

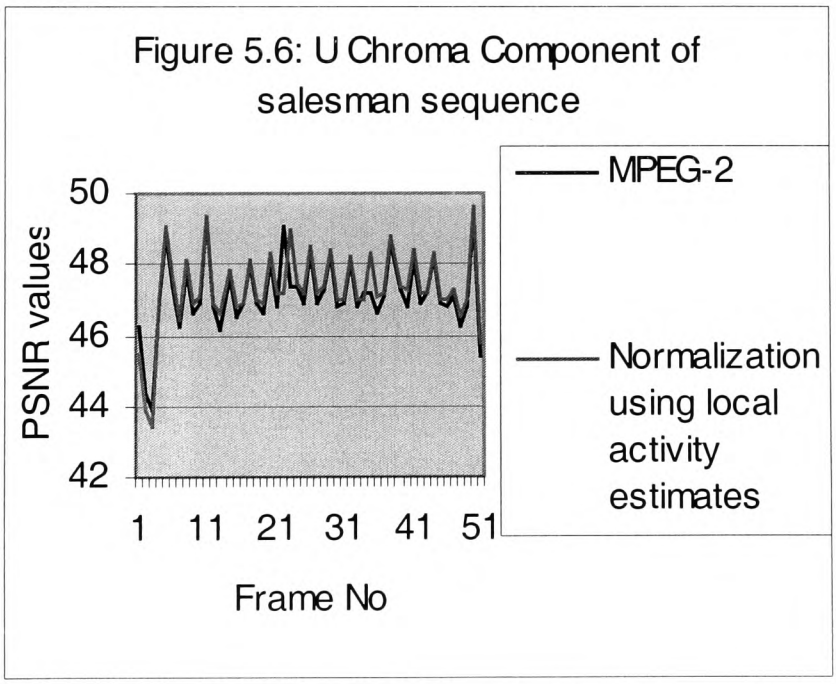
Figure 5.6: U Chroma Component of salesman sequence
PSNR values
50
48
46
44
42
1
11
21
31
41
51
Frame No
MPEG-2
Normalization using local activity estimates

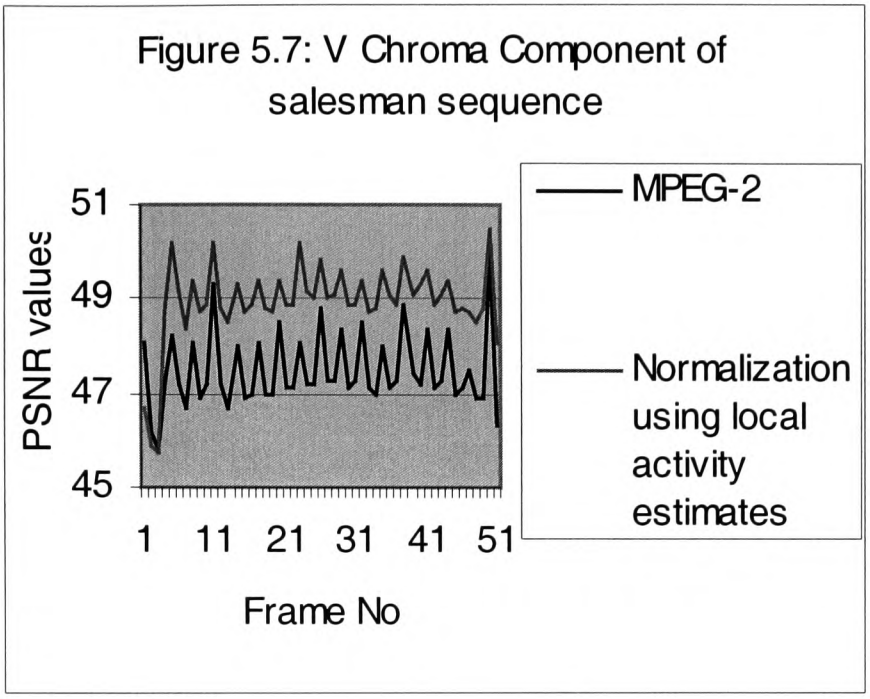

Figure 5.7: V Chroma Component of salesman sequence

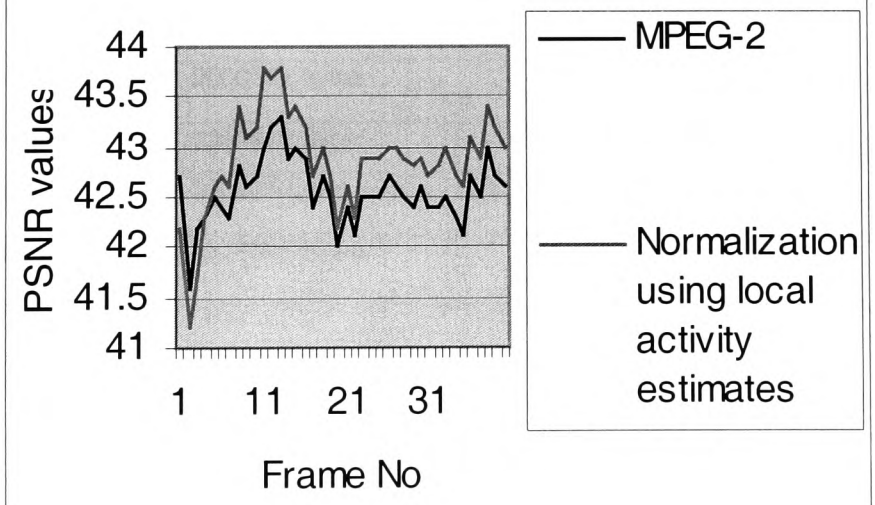

Figure 5.8: U Chroma Component of calendar sequence

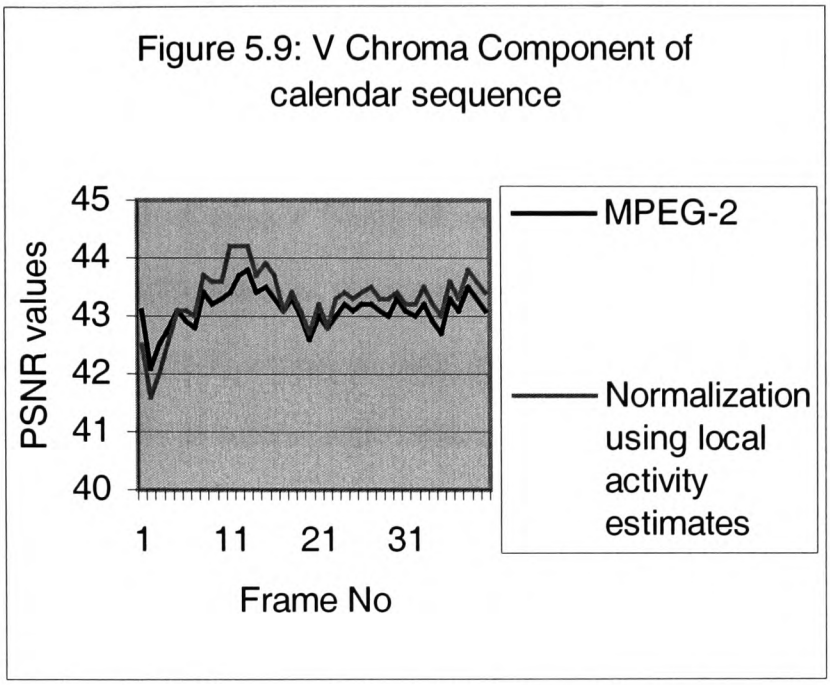

Table 5.1 : Bit rates produced by the proposed scheme versus MPEG-2		
Test Sequences	**Normalization using local activity estimation**	**MPEG-2**
Miss America (50 frames)	1275359 bytes	1275213 bytes
Susie (50 frames)	2500311 bytes	2500740 bytes
Mobile (40 frames)	1999972 bytes	2000711 bytes
Trevor (50 frames)	293805 bytes	293847 bytes
Salesman (50 frames)	1276342 bytes	1276037 bytes

5.4. Improving the rate distortion performance by using a family of exponential modulators

We investigated the potential of using a family of exponential modulators in order to improve the rate distortion performance for the same final number of bits as the MPEG-2 standard. The motivation here is to attempt to stabilise the undesirable variation of the normalisation estimate in order to achieve more optimal R-D performance. Note that we can not simply substitute the normalised activity estimate *with a constant value* because a potentially wrong choice will lead to R-D performance degradation. Since its evident from equation (5.2) that there is undesirable variation both from the buffer estimate and the normalised activity estimate, we attempt to reduce the *total variation* by modulating the normalisation part. So instead of using only equation (5.3) for normalisation, we additionally normalise using:

$$N\_act_j^* = N\_act_j * e^{-k*N\_act_j} \qquad k \in R^+, \qquad k >= 1 \tag{5.8}$$

This in effect re-maps the range of the normalisation function described in equation (5.3) from the interval (0.5,2) to smaller range intervals. For example when k=1 the interval is (0.27,0.38), when k =2 the interval is (0.04-0.14) etc. It can be observed that the proposed family of exponential modulators gives more control to the buffer estimate than to the normalised activity estimate, seeking an alternative balance point between them. At the same time, it enables more quantization parameters to be packed in the lower end of the quantization spectrum while still retaining certain adaptivity. It finally aids in a more uniform information loss distribution across macro-blocks and frames.

This more constant information loss distribution aids in turn to further improvements in PSNR performance, since less overhead bits are needed in order the decoder to be informed about changes in the quantization parameters. It can be observed from equation

(5.2) that reduction of overheads implies that the buffer estimate Qj becomes smaller for the target number of bits allocated to a macroblock and as a result the quantization parameter *mquant* decreases. Consequently, we can achieve less information loss for the same target number of bits per macro-block in the quantization phase of MPEG-2. Thus, continuous reduction of overheads on a macroblock basis will result in PSNR improvements on a frame basis for the same target number of bits as the standard.

Regarding computational complexity, the proposed family of exponential modulators costs just four extra operations per macro-block, namely one negation of N_actj, one multiplication with the real value k, one exponentiation of the result and one multiplication of the exponentiated result with the normalised activity estimate. Due to the low computational cost the proposed family of exponential modulators is suitable for real time applications.

The distribution of the quantizer moderators (*mquants*) of the proposed family of exponential modulators will peak at a different point (very slightly higher) than the one at MPEG-2 rate control at the low end of the quantization spectrum. This will prevent buffer overflows. It would be impossible for the proposed scheme to have the quantizer moderators distribution peaking at the same or lower point as compared to MPEG-2 since the determination of the quantizer moderators is more buffer oriented. Also the savings in overheads, due to the more uniform information loss distribution further aid in the avoidance of buffer overflows. A further interesting property of the proposed scheme is that the range of the quantizer moderators will be smaller at the lower end of quantization spectrum.

We tested extensively the proposed exponential modulation versus MPEG-2 in terms of rate distortion, for the same final number of bits. Improvements up to 3.5 db along the luminance (Y) and up to 3.5db and 3db across the two chrominance components (U,V) are

reported. It is worth noticing that more than 98% of the frames tested showed improvements in both luminance and chrominance components. Figures [5.10-5.14] summarise the performance results for the luminance component and Figures [5.15-5.18] for the chrominance components for a set of commonly used test sequences. Table 5.2 compares the final number of bits produced for the two schemes, while Table 5.3 indicates the savings in overheads due to the more uniform information loss distribution. Finally, from our experiments the optimal value of the real k in equation (5.8) was found to be 1.

Figure 5.10: Luma Component of miss america sequence

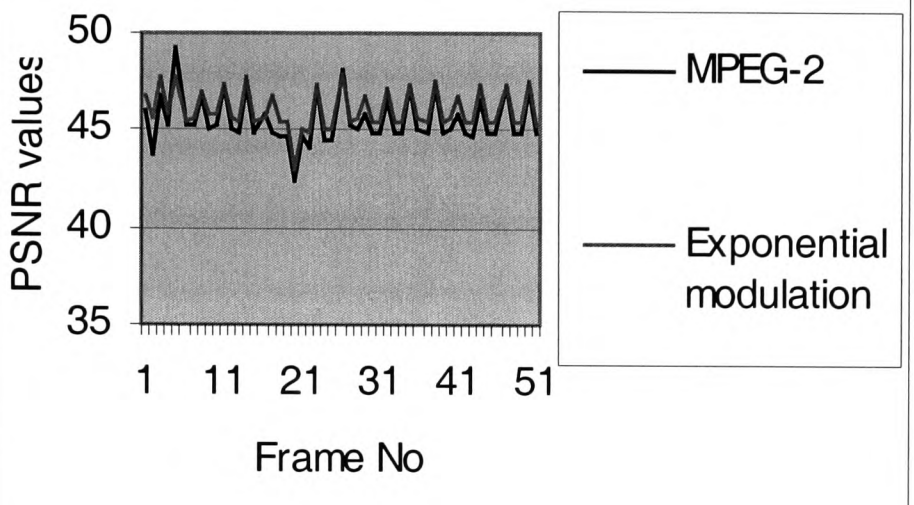

Figure 5:11: Luma Component of calendar sequence

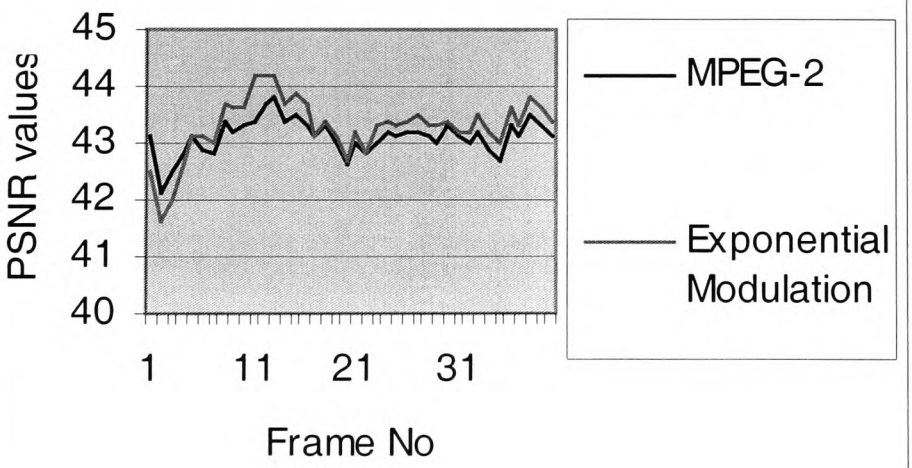

Figure 5.12: Luma component of susie sequence

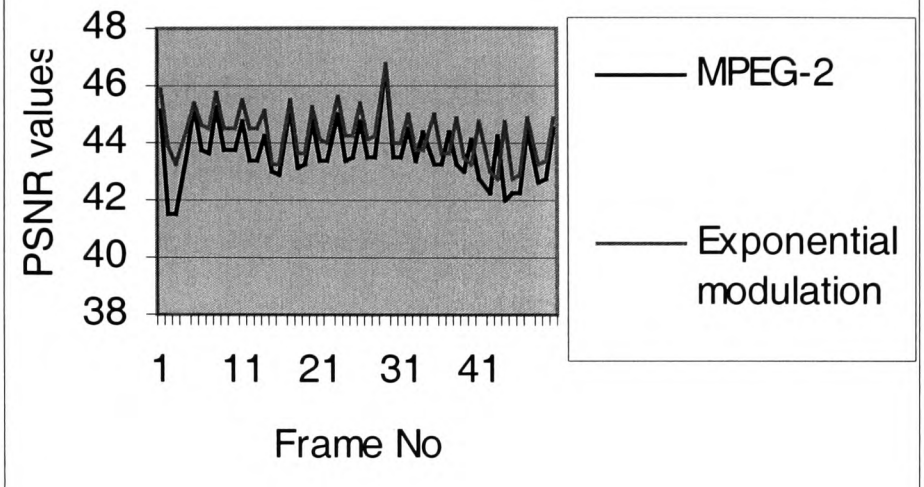

Figure 5.13: Luma Component for salesman sequence

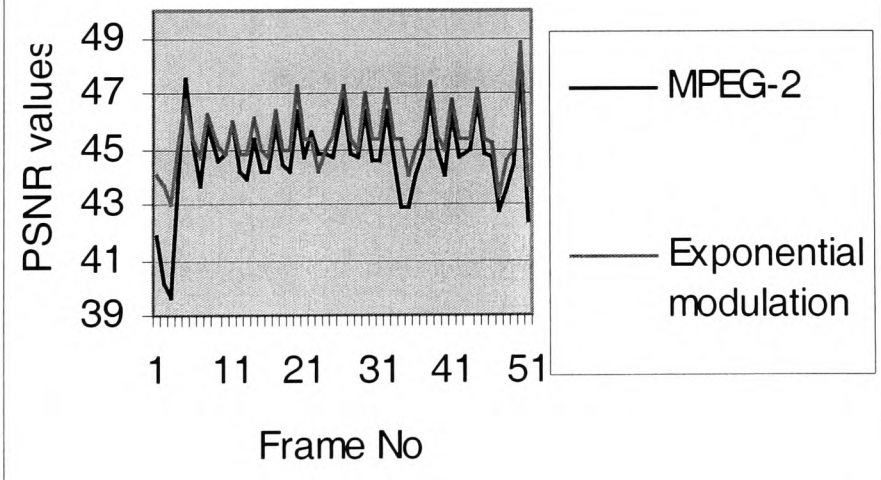

Figure 5.14: Luma Component for trevor sequence

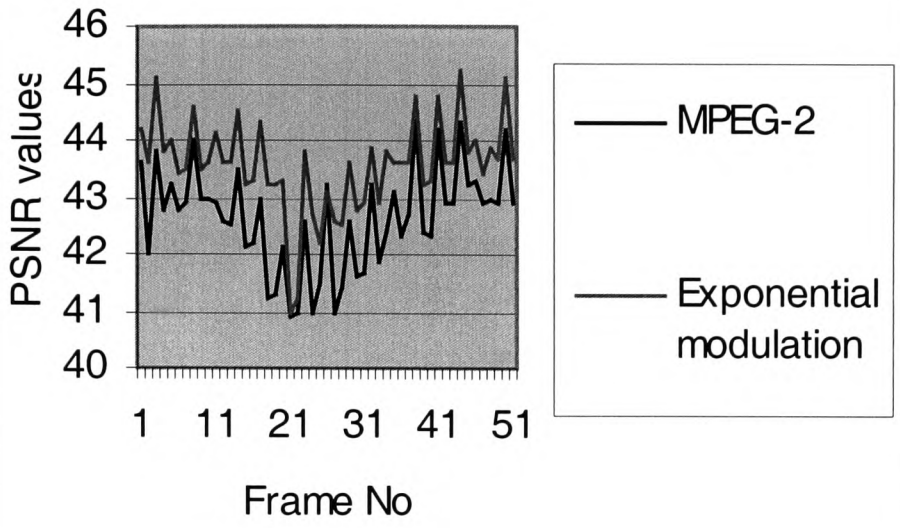

Figure 5.15: U Chroma Component for salesman sequence

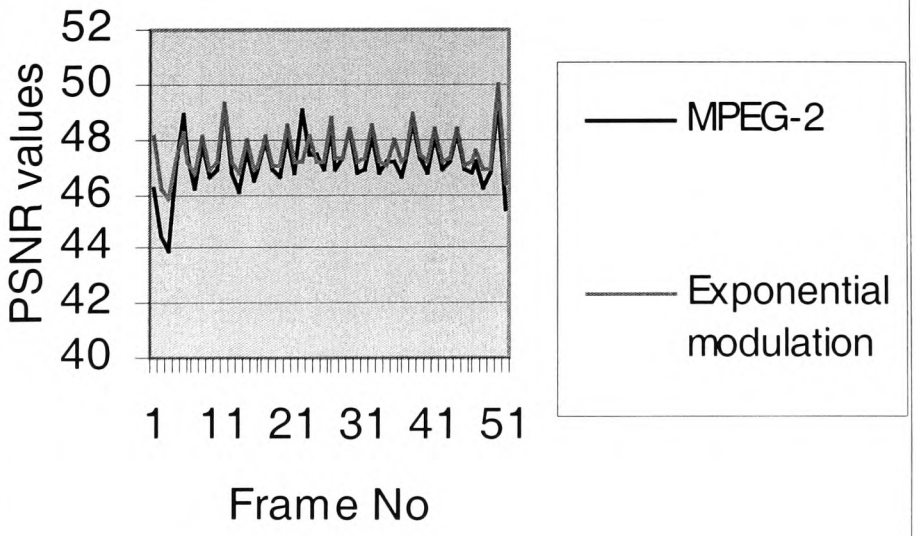

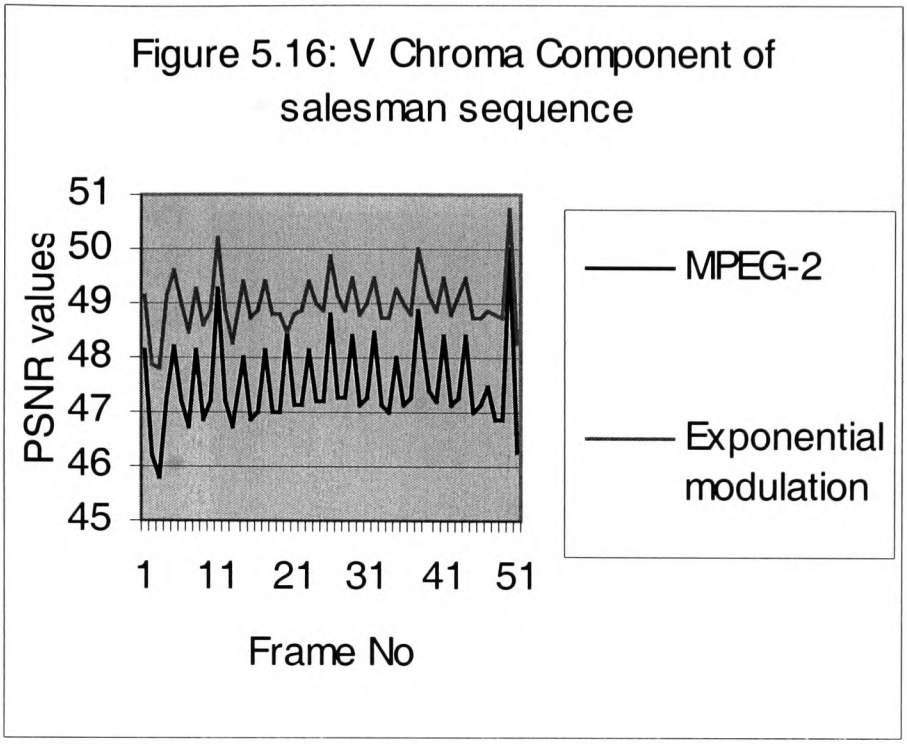

Figure 5.16: V Chroma Component of salesman sequence

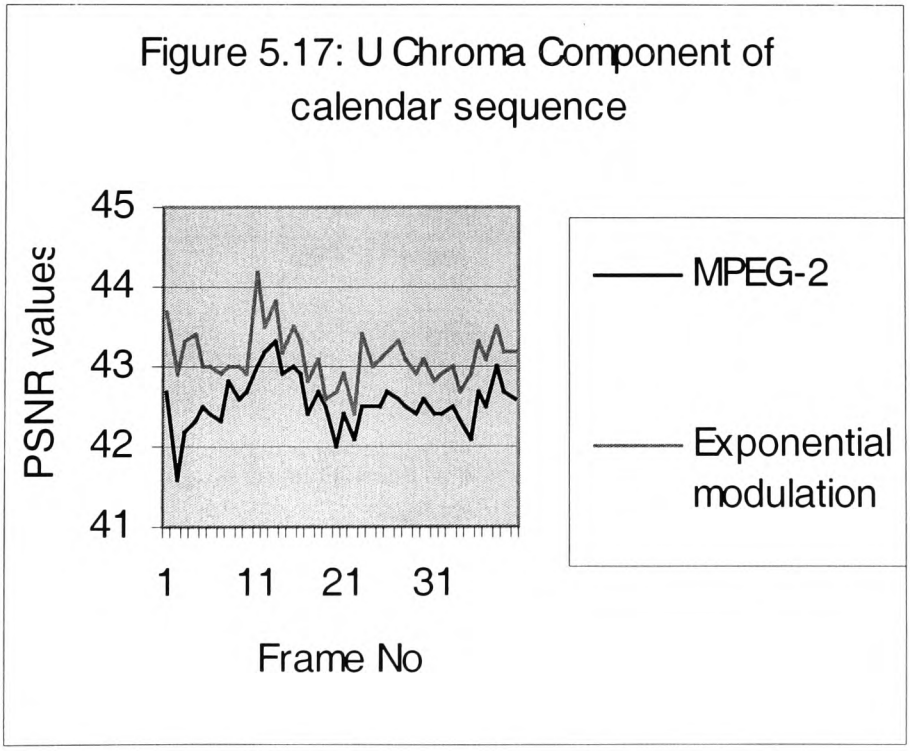

Figure 5.17: U Chroma Component of calendar sequence

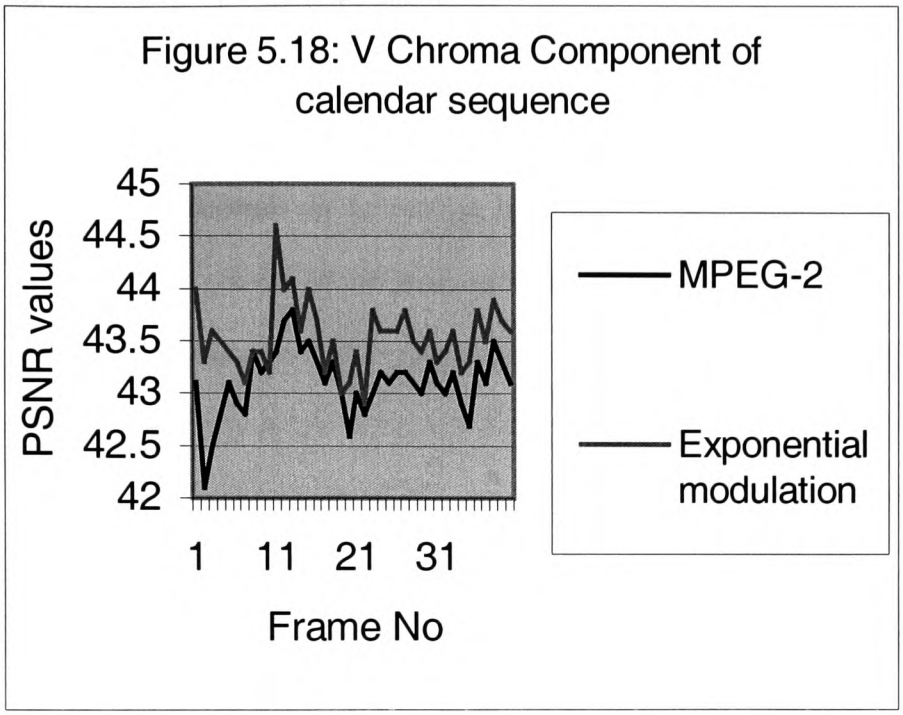

Table 5.2 : Bit rates produced by the proposed scheme versus MPEG-2		
Test Sequences	**Exponential function for normalization (Nact *e(-k*N_act))**	**MPEG-2**
Miss America (50 frames)	1275099 bytes	1275213 bytes
Susie (50 frames)	2501166 bytes	2500740 bytes
Mobile (40 frames)	1998400 bytes	2000711 bytes
Trevor (50 frames)	293717 bytes	293847 bytes
Salesman (50 frames)	1279982 bytes	1276037 bytes

Table 5.3: Bit savings in transmission of the changes of the final modulation factors			
Test Video Sequences	**Bits transmitted using the exponential function for normalization**	**Bits transmitted using the MPEG-2 normalization function**	**% savings in bits**
Miss america	23710	31290	24.3
Calendar	9485	65855	85.6
Susie	56390	82265	31.5
trevor	7450	17430	57.3
salesman	20885	36090	42.2

5.5 Low computational cost activity estimates

As evidenced by equation (5.3), the normalised activity estimate N_actj for each macroblock to be encoded depends on the relation between a variance based local activity estimate and on the average activity of the previously encoded frame measured in terms of variance. We wanted to investigate if there are activity estimates other than variance that reduce the undesired variability of the normalisation process (thus being more optimal in R-D terms) for the same final number of bits produced and for the same normalisation function (equation 5.3) as the standard.

We propose the standard deviation of pixel values in a block and the sum of absolute differences between pixel values and the block mean (SAD) as alternative activity estimates for improving the rate distortion performance.

Formally, the standard deviation of an 8*8 block of pixels is defined as:

$$\text{std\_dev}_{\text{blk}} = \sqrt{1/64 \times \sum_{k=1}^{64} (P_k - P\_mean)^2} \qquad (5.9)$$

where $P\_mean = \frac{1}{64} \times \sum_{i=1}^{64} pi$ represents a mean value of the block and Pk $(k \in [1, 64])$ denotes any pixel value in the block.

In the context of MPEG-2 rate control, the 8*8 sub-block with the minimal standard deviation can be used as a representative for the activity of the macroblock to be encoded. Also the average activity of the previously encoded frame is now calculated based on standard deviation. The extra overhead for using standard deviation for activity measure, as compared to variance, is just 4 operations per macroblock for determining the square roots of the four constituent 8*8 sub-blocks.

The sum of absolute differences between pixel values and the block mean (SAD) of an 8*8 block is defined as:

$$SAD_{blk} = 1/64x \sum_{k=1}^{64} abs(P_k - P\_mean) \qquad (5.10)$$

where $P\_mean = \frac{1}{64} \times \sum_{i=1}^{64} p_i$ represents a mean value of the block and Pk ($k \in [1, 64]$) denotes any pixel value in the block. The 8*8 sub-block with the minimal SAD can be used as a representative for the activity of the macroblock to be encoded. Also the average activity of the previously encoded frame is now calculated based on SAD. No extra overhead by using this measure is imposed as compared to variance, because the 64 extra multiplications per macroblock that the variance estimate needs are substituted by 64 estimations of absolute values of differences.

To assess the rate distortion performance of the proposed activity estimates, namely the SAD and the standard deviation we run extensive experiments on commonly used video sequences. We report improvements up to 2.8 db for both the SAD and the standard deviation estimates for the same final number of bits. These PSNR performance results are shown in Tables [5.19-5.28] from where it can be seen that the proposed estimates outperform the variance based estimate used in MPEG-2 rate control for the same final number of bits as the standard. The final number of bits produced for the proposed activity estimates as compared to the bits produced by MPEG-2 is shown in Table 5.4. Finally, Tables 5.5 and 5.6 show that the number of bits needed for informing the decoder about changes in the quantization parameters is substantially reduced by using the proposed estimates. This implies that the quantization parameter *mquant* per macro-block changes less frequently and as such the information loss distribution produced by the proposed estimates is more uniform as compared to MPEG-2. The positive effects of a more

uniform information loss distribution in PSNR terms for the same compression rates as the standard, is explained in detail in the previous section.

Figure 5.19: Luma Component of miss america sequence

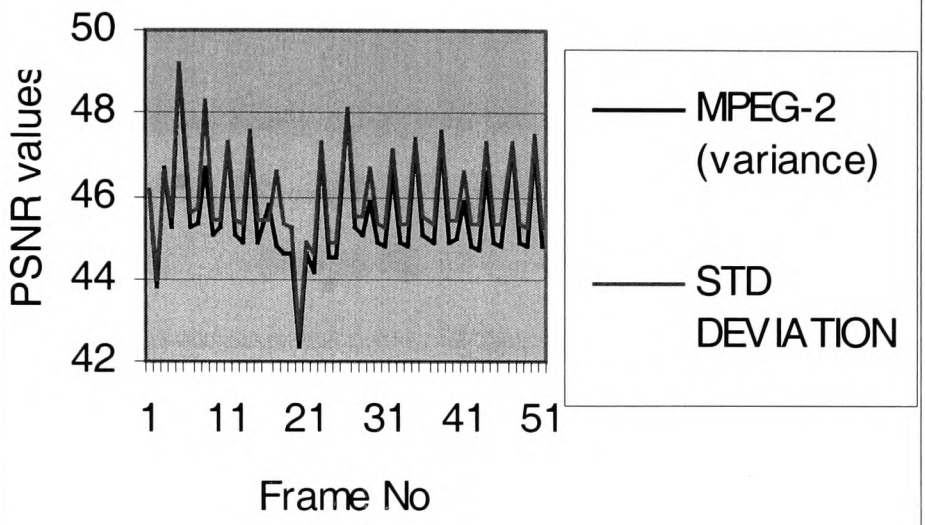

Figure 5.20: Luma Component of miss america sequence

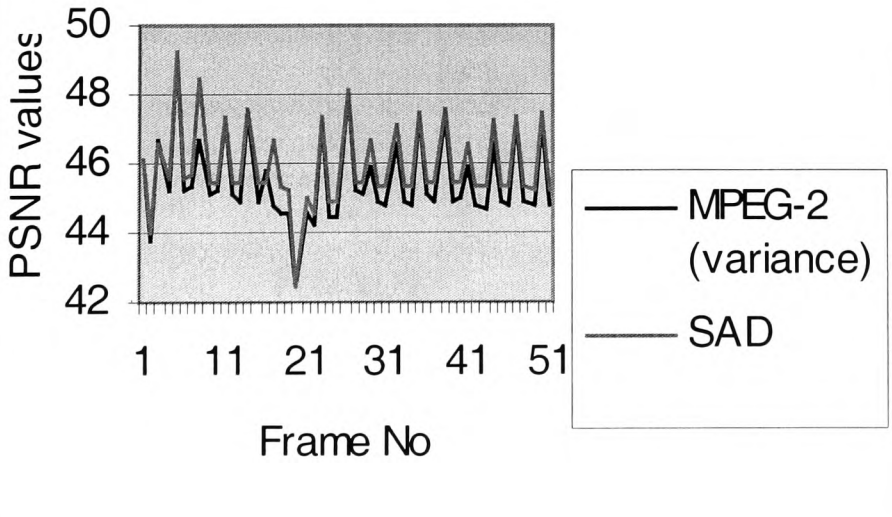

Figure 5.21: Luma Component of calendar sequence

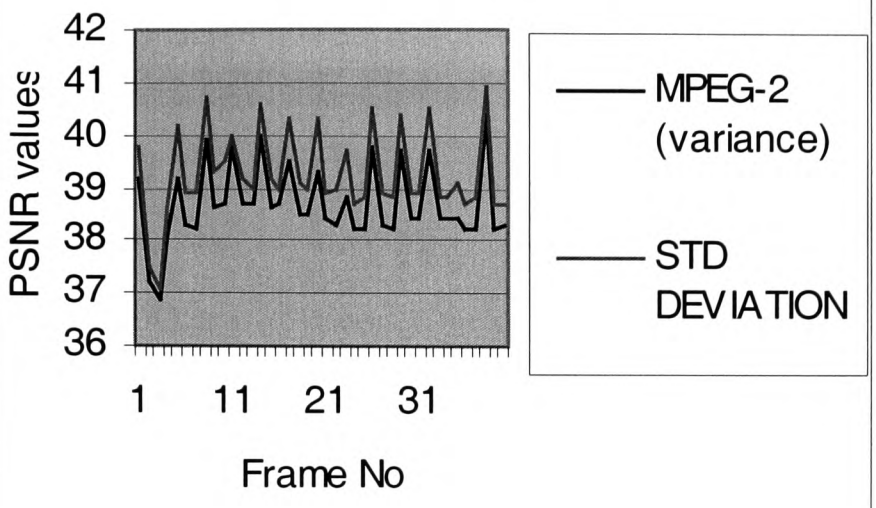

Figure 5.22: Luma Component of calendar sequence

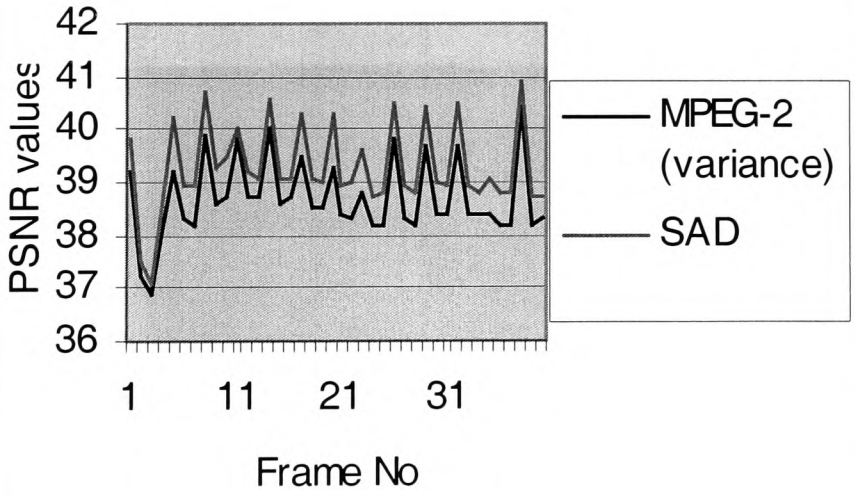

Figure 5.23: Luma Component of susie sequence

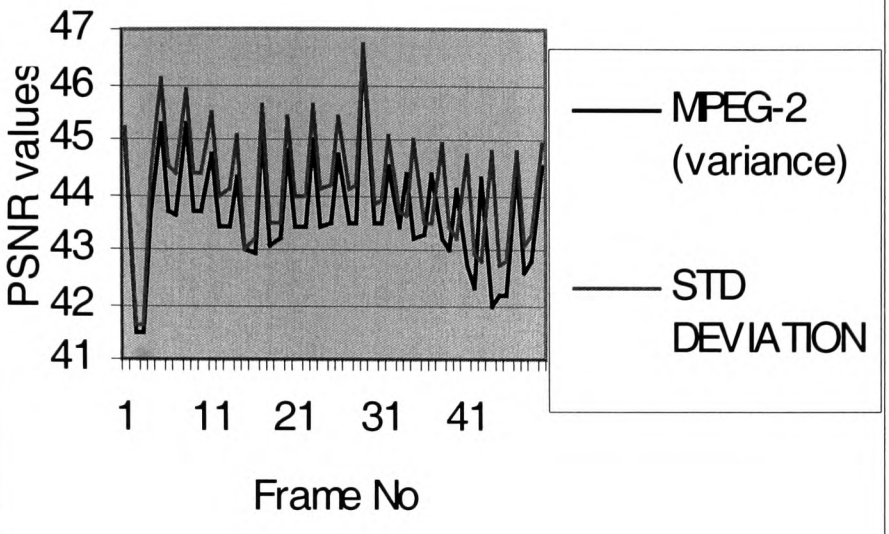

Figure 5.24: Luma Component of susie sequence

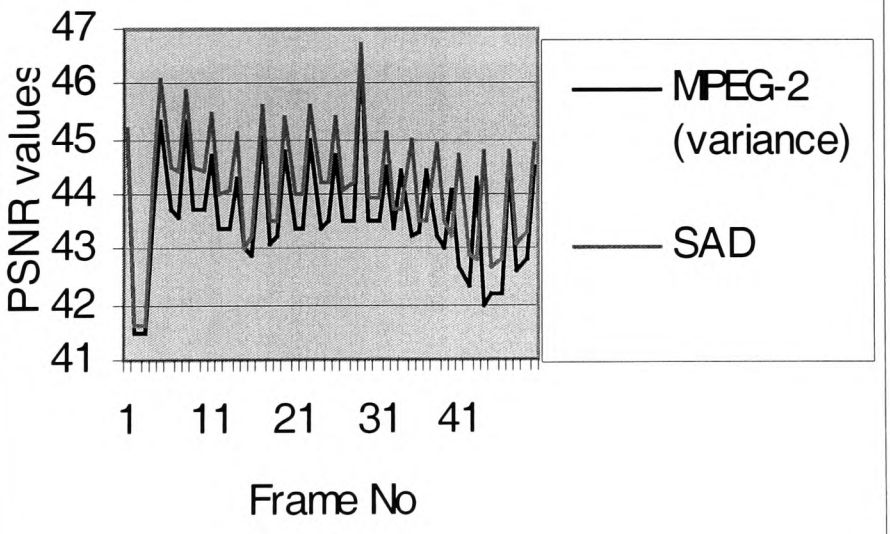

Figure 5.25: Luma Component of salesman sequence

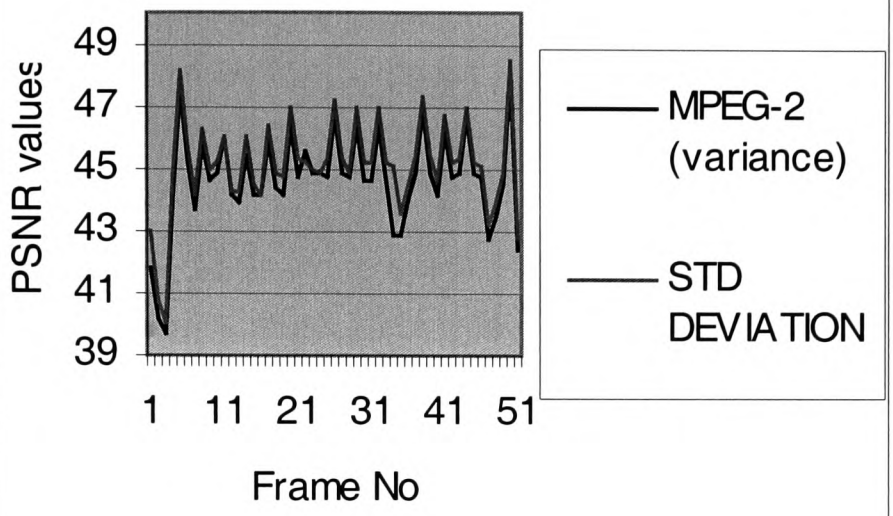

Figure 5.26: Luma Component of salesman sequence

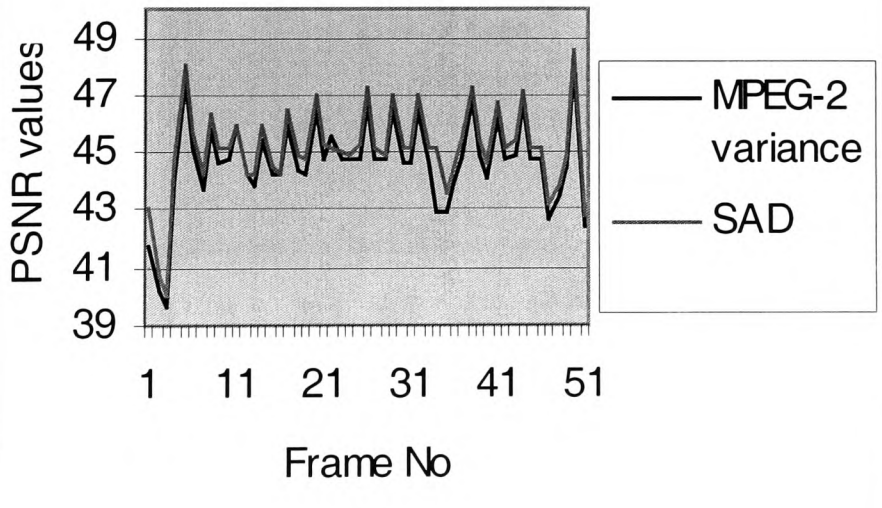

Figure 5.27: Luma Component of trevor sequence

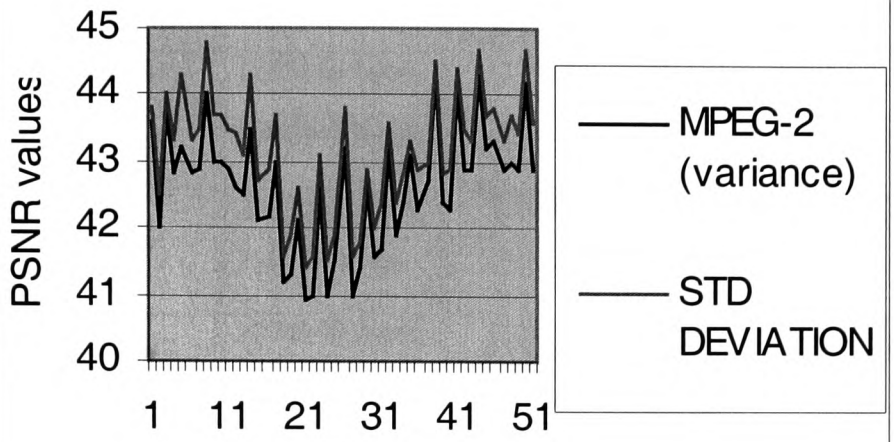

Figure 5.28: Luma Component of trevor sequence

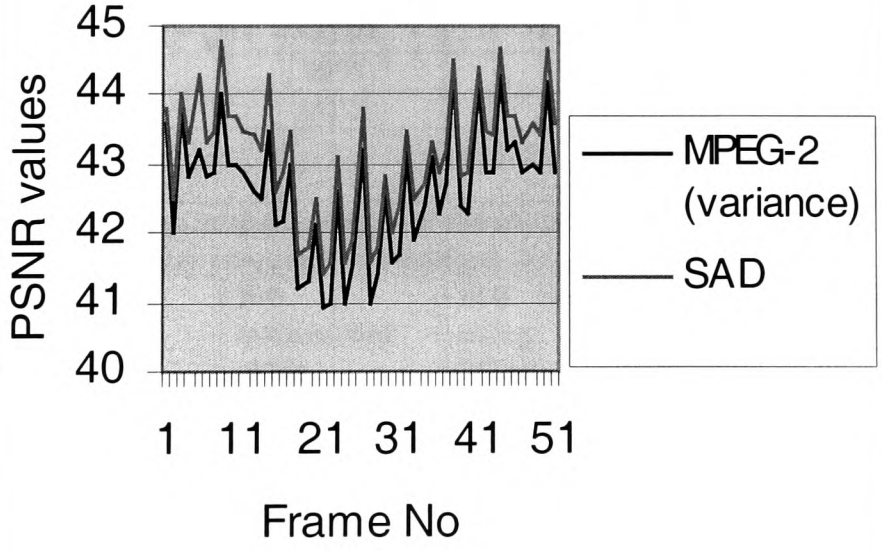

Table 5.4: Comparison of the final number of bits produced			
Test Sequences	**SAD Activity estimate**	**Standard deviation activity estimate**	**MPEG-2**
Miss America (50 frames)	1275165 bytes	1275161 bytes	1275213 bytes
Susie (50 frames)	2500347 bytes	2500293 bytes	2500740 bytes
Mobile (40 frames)	2000223 bytes	2000142 bytes	2000711 bytes
Trevor (50 frames)	293814 bytes	293849 bytes	293847 bytes
Salesman (50 frames)	1276290 bytes	1276278 bytes	1276037 bytes

Table 5.5: Bit savings in transmission of the changes of the quantization parameter (mquant) in SAD case			
Test Video Sequences	**Bits transmitted using SAD for activity estimation**	**Bits transmitted using variance based activity estimation (MPEG-2)**	**% savings in bits**
Miss America (50 frames)	26550	31290	15.15
Mobile (40 frames)	24010	65855	63.54
Susie (50 frames)	51310	82265	37.63
Trevor (50 frames)	9995	17430	42.66
Salesman (50 frames)	25125	36090	30.38

Table 5.6: Bit savings in transmission of the changes of the quantization parameter (mquant) in standard deviation case			
Test Video Sequences	**Bits transmitted using standard deviation for activity estimation**	**Bits transmitted using variance based activity estimation (MPEG-2)**	**% savings in bits**
Miss America (50 frames)	26880	31290	14.09
Mobile (40 frames)	25460	65855	61.34
Susie (50 frames)	52800	82265	35.82
Trevor (50 frames)	9840	17430	43.55
Salesman (50 frames)	25620	36090	29.01

5.6 Review of the R-D approaches in the context of video coding

In general, all existing work on rate-control with R-D optimization methods can be roughly categorised into analytic approaches and empirical approaches. The empirical approaches can be further divided, according to the distortion criterion they seek to minimise, into techniques that attempt to minimise the maximum distortion (MINMAX) and the ones that attempt to minimise the average (or total) distortion (MINAVE) for a given bit rate. The class of MINMAX approaches is dominated by mostly trellis-based techniques, whereas the class of MINAVE approaches can be classified as both trellis-based techniques and model-based techniques. Finally, the class of model-based techniques can be further divided into two major categories depending on whether the bit rate control is based on pre-analysis or prediction. In pre-analysis control schemes, the quantization settings of a frame can be made dependent on future frames, whereas in predictive control schemes, the quantization settings are only dependent on the current and the previously encoded frames. The purpose of this section is to assess all these rate distortion approaches in a real time video coding framework, and explore the possibility of converting those techniques into a real-time framework by revealing their advantages and disadvantages.

5.6.1 Analytic model based approaches

These approaches attempt to predict the R-D characteristics of an input source based on probabilistic models [72,73,90-94,99]. One typical example is the logarithmic rate model [72] which can be outlined below:

$$r(q)=\alpha+\beta*\log(\frac{1}{q}) \qquad (5.11)$$

Where the parameters α and β can be found through curve fitting and they may also

depend on the quantizer's step size q . The main disadvantage of the above models is that they are too inaccurate in terms of the number of bits produced to be useful in a rate control context. Typically, errors in bit rates range from 40% for I frames, up to 150% for P frames, and even up to 400% for B frames. By introducing a third parameter γ to control the curvature of the rate function, another example of existing models can be described [73] as follows:

$$r(q)=\alpha+\frac{\beta}{q^{\gamma}} \tag{5.12}$$

These models improve the bit rate error in comparison with that of logarithmic models.But its accuracy is still unsatisfactory for rate-distortion performance optimisation, especially for P and B frames inside low activity video sequences.

A careful examination of the above models reveal the following four issues:

- Firstly, it is innaccurate to apply such analytic models to R-D optimizations at frame or macroblock level, since video coding is a highly non-linear process, which can not be characterised by those simple models as given above. The innaccuracy of the rate models is further expanded by the fact that practical video encoders also use techniques such as run-length coding, and quantization with wider range of quantization steps, in order to achieve the best possible compression efficiency [77].
- Secondly, the models given above virtually assume that the distortion (in terms of MSE measurement) is proportional to the quantization step. Yet the encoding is a non-linear process, which makes the estimation error even larger [60].
- Thirdly, to improve the accuracy of predicting R-D characteristics, either the models themselves have to be designed into more complicated forms or more control points have to be used for data fitting [60]. In both cases, the computational complexity will

prevent it from being used on real-time basis.

- Finally, the above models only attempt to predict the R-D characteristics of a video source based on a set of simple mathematical formulas. Due to the variety of the statistics embedded in different video sequences, which may not fit in well with the probabilistic models, it is unlikely for those models to perform optimally.

5.6.2 Empirical approaches

Empirical approaches attempt to optimise the R-D performance of a video coding system based on observed data or previously processed data. This category can be further analysed in two broad classes according to the distortion criterion they seek to optimise [78].The first class seeks to minimise the average (or total) distortion measure for a given bit rate or vice versa [58-60]. This class of empirical approaches can be referred to as the MINAVE approaches. The philosophy behind it is that if the average/total distortion is minimised, the best quality of encoding a video sequence is obtained in the long run. The second class is represented by so called MINMAX approaches. Their goal is to minimise the maximum source distortion for a given bit rate, or vice versa. The philosophy behind MINMAX approaches is that, by minimising the maximum source distortion, no single distortion will be extremely bad and hence the overall quality will become stable. Representative techniques proposed in both classes include dynamic programming [58,78] and Lagrange multiplier based optimisations [95,59,62,74-76]. However, all existing techniques involving dynamic programming need to construct a trellis of R-D characteristics that grows exponentially with the size of the input source. Furthermore, when they are combined with Lagrange multiplier based techniques for R-D optimisation, multiple pass and iterations over the input source data are often necessary for the estimation of the optimal R-D characteristics. Hence, these approaches are not suitable for on-line rate

control design. Their computing cost and level of complexity is often high. Nonetheless, an interesting sub-class of MINAVE approaches is the one that uses models (e.g. different kinds of splines) to predict the R-D characteristics from a limited set of controlling points [60,96].In these approaches, the predicted R-D controlling points along with the original ones are fed into an optimisation process (potentially involving multiple iterations) based on the Lagrange multiplier method. In this way, both the MINAVE distortion criterion and the bit rate criterion can be satisfied. As a matter of fact, the model based empirical approaches aim at reducing the computational complexity at the expense of accuracy in estimating the R-D characteristics of the input source. In comparison with the analytic approaches as described above [60] they are shown to exhibit greater accuracy in estimating the R-D characteristics at frame level. Model based approaches can finally be subdivided into pre-analysis control schemes with delayed decision and predictive control schemes, according to the encoding delay allowed [60]. In the delayed decision pre-analysis control schemes, the R-D characteristics of the whole group of pictures (GOP) have to be processed/optimised before the first frame of the GOP can be encoded, thus incurring an encoding delay of one GOP. On the other hand, the basic premise behind predictive control schemes is that, inside a GOP, the frame to be encoded is likely to have similar R-D characteristics with *the last encoded frame of the same type.* This implies that it is sufficient to consider *only one set of R-D characteristics per frame type* for the whole GOP optimization and also that R-D characteristics of future frames can be approximated by R-D characteristics of the most recently encoded frames of the same types. Therefore, while the optimisation is still performed on a GOP basis, the current frame can be immediately encoded and sent to the output channel after its quantization settings have been estimated. Subsequently, the bit budget for the GOP will be updated along with the GOP structure and the procedure will be repeated for a newly arrived frame until all frames

in the GOP have been processed. Thus, there will be only one frame encoding delay. Comparison of the two approaches [60] reveals that predictive schemes further reduce the computational complexity at the expense of sub-optimality in the estimation of the R-D characteristics. The reduction in computational complexity is due to the fact that, instead of constructing controlling points for every frame to be encoded, predictive schemes use one set of controlling points per frame type, which is updated after the current frame is encoded. The key point in predictive rate control schemes is that they are only *slightly* sub-optimal as compared to the delayed decision pre-analysis schemes, which implies that the assumption about the similarity of R-D characteristics between frames of the same type inside a GOP is a valid one. This fact will be used as a foundation for our proposed algorithms in online rate control design using the Lagrange multiplier method in the latter sections.

However, there are two problems associated with the model-based empirical approaches, which relate to computational complexity and the dependency of the quantizers among different frame types inside a group of pictures (GOP). Computational complexity and the dependent quantization are correlated in the sense that frame dependent quantization promotes computational complexity. Typically, the I-frames inside a GOP are the main information carriers since one or more P frames will be predicted from them and they are not predicted themselves from any other frame. Due to the fact that the Mean Square Error (MSE) of the reference frames directly influences the MSE of the predictive frames [60] we can not be frugal in selecting fixed quantizers for the I-frames. In order to achieve a reasonable R-D optimization, we would have to grow a trellis for every I-frame in a GOP. Trellis growth often incurs exponential increase of computational cost with respect to the size of the input source. More details of the discussion will be provided in Section 5.7.1 of this chapter. An ad-hoc selection of quantization steps for I-

frames could potentially run the risk of producing sub-optimal results that would fail to justify its computational overhead. In addition, such a policy could even spoil the quality of successive P and B frames or even cause problems of overflows and underflows in the MPEG-2 buffer. For those model-based empirical approaches, the complexity issue could become worse due to the inter-dependency of different frame types inside a GOP when quantization step is selected. As an example, for every controlling point (R-D pair) of an I-frame, there is a corresponding set (called *representative* set) of controlling points in a P-frame. Therefore, the controlling points in P-frames can be represented as:

$$N_{control\_points\_P} = N_{control\_points\_I} * N_{control\_points\_rep\_set} \qquad (5.13)$$

Where $N_{control\_points\_P}$ denotes the number of controlling points in a P-frame, $N_{control\_points\_I}$ denotes the number of controlling points in an I-frame and $N_{control\_points\_rep\_set}$ denotes the number of controlling points in the representative set. Such a representative set, for instance, could have the quantiser step size being {1,2,3,5,8,13,21,31}, which capture the exponential decay property. For B-frames, the complexity increases even more since they are bi-directionally predicted from two P-frames and they need *even a greater number* of controlling points. Regardless of trellis growth or not, the consequence is that the computational overhead of the model based empirical approaches is still high since considerable number of controlling points are generally needed for the R-D optimization.

Finally, in terms of the encoding delay, the empirical based methods can be subdivided into the GOP delay methods and the frame delay methods [60]. GOP based delay methods would require the entire group of pictures to be fed in and processed before encoding its first frame. Trellis based and spline based approaches fall into this category. As a result, they would be more suitable for off-line applications rather than online ones.

An on-line rate control algorithm suitable for real time video compression needs to

combine the simplicity of a rate/distortion model with the improved estimation of R-D characteristics, offered by empirical approaches, at a low computational cost. The two rate control algorithms we proposed here are designed based on this principle, which adopts the rate-control model used in MPEG-2.

5.7 Towards online rate control using the Lagrange multiplier method in MPEG-2

From the above discussion and the description of the MPEG-2 rate control algorithm in Section 5.2, we can infer the following:

- MPEG-2 is designed for low complexity online video coding of broadcast quality. The rate control algorithm used in the standard is "rate based only", and hence it is not optimal in R-D terms.
- The R-D optimizations proposed in the literature focus on reducing the computational cost and encoding delay as compared to the optimal R-D estimation, while a reasonable estimation of the R-D characteristics is retained. However, they are still computationally intensive especially when dependent quantization among frames is taken into account. In addition, the encoding delay incurred is at least one frame (e.g. predictive control based approaches). Therefore, these approaches are not suitable for on-line rate control.
- The assumption about similarities in R-D characteristics *between frames of the same type* is valid, which can be confirmed by both experiments and reports by the existing published work [60]. Predictive control approaches result in *slightly sub-optimal* R-D estimates as compared to delayed decision pre-analysis approaches. The significance with the former lies in the fact that the computational cost and the encoding delay are significantly reduced.

Motivated by the last observation, we investigated the similarity of the R-D characteristics between adjacent macroblocks in the frame to be encoded. From our extensive experiments, it is observed that adjacent macroblocks in a frame exhibit similar rate-distortion characteristics due to the high pixel correlation and the differential motion vector encoding. In this respect, only a limited neighborhood of the macroblock to be encoded needs to be considered for rate distortion modeling. In the MPEG-2 framework, we can further observe that the correlation due to the differential motion vector encoding is broken at the beginning of every slice (group of macroblocks). This leaves only a small history window of previously encoded macroblocks on the same slice to be considered and thus it is reasonable to assume that the previous macroblock of the one to be encoded is the most correlated one in terms of rate distortion characteristics. Hence, a *localized modeling technique* can be designed to reduce the search intensity when Lagrange multiplier theory is applied to the rate control design. This makes it the key feature in our proposed rate control algorithm design.

Based on localized modeling, we can re-formulate the rate control problem in the MPEG-2 standard (described in Section 5.2) *for the macroblock to be encoded* as follows:

Given a macroblock to be encoded, which is of size N (256 pixels), and a range of quantization parameters $[\text{mquant}_{\min}, \text{mquant}_{\max}]$, find q* = mquant with $\text{mquant} \in [\text{mquant}_{\min}, \text{mquant}_{\max}]$, such that:

$$q^* = \arg\left(\min \frac{1}{N} d(mquant) \right) \tag{5.14}$$

subject to the condition that the macroblock bit rate $r(q^*)$ is not greater than the target rate set by MPEG-2.

According to the Lagrange multiplier method, the following combined cost function can be produced:

$$T_{\lambda(t)}(x(t)) = e_q(t) + \lambda(t) * r_q(t) \qquad (5.15)$$

where, at time t of encoding, $\lambda(t)$ is the Lagrange multiplier used for $x(t)$, the macroblock to be encoded and $e_q(t)$ and $r_q(t)$ are the corresponding distortion and rate for the quantizer step q.

A theorem presented by Shoham and Gersho [61], states that the quantizer step q* corresponding to a rate $r_{q*}(t)$ that minimizes equation (5.15) for a given Lagrange multiplier $\lambda(t)$, is also a solution to equation (5.14) for a target rate $r_{q*}(t)$. Since we use as the distortion measure for the current macroblock the well known Mean-Square-Error (MSE), the term $e_q(t)$ in equation (5.15) actually denotes the normalized sum of the distances between original and reconstructed pixels in the current macroblock. Hence, equation (5.15) can be rewritten as:

$$T_{\lambda(t)}(x(t)) = \frac{1}{N} * \sum_{i=1}^{N} (x_i(t) - \overline{x_i}(t))^2 + \lambda(t) * r_q(t) \qquad (5.16)$$

where N is the macroblock size (256 pixels), $x_i(t)$ and $\overline{x_i}(t)$ represent the original pixel and the reconstructed one in the same macro-block.

To minimize $T_{\lambda(t)}(x(t))$ with respect to rate , we have:

$$\frac{\partial(T_{\lambda(t)}(x(t)))}{\partial(r_q(t))} = \frac{-2}{N} * \sum_{i=1}^{N} (x_i(t) - \overline{x_i}(t)) * \frac{\partial(\sum_{i=1}^{N} \overline{x_i}(t))}{\partial(r_q(t))} + \lambda(t) = 0 \qquad (5.17)$$

For the current macroblock to be encoded, we approximate the derivative of the sum of the reconstructed pixel values with respect to the estimated bit rate as follows:

$$\frac{\partial(\sum_{i=1}^{N} \overline{x_i}(t))}{\partial(r_q(t))} = \frac{\sum_{i=1}^{N} (\overline{x_i}(t) - \overline{x_i}(t-1))}{r_q(t) - r_{q1}(t-1)} \qquad (5.18)$$

where $r_q(t)$ represents the estimated bit rate of the macroblock to be encoded corresponding to a quantizer step size q, and $r_{q1}(t-1)$ represents the actual bit rate of the previously encoded macroblock using a quantizer step of q1.

Substituting equation (5.18) in (5.17) and solving for the estimated bit rate for the current macroblock q will yield:

$$r_q(t)=r_{q1}(t-1)+\frac{2*\sum_{i=1}^{N}(x_i(t)-\overline{x_i(t)})}{N}*\frac{\sum_{i=1}^{N}(x_i(t)-\overline{x_i(t-1)})}{\lambda(t)} \quad t>0 \tag{5.19}$$

We could have solved the minimization problem of equation (5.16) with computationally expensive methods. Such techniques include encoding and reconstructing the current macroblock for every possible quantization step to estimate its R-D characteristics (trellis growing) or using a certain number of controlling points and interpolating the rest of the R-D data by using splines. The high computational complexity of such approaches will be analyzed in Section 5.7.1.

Essentially, the above design relates the estimated rate of the current macroblock to the actual rate of a previously encoded macroblock via a Lagrange multiplier (λ value). To jointly improve the distortion performance, we propose two options *in the same Lagrangian formulation*. The first option is to relate a distortion metric (e.g. MSE) of the current macroblock to the corresponding metric of a previously encoded. The second option is to relate the quantizer step size for the current macroblock with the quantizer step size of a previously encoded macroblock. Among the two options, the second option is justified due to an approximation result in quantization theory [79] which explicitly relates the MSE with the quantizer step size on a macroblock basis. To this end, our low-cost approach can be evidenced by the simple approximation we use for the derivative estimation in equation (5.18).

Equation (5.19) forms the basis of our rate control algorithm design and is used to derive the quantizer moderator *mquant* in MPEG-2 for the macroblock to be encoded. Starting from a fixed Lagrange multiplier λ, we can control the actual rate of the macroblock to be encoded on line, based on the information of R-D statistics from the previously encoded macroblock only. It should be noted that, in equation (5.19), the actual rate produced by encoding the previous macroblock (i.e *r(t-1)*) is always known before the current macroblock is encoded and as such it can be treated as an available constant. In addition, the recursion between different values of λ, except $\lambda(t=0)$ that is a fixed constant, is of the following form:

$$\lambda(t) = \lambda(t-1) \pm c \qquad t > 0 \tag{5.20}$$

Where *c* denotes a constant step size whose sign depends on the feedback mechanism.

From equation (5.19), we can also observe that the Lagrange multiplier could be regarded as a global moderator for estimation of bit rate as the current macro-block is encoded.

In contrast to traditional R-D approaches where the quantizer step size for the whole frame to be encoded is determined after multiple iterations on the Lagrangian formulation, MPEG-2 determines the quantizer step size on a macroblock basis and based on a "rate only" model (Section 5.2). Consequently, by using a Lagrangian formulation which incorporates distortion explicitly in the feedback mechanism on a macroblock basis, we expect to improve the accuracy of the rate model used by MPEG-2 in R-D terms. In the context of MPEG-2, this will result in improving the accuracy in estimating the modulation parameter Q_j which indicates the contribution of the buffer fullness in the estimation of the macroblock quantizer step *mquant* in equation (5.2) .

From the discussion in Section 5.2, we can infer that MPEG-2 performs an accurate quantization step assignment per macroblock when every macroblock rate is equal to the target bit rate set by the standard. The target rate is the same for all macroblocks inside a frame and hence can be treated as a constant. Consequently, a uniform information loss distribution is assumed since the same number of bits is allocated for every macroblock. Suppose that we are to encode a macroblock at time t. According to the MPEG-2 rate control scheme, the buffer fullness at that instant will be:

$$d^x j(t) = d + \sum_{i=1}^{t-1}(actual\_rate(i) - target\_rate) \tag{5.21}$$

Where d denotes the buffer occupancy from previous frames, *actual_rate(i)* the rate produced by macroblock i and *target_rate* the target rate per macroblock set by the standard.

From our rate control design highlighted by equations (5.19-5.20), a more optimal R-D based approach can be designed as follows:

$$d^x j(t)_{corr} = d + \sum_{i=1}^{t-1}(actual\_rate(i) + \delta(i) - target\_rate) \tag{5.22}$$

where (actual_rate(i)+ δ (i)) is the right hand side of equation (5.19)

Hence, the quantization step size in equation (5.2) will now be determined by:

$$mquant = \frac{d^x j(t)_{corr} * 31}{r} \quad = \quad Q_j \tag{5.23}$$

Where r is the reaction parameter (constant) discussed in Section 5.2 and $d_j^x(t)_{corr}$ is now the corrected estimate from equation (5.22). The normalisation of the buffer estimate by using equation (5.23) has to be performed in order to avoid the problems of overflow and underflow.

The feedback criterion is another important part of our scheme. We can reward the buffer if the previous macroblock produces less bits than it was expected and penalize the buffer on the contrary.

Finally, the proposed algorithm can be summarized by the following pseudo-codes:

if $(r(t-1) < B(t-1))$
{
decrease λ *according to* (5.20)
calculate the estimated bit-rate of
the current macroblock according to (5.19)
calculate the corrected buffer estimate according to (5.22)
calculate mquant according to (5.23)
}
else
{
increase λ *according to* (5.20)
calculate the estimated bit-rate of
the current macroblock according to (5.19)
calculate the corrected buffer estimate according to (5.22)
calculate mquant according to (5.23)
}

Where *r(t-1)* is the actual bit rate produced by the previous macroblock, *B(t-1)* is the expected rate of the previous macroblock and the Lagrange multiplier is the control parameter for the feedback scheme. The above operations apply to all macroblocks inside a frame, except the first one. For the first macroblock, the estimate for the actual rate *r(t=0)* is calculated as in MPEG-2. This design only applies to P and B frames inside a GOP in our algorithm design. For I-frames, the MPEG-2 scheme is retained.

In an MPEG-2 context, the R-D statistics of the previously encoded macroblock along with its quantization step size *mquant* are already known when the current macroblock is processed. Hence, they do not need to be estimated again. Consequently, we

would only need to calculate the distortion metric (in the MSE approach) for the current macroblock before it is encoded, and use this metric to estimate its bit rate in the Lagrangian formulation. In the case of using the quantizer step size approximation, we do not need any extra operations since MPEG-2 calculates *mquant* for the current macroblock anyway. In this case we can directly use the quantizer step size for the current macroblock to estimate its bit rate. It should be noted that since we consider the problem of visually weighted quantization [80,81] as a separate one, it remains to be our primary aim to improve the performance of the MPEG-2 rate control algorithm *in terms of R-D performance*. To this end, although the quantizer step size per macroblock as calculated by MPEG-2 is a combined estimate of buffer fullness and visual weighting (see Section 5.2), we only use the buffer fullness part in the approximation for the quantizer step size.

By examination of the above rate control design and the relationship between the MSE and quantization, our second proposed rate control algorithm can be formulated. Specifically, the quantization theory [79] reveals the fact that the Mean Square Error (MSE) is approximately proportional to the square of the quantization step size for the macroblock to be encoded, which can be described as follows:

$$\frac{1}{N} * \sum_{i=1}^{N} (x_i(t) - \bar{x}_i(t))^2 \approx \frac{(Q(t))^2}{12} \tag{5.24}$$

where t refers to the current time indicating the macroblock to be encoded. Hence, the cost function in equation (5.15) can be rewritten as:

$$T_{\lambda'(t)}(x(t)) = \frac{(Q(t))^2}{12} + \lambda'(t) * r'(t) \tag{5.25}$$

where $Q(t)$ is the quantization step size for the current macroblock to be encoded, $r'(t)$ is the expected bit rate for the current macroblock when $Q(t)$ is used as the quantization step

and $\lambda'(t)$ is the Lagrange multiplier. Our objective is to minimize the combined cost function with respect to the bit rate estimate of the current macroblock. This gives us:

$$\frac{\partial(T'\lambda'(t)(x(t)))}{\partial(r'(t))} = \frac{Q(t)}{6} * \frac{\partial(Q(t))}{\partial(r'(t))} + \lambda'(t) = 0 \tag{5.26}$$

We approximate the derivative of the quantizer step size with respect to the estimate of the bit rate for the current macroblock as follows:

$$\frac{\partial(Q(t))}{\partial(r'(t))} = \frac{Q(t) - Q(t-1)}{r'(t) - r'(t-1)} \tag{5.27}$$

Substituting equation (5.27) in (5.26) and solving for the estimate of the bit rate for the current macroblock yields:

$$r'(t) = r'(t-1) + \frac{Q(t)}{6} * \frac{Q(t-1) - Q(t)}{\lambda'(t)} \qquad t > 0 \tag{5.28}$$

The rest of the procedure in determining the quantization step *mquant* is exactly the same as in the Mean Square Error case (MSE). The main difference here is that the computational cost is even lower. This is because the quantizer step sizes of the current and previous macroblocks are already available and so is the bit rate of the previously encoded macroblock. This eliminates the reconstruction of the current macroblock and saves the computing cost on all operations involved, which include inverse quantization, IDCT, adding the errors in place and calculating the Mean Square Error (MSE).

The proposed algorithms attempt to combine the simplicity of the MPEG-2 rate control scheme to the R-D optimizations described in Section 5.6.2. Instead of iterating multiple times for R-D optimization over a number of controlling points in order to estimate the quantization step size for the current frame/macroblock, we can achieve this online and with low computational cost based on a combination of the localized modeling principle

and the Lagrange multiplier theory.

A rate control algorithm design on top of MPEG-2 and based on the features just described would have the following properties:

- It would improve the estimation of the R-D characteristics as compared to MPEG-2 rate control scheme due to the explicit consideration of distortion in the selection of the quantizer step size on a macroblock basis.
- Compared to the least computational cost techniques described in Section 5.6.2 for R-D optimization (predictive control using controlling points), the proposed schemes would reduce the computational cost even further. Due to the localized modeling, the proposed algorithms require reconstructing the current macroblock only once (MSE approach) or not at all (quantizer step size approach), as opposed to multiple reconstructions needed in the R-D techniques involving a number of controlling points.
- The encoding delay would also be reduced with the proposed schemes, compared with the least computationally intensive R-D approaches. The predictive control schemes would require the R-D optimization process to be completed for the whole frame before the first macroblock of this frame is actually encoded and sent to the output channel. Furthermore, for every frame to be encoded, the optimization is still performed for the whole group of pictures, which potentially imply multiple iterations in the Lagrangian formulation. In the proposed schemes, the first one is based on the MSE criterion, and it would be able to improve the R-D performance on the fly and send the encoded macroblock to the channel with *only one macroblock* delay. The second proposed scheme, which is quantizer step based, would require *zero delay* since no macroblock reconstruction is necessary.

5.7.1 Complexity analysis

To highlight our low cost approach in designing the proposed algorithms, this section contributes a detailed complexity analysis in comparison with representative existing R-D based rate control algorithms. A fair measure of computational cost for the rate control problem in MPEG-2, in a rate distortion sense, will have to incorporate two factors [82]. The first factor is the number of comparisons needed for finding the optimal trellis path in the optimization stage and the second is the number of individual operations needed for constructing the controlling points on the rate distortion curve. Clearly, for a frame with N macroblocks and X controlling points on the rate distortion curve, X^N comparisons are needed in the optimization stage for the optimal trellis path. The number of operations needed for constructing a controlling point (rate, distortion pair) can be analyzed as follows:

- Number of operations needed for the DCT calculation per macroblock ((luminance + chrominance) 8*8 blocks). We denote these operations by the letter D.
- Number of operations needed for the quantization per macroblock ((luminance + chrominance) 8*8 blocks). We denote these operations by the letter Q.
- Number of operations needed for entropy coding of the quantised DCT coefficients. Only at this stage the rate is known for a controlling point. We denote these operations by the letter E.
- Number of operations needed for inverse quantization per macroblock ((luminance + chrominance) 8*8 blocks). We denote these operations by the letter L.
- Number of operations for the IDCT calculation per macroblock ((luminance + chrominance) 8*8 blocks). We denote these operations by the letter I.

- Number of operations needed for adding the errors between the current macroblock and its best match on the reference frame in place. We denote these operations by the letter A.
- Number of operations for the mean square error calculation (MSE) per macroblock. Only after this step, the distortion is known. We denote these operations with the letter M.

An optimization algorithm with respect to the quantizer step size that is trellis based and uses X controlling points would need N*X*(D+Q+E+L+I+A+M) + x^N operations, which makes it extremely difficult for real time video coding. In the case of model based empirical approaches (i.e different kinds of splines) the number of operations depends on both the frame type and the spline type. In general, due to the inter-dependency in quantization between predictor and the predicted (or bi-directionally predicted) frames, the number of controlling points for I frames is smaller than the number of controlling points for P frames. In turn, since B frames are predicted from two P frames, the number of controlling points for P frames is smaller than that of controlling points for B frames. In addition, the number of operations needed to fit a spline model depends on the type of spline and includes both the operations (additions + multiplications) for estimating the rate/distortion but also the operations needed to estimate the spline coefficients. In general simpler splines need less operations. If we denote the operations needed to fit a spline model with the letter S, we have:

$$N*X_I*(D+Q+E+L+I+A+M+S)<N*X_P*(D+Q+E+L+I+A+M+S)<N*X_B*(D+Q+E+L+I+A+M+S)$$

(5.29)

where X_I, X_P, X_B denote the number of controlling points for I,P,B frames respectively.

The main difference between predictive control schemes and delayed pre-analysis control schemes in terms of the number of controlling points used in the optimization is that for the former there is only one set of controlling points per frame type, compared to one set per individual frame for the latter. So the total number of operations in a GOP based R-D optimization for a delayed pre-analysis control scheme would be:

$$W_I*N*X_I*(D+Q+E+L+I+A+M+S)+W_P*N*X_P*(D+Q+E+L+I+A+M+S)+W_B*N*X_B*(D+Q+E+L+I+A+M+S)$$

(5.30)

where W_I, W_P, W_B denote the number of I,P,B frames inside a group of pictures.

Whereas, the total number of operations in a GOP based R-D optimization for a predictive control scheme would be smaller, which can be worked out as:

$$N*X_I*(D+Q+E+L+I+A+M+S)+N*X_P*(D+Q+E+L+I+A+M+S)+N*X_B*(D+Q+E+L+I+A+M+S)$$

(5.31)

This is because the controlling points for each frame type have to be constructed only once and would not be updated until the current frame is encoded .

In contrast, the proposed algorithm based on the Mean Square Error (MSE) in Section 5.7 is not trellis based and does not need controlling points or spline models for optimization. So, the required amount of operations over a group of pictures is:

$$N*W_I*(D+Q+E+L+I+A+M)+N*W_P*(D+Q+E+L+I+A+M+S)+N*W_B*(D+Q+E+L+I+A+M+S) \quad (5.32)$$

The second algorithm proposed in Section 5.7 has an even smaller computational cost, since it does not involve macroblock reconstruction. So the number of operations over a GOP is:

$$N*W_I*(D+Q+E)+N*W_P*(D+Q+E)+N*W_B*(D+Q+E) \quad (5.33)$$

In the above complexity analysis, we only considered the operations needed for the construction of the controlling points with respect to the length of the input source when this length is measured in macroblock units. We did not consider the number of iterations

over this set of controlling points in order the optimization constraints to be satisfied. This is the case in the R-D optimization methods proposed in the literature, but not for our proposed algorithm design since we only use the Lagrangian formulation as a feedback mechanism to improve the rate prediction for the macroblock to be encoded. Although fast methods for reducing the number of iterations exist [61], this number is usually greater than one. The number of iterations can not be expressed directly as a function of the length of the source, since it has to do more with the specific optimization method chosen and the constraints imposed on the problem. It actually indicates the number of comparisons needed in order the minimum Lagrangian cost to be found. Nonetheless, the number of iterations may still be important in terms of the absolute number of operations, if the optimization method is slowly converging [60].

Even with the fact that only the total number of operations for the construction of controlling points on a GOP basis is counted, it is evident that both the rate control algorithms proposed are of smaller computational complexity as compared to delayed pre-analysis control schemes. As compared to the predictive control schemes, the proposed algorithm design is also of lower complexity. This is because spline based predictive control schemes would still need a number of controlling points per frame type, which is usually more than the number of frames of this type inside a group of pictures in an MPEG-2 context. In this case, without considering again the multiple iterations of the predictive control schemes, it can be worked out that the total number of operations in equations (5.33) and (5.32) is less than the operations in equation (5.31).

Although direct buffer state feedback schemes are usually of lower computational complexity as compared to traditional R-D approaches, their complexity still depends on the number of controlling points used in the optimization. The only difference is that such schemes would have to rely on current or past information as opposed to the ability of

predicting future information, which is the case in traditional R-D approaches. Any such optimization scheme that does not utilize localized modeling and excluding the number of iterations for the optimization constraints to be satisfied would need the number of operations per group of pictures given in equation (5.31). An example of such work can be found in Chen and Wong [63].Even direct buffer state feedback schemes that attempt to minimise the Lagrangian formulation of equation (5.15) on a single macroblock basis could be computationally expensive because of the techniques used to collect the R-D data. In relevant work found in Choi and Park [59], curve fitting techniques are used to obtain the R-D data points. In terms of complexity, these techniques are still computationally intensive and thus this part of the optimization will still have to be performed offline. This is because in curve fitting techniques the number of operations needed is dependent on the relation between rate and distortion in an MPEG-2 context, on the number of control points used in the interpolation method and on the number of control points that need to be estimated from the fitting process. Given that most proposed R-D models are either exponential or logarithmic (Section 5.6.1) , that the interpolation accuracy is increased with the number of interpolators and that in MPEG-2 we need to consider 32 quantization choices per macroblock, the computational cost can still be high.. Schemes like the aforementioned are apparently more computationally intensive than our proposed rate control algorithms which use a combination of localised modelling and of low cost R-D estimation online.

In the context of TM5 technique, each macroblock of the current frame will be reconstructed after the frame is encoded for two reasons. Firstly, the reconstructed frame may be used as a reference for the next frame to be encoded. Secondly, the PSNR value needs to be calculated to indicate the image quality in the reconstructed video sequences. To this end, it is irrelevant in terms of operations if a macroblock is reconstructed

immediately after it is encoded or if it is reconstructed with the rest of the macroblocks after the whole frame is encoded. That's why we do not count the operations for reconstructing the previous macroblock in equation (5.19) in the complexity analysis. In conclusion, the complexity of the two rate control algorithms we proposed can be regarded as the same level as that in the current MPEG-2 rate control scheme.

5.7.2 Experiments

The proposed rate control algorithms were tested versus the MPEG-2 rate control algorithm for a variety of video sequences including both fast (e.g. calendar sequence) and slow motion ones (e.g. Miss America). In order to test the performance of both the proposed schemes under different channel rates, we run the experiments at the low, medium and high ranges of MPEG-2, based on the TM5 implementation. This roughly corresponds to channel rates of 1.152, 5 and 10 Megabits per second respectively. The testing under different channel rates is important since it implies different R-D behavior [77].We also tested the proposed schemes under small (20*16 Kbits), medium (80*16 Kbits) and large (160*16Kbits) buffer capacities to ensure that the proposed improvements in R-D estimation would not violate buffer constraints. The initial choice for the Lagrange multiplier in both the proposed algorithms was set to 1000 with increments or decrements of a fixed step size of 20. In the proposed rate control algorithms, the target settings for each frame in a group of pictures is determined by the MPEG-2 algorithm, as opposed to explicit target settings set by the algorithms proposed in the literature [60].

On the average, improvements from 0.5db to 1db per frame were observed for the same final number of output bits produced in all the test cases. The PSNR performance of the online rate control algorithm described in Section 5.7 (MSE based) versus MPEG-2 is shown in Figures 5.29-5.33 for the same number of target bits. Figures 5.34-5.38 compare the PSNR performance of the second proposed algorithm in Section 5.7 (Quantizer step size based) versus MPEG-2 while the target bit rate is maintained the same. The compression rates for both schemes versus MPEG-2 are shown in Table 5.7.

As expected, both the proposed algorithms trade computational complexity for sub-optimality in estimating the R-D characteristics of a video sequence, which is a common

characteristic of all "buffer feedback" based schemes. It is worth noticing though, that the average PSNR improvements in model based empirical approaches rarely exceed 1dB per frame [60],yet their complexity in terms of absolute number of operations is high as analyzed in Section 5.7.1. In addition, any simplification of the spline models (e.g. piece-wise linear splines instead of piece-wise cubic splines [60])is shown to induce losses of up to 0.2 db per frame for the same number of bits produced. This factor seriously questions the gains of model-based empirical approaches in terms of R-D optimization versus computational complexity, especially in the context of low end-to-end delay video coding. It can also be seen from the results that for each test video sequence the two rate control methods perform virtually the same in PSNR terms for the same bit rates. This is expected since they both rely on a combination of localized modeling for reducing the computational cost and a Lagrangian formulation for improving the estimation of R-D characteristics. Finally, both the proposed algorithms will reduce the encoding delay as compared to the R-D approaches described in Section 5.6.2.

The proposed MSE based rate control algorithm will induce an encoding delay of *one macroblock only* as compared to predictive control approaches that require at least one frame encoding delay. The quantizer step size based rate control algorithm will induce *zero encoding delay.*

Traditional rate distortion approaches can be sped up with parallel implementation or with pipelined compression [58,60], although this may require special hardware or software. They are still relevant in the context of real time video coding because there are real time applications which can afford high end-to-end delay [60].Furthermore, when the delay and computational cost are not an issue, these techniques are shown to perform close to the optimal in estimating R-D characteristics of an input source [58,60].However, standards such as MPEG-2 or H.263 are designed for low end-to-end delays and based on

simple designs not only for their rate control but for all stages of the compression system. Indeed, there may be applications such as videophones or video-conferencing that high end-to end-delay is not acceptable. It is in this light that low cost rate control algorithms, which are still model based but also locally R-D optimized, are extremely important in any attempt to improve the online rate-distortion performance of video coding systems.

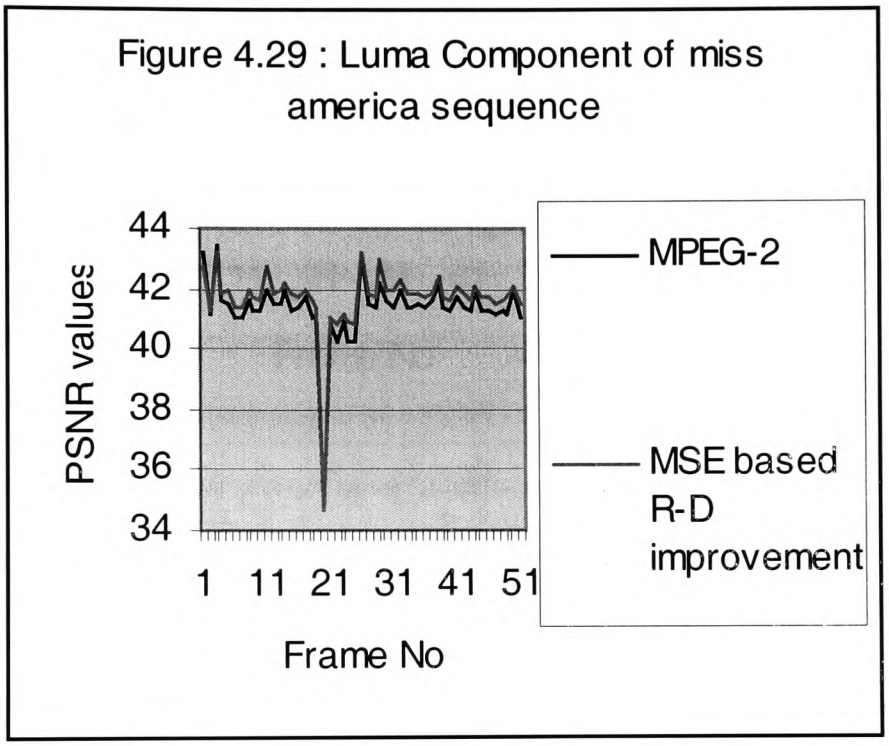

Figure 4.29 : Luma Component of miss america sequence

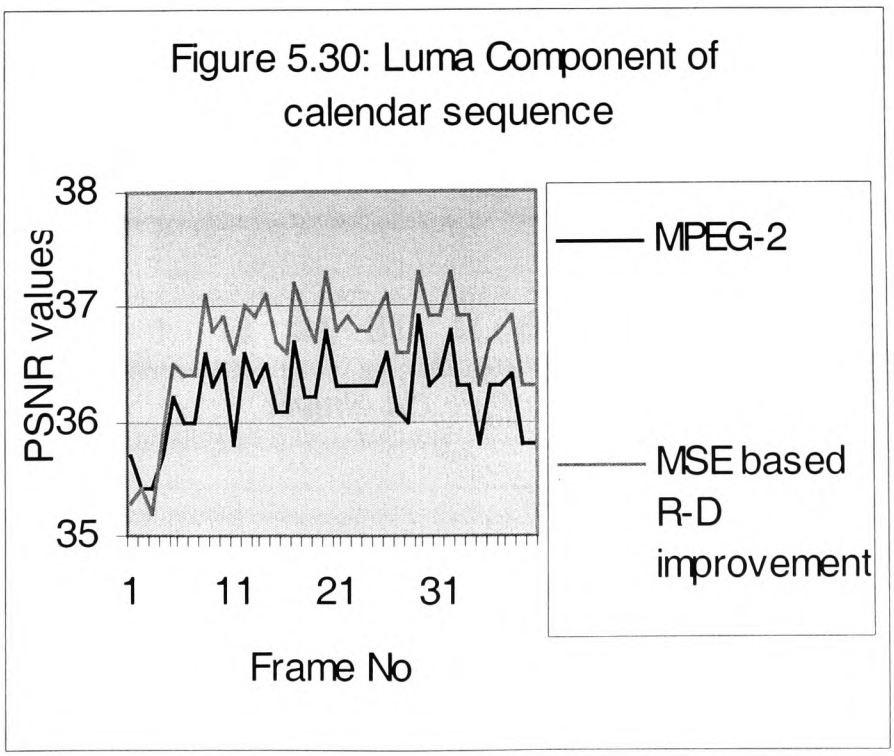

Figure 5.30: Luma Component of calendar sequence

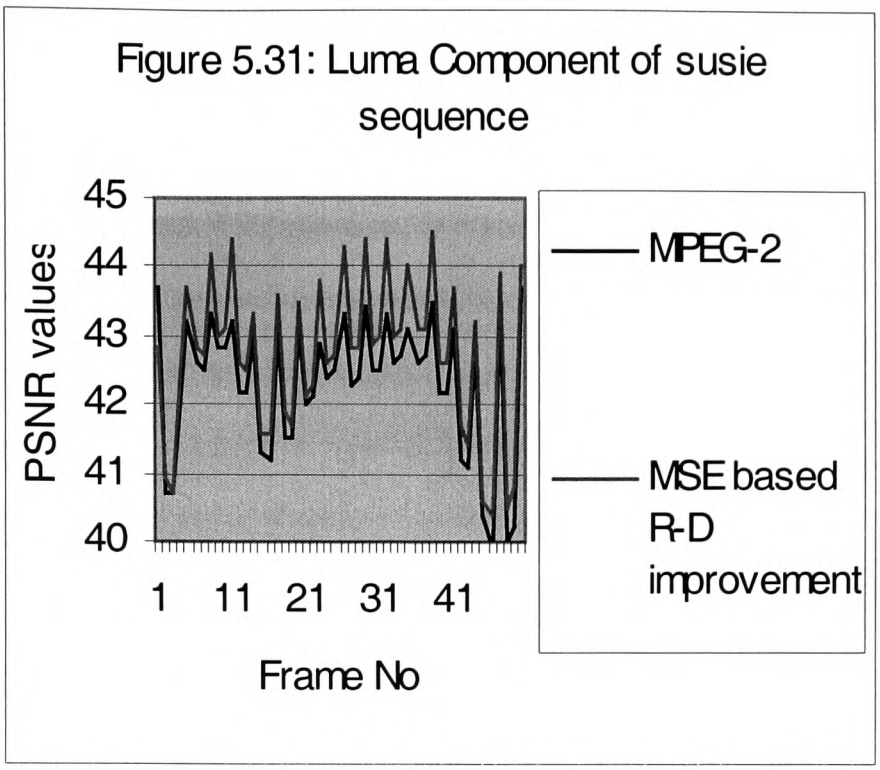

Figure 5.31: Luma Component of susie sequence

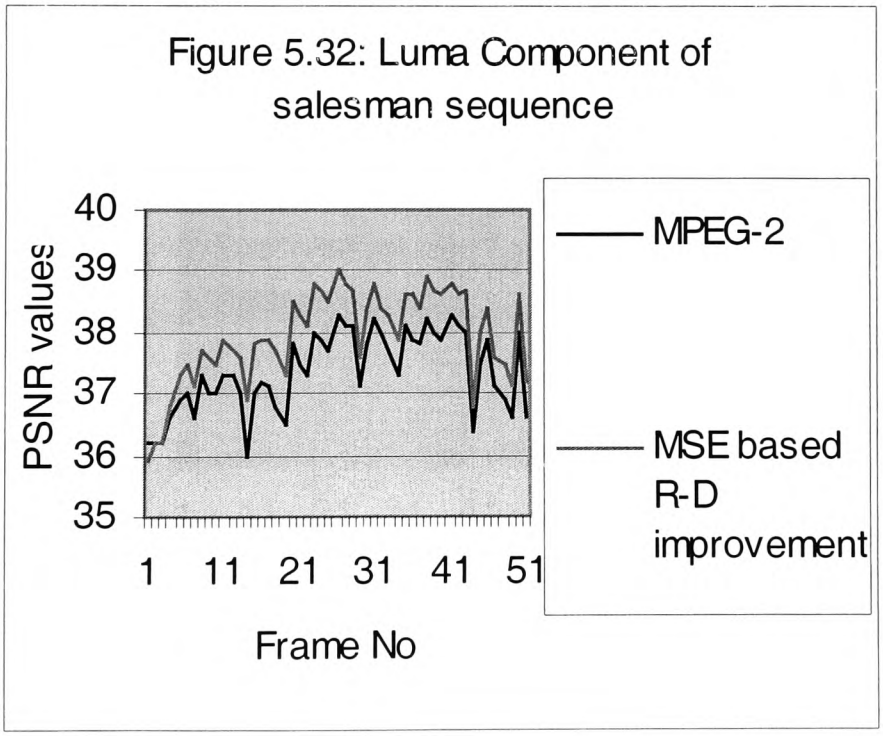

Figure 5.32: Luma Component of salesman sequence

Figure 5.33: Luma Component of trevor sequence

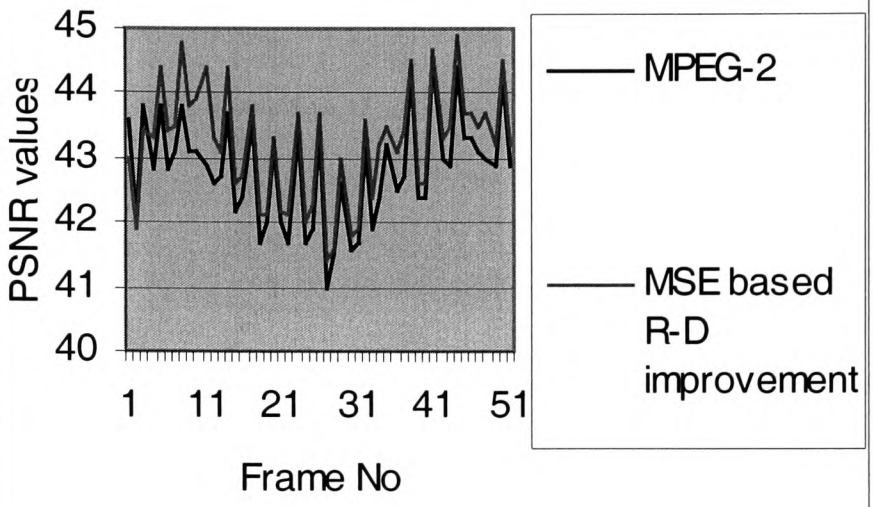

Figure 5.34: Luma Component of miss america sequence

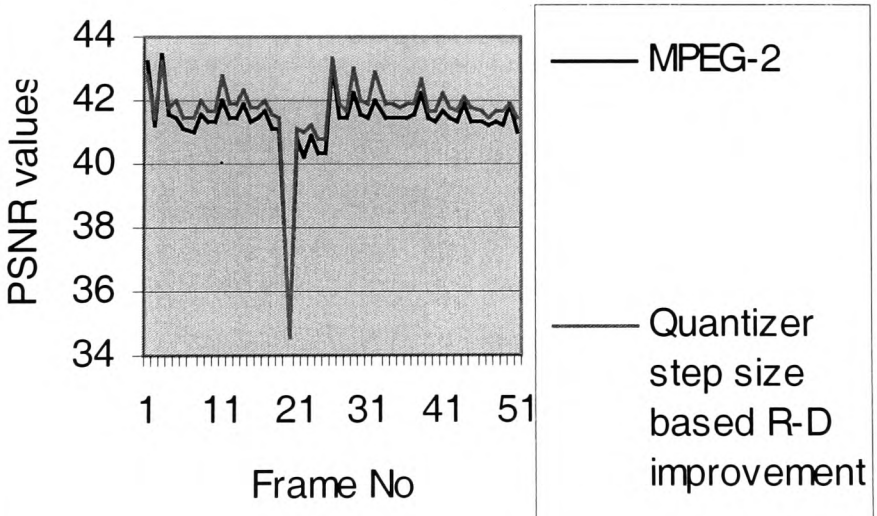

Figure 5.35: Luma Component of calendar sequence

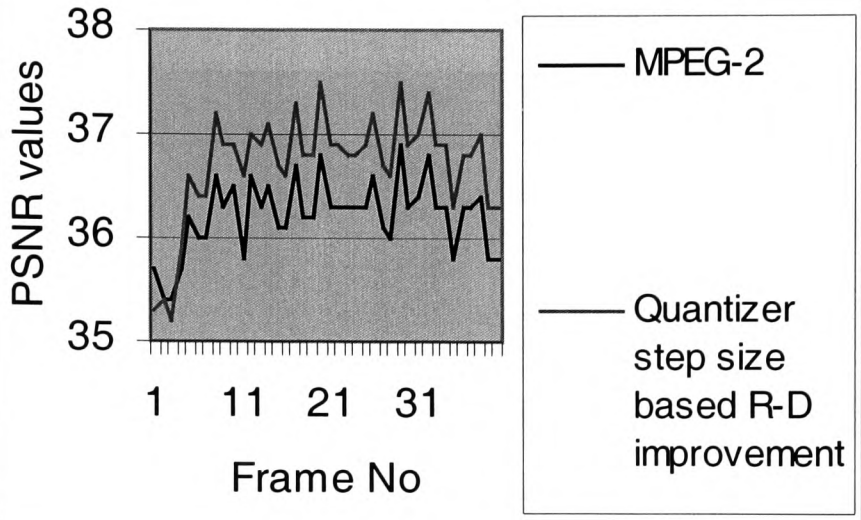

Figure 5.36: Luma Component of susie sequence

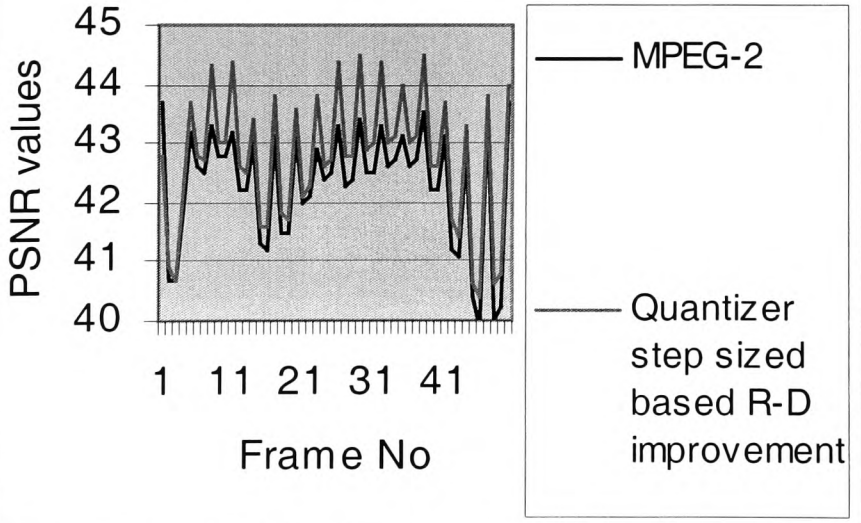

Figure 5.37: Luma Component of salesman sequence

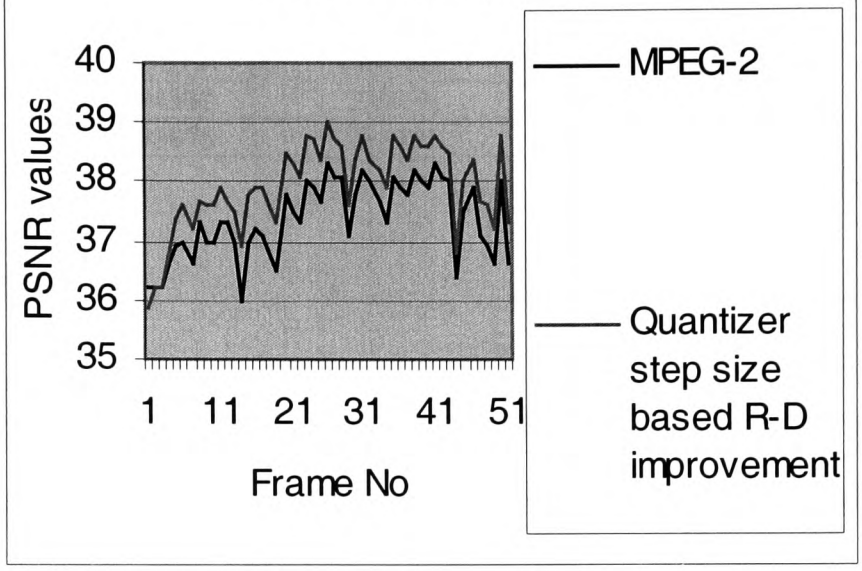

Figure 5.38: Luma Component of trevor sequence

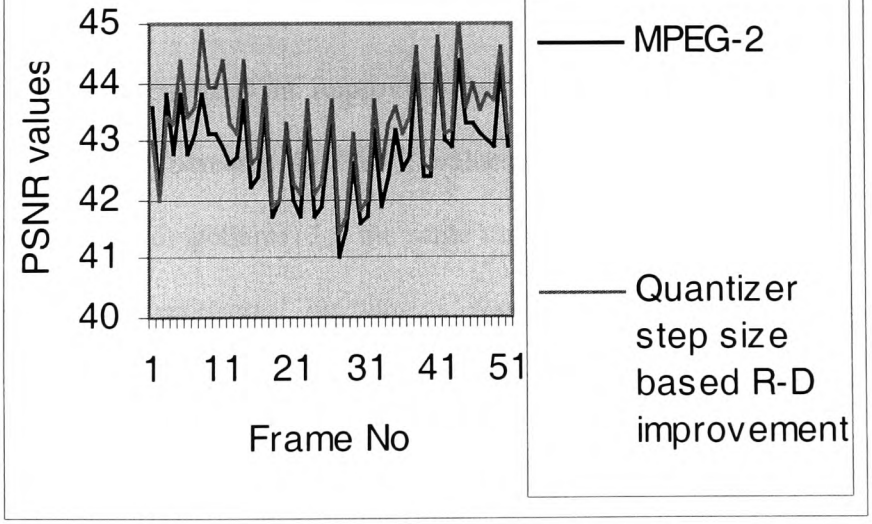

Table 5.7: Comparison of the final number of bytes produced			
Test Sequences	**MPEG-2**	**MSE based R-D improvement**	**Quantization step size based R-D improvement**
Miss America	294048	293921	293873
Calendar	833855	833800	833800
Susie	1458991	1458444	1458350
Salesman	294302	294076	294082
Trevor	293878	293831	293800

5.8 Conclusions

In this chapter, the problem of *low computational cost R-D improvements* of the MPEG-2 rate control scheme was considered. It was shown that for low encoding delay video compression, there exist schemes which improve "on the fly" the R-D performance of the rate control algorithm of the standard. In the first part of the chapter, four *improved activity estimation schemes* in R-D terms were proposed. It was shown that *local activity estimation,* based on the distance of the activity of the currently encoded macroblock as related to the activity of adjacent macroblocks and to the average activity of the previously encoded frame, may be beneficial in improving the R-D performance of the standard. Experiments showed that increases in PSNR values of encoded frames up to 2.5db (luminance+chrominance components) for the same number of bits as the standard can be achieved. Subsequently, *exponential modulation* was used to reduce the unnecessary fluctuation of the quantizer step size per encoded macroblock. The reduction in this fluctuation results in a more uniform quality across macroblocks of the encoded frame, while at the same time more quantization parameters are packed in the lower end of the quantization spectrum. This improves the PSNR values per frame since the majority of the macroblocks are assigned lower quantization parameters. The increase in bit production due to smaller quantizer step sizes is offset by the reduction in the overheads transmitted. It

was shown that the proposed modulators achieved per frame improvements up to 3.5db in the luminance and 3.5 and 3db in the two chrominance components respectively for the same final number of bits as MPEG-2. Two *novel statistical estimates* were also proposed in order to reduce the quantization step assignment fluctuations in MPEG-2 rate control. It was shown that the variability in the activity normalization phase of the quantizer step size selection, caused by *the extra sensitive to changes* variance, can be reduced by using the Sum of Absolute Differences (SAD) and the standard deviation of pixel samples (STD) instead. Thus, more uniform quality can be achieved across macroblocks of a frame, for the same normalization function as the standard, since less overheads need to be transmitted in order to indicate quantizer step size changes. Improvements up to 2.8db per frame for both the proposed statistical estimates were observed for the same final bit rate as the standard.

In the second part of the chapter, the "rate only" based rate control scheme of MPEG-2 was enriched by explicitly including distortion in the estimation of the quantization step through a low cost Lagrangian formulation. Two *locally optimal* algorithms in R-D terms were proposed and their complexity was assessed in terms of absolute number of operations versus a variety of well known R-D optimization approaches. It was shown that, whereas well known computationally intensive R-D approaches rarely achieve improvements of over 1db per frame, the proposed schemes achieved 0.5db-1db improvements per frame *for a much lower computational cost and encoding delay* for the same number of bits as the standard.

The proposed low cost activity estimates for improving the R-D performance along with the locally optimal (in R-D terms) Lagrangian based schemes, could have significant potential in real time applications or in applications where the PSNR performance is at premium. Typical examples include surveillance systems, video aided terrain mapping etc.

CHAPTER 6- THESIS CONCLUSION AND FURTHER RESEARCH

This thesis reported on the design, development and analysis of ten low cost algorithms and four estimates for image and video compression. The proposed algorithms and estimates refer to the JPEG-LS standard for still image compression and to the MPEG-2 and MPEG-4 standards for video compression.

In the third chapter, three algorithms were proposed for JPEG-LS. Initially, a multilevel information loss distribution is developed in order to indirectly optimize the image quality in visual terms. The HVS principle followed, reflects the different tolerance of the human visual system across different textures and the prediction scheme of the standard was modified to reflect this principle. Specifically, the retaining of information as much as possible in smooth textures was enforced, whereas information loss was increased in rough areas where the HVS is less sensitive. In this manner a better balance between visual quality and compression rates was achieved. The multilevel information loss distribution was shown to produce higher compression rates and better visual quality than JPEG-LS. It was also shown to be very competitive even in PSNR performance for the same compression rates as the standard, provided a suitable triplet of information loss parameters was chosen. Subsequently, the possibility of adding rate control to the standard was investigated. Two low cost rate control algorithms were designed based on the suggested information loss distribution and their performance in both PSNR terms and visual quality was assessed. It was shown that in contrast to computationally expensive rate distortion techniques for optimizing the R-D performance, it is possible to optimize the visual performance via low cost schemes and produce images of better visual quality for the same compression rates as JPEG-LS. Since every rate control scheme has to enforce the compression rate close to a defined target, whereas the standard just exploits the natural compressibility without considering rate control, both of the rate control schemes proposed

showed an average degradation of 2-3 db in PSNR terms for the same compression rates as the standard. It was also shown that the two proposed low cost rate control schemes are capable of controlling the compression rates in the ranges 2:1 and 3:1. This is important in the context of digital photography where users may decide to compress an image at a compression rate of their choice or alternatively to fit an image in the space of a previously deleted image. The third chapter concluded with potential applications of one of the rate control algorithms in the context of medical imaging. The domain of medical imaging imposes stricter requirements as compared to the domain of the entertainment industry in terms of the information loss distributions, since in applications such as wound/rash healing we can afford to lose less information on edges. Despite this fact, one of the rate control schemes proposed, managed to outperform JPEG-LS by retaining smooth texture better than the standard for the same compression rates even in this application domain. In the case of medical imaging, the compression rates were also controlled in the ranges 2:1 and 3:1.

The key point in the HVS based, multilevel information loss distribution, was the characterization of texture according to the JPEG-LS prediction scheme. A refined JPEG-LS prediction scheme with more than three texture denominations could improve both the results in terms of the information loss distribution and consequently the HVS based rate control algorithms. This of course would increase the complexity of the algorithms but it still is a future direction to be considered, especially in applications where the visual quality is of outmost importance.

In the fourth chapter, four low cost algorithms were presented for utilizing pixel value trends in improving compression rates and MSE performance in the MPEG-4 and JPEG-LS standards. In the MPEG-4 case, the pixel trend considerations for the padding problem in boundary macroblocks resulted in the proposed Linear Extrapolated Padding technique

(LEP). When this technique was applied in padding the reference macroblock in the horizontal direction, it resulted in compression improvements of up to 6.9% as compared to MPEG-4. No significant compression improvements were found when LEP was also applied in the vertical direction. For severely distorted boundary macroblocks, the Extrapolated Average Padding (EAP) technique was also proposed and a hybrid algorithm that dynamically chooses the most appropriate of the two padding techniques proposed was designed. The choice of the optimal padding technique depended on a simple measure of distance mismatch as compared to a fixed threshold. Improvements in compression rates of up to 9% were observed with the hybrid padding scheme, as compared to the padding scheme of the MPEG-4 standard.

In this direction, a more elaborate mismatch measure and a dynamic threshold could enhance the performance of the hybrid scheme. The low computational complexity was a prime factor in the proposed design and this justifies the simple design choices.

The fourth chapter concludes with two low cost algorithms for adding diagonal edge detection in JPEG-LS. The standard does not include diagonal edge detection since it is limited to horizontal and vertical edges only. Although this is the case in most images, in the presence of diagonal edges, JPEG-LS will perform poorly in MSE terms due to inadequate prediction. The proposed two algorithms exploit pixel trend variation via local gradients in order to detect diagonal edges accurately and use a weighted scheme for the predicted values, based on the pixel correlation inside the predictive template. The two schemes show improvements in MSE terms of 3 and 2% correspondingly for the same compression rates as the standard. It is worth noticing that the two algorithms for diagonal edge detection do not change the compression rates of the standard. This is expected since no modification in the entropy coding scheme of JPEG-LS was attempted. The more

accurate prediction resulting from the proposed schemes could be used for improving the statistical context modeling, which is a key element of JPEG-LS.

A more elaborate diagonal edge detection could be a way forward but it would involve increasing the computational complexity. As in chapter two, the simple design choices taken were aimed in low computational cost schemes.

In the fifth chapter, the issue of low cost improvements of the rate distortion performance in MPEG-2 based video coding was addressed. Four improved estimates were proposed for improving "on-the-fly" the rate distortion performance of the MPEG-2 rate control scheme. They all aimed in reducing the unnecessary fluctuations of the quantizer step size assignment per macroblock, for the rate control scheme of the standard. Ideas like local activity estimation, exponential modulation and alternative statistical estimates (sum of absolute differences between sample pixels and mean and normalization based on standard deviation instead of variance) were explored. It was shown that the activity normalization phase of MPEG-2 is not optimal in R-D terms and as such, the above estimates can provide low cost solutions for R-D improvements. The PSNR performance of exponential modulation showed improvements of up to 3.5db, the local activity estimation of up to 2.5db and the SAD and STDEV of up to 2.8db for the same final number of bits as the standard for a variety of commonly used video sequences.

A more elaborate activity estimation and normalization process could improve R-D performance in MPEG-2, but this would result in increasing the computational complexity.

Chapter 5 concluded by presenting two low cost algorithms for online R-D improvements in MPEG-2 rate control, which are based on the buffer based rate control scheme of the standard but they also use Lagrangian theory for local optimization. By minimizing locally the Lagrangian R-D formulation by a simple derivative approximation, we can improve in a computationally inexpensive manner the "rate only" buffer feedback mechanism of

MPEG-2 by explicitly considering distortion in the estimation of the quantizer step size per macroblock. The value of the proposed algorithms stems from the fact that PSNR improvements of 0.5-1db are achievable for the same number of bits as the standard, with extremely low computational cost optimizations and encoding delay. This has to be compared to the 1db improvements for the same number of bits as MPEG-2, of well known R-D optimization approaches which are computationally very intensive, they incur high encoding delays and as such they are realistically only applicable offline. A detailed complexity analysis of the proposed two algorithms versus a variety of well know R-D approaches is included in the chapter.

Both the proposed schemes used the rate distortion characteristics of the previously encoded macroblock only in the Lagrangian formulation. R-D optimization approaches that consider a limited window of macroblocks in the past or future, can be used for improving even more the rate distortion performance of the MPEG-2 rate control scheme. Although this direction is possible, it will undoubtedly increase complexity since the number of operations needed for the collection of the R-D characteristics and the number of iterations needed for the optimization method to converge will be higher.

References

1. C.J. van den Branden Lambrecht and O.Verscheure, "Perceptual quality measure using a spatio-temporal model of the human visual system,", in Proc. of IS&T/SPIE Digital Video Compression '96, (San Jose, CA), pp 450-461, Feb. 1996.

2. C.A. Burbek and D.H. Kelly, "Spatio-temporal characteristics of visual mechanisms", excitatory-inhibitory model," Journal of the Optical Society of America, Vol 70, pp 1121-1126, Sep. 1980.

3. G.E. Legge and J.M.Foley, "Contrast masking in human vision", Journal of the Optical Society of America, Vol 70. pp. 1458-1471, Dec 1980

4. B.A.Wandell, Foundations of Vision, Sinauer Associates, Inc, 1995

5. ISO/IEC JTC 1/SC 29/WG1 FCD 14495-public draft, July 16th, 1997. http://www.jpeg.org/public/jpeglinks.htm

6. JTC 1.29.14, 15444: Call for contributions for JPEG-2000, http://www.jpeg.org

7. MPEG-2 encoder v.1.1a, MPEG Software simulation Group, (online) http://www.mpeg.org/tristan/MPEG/MSSG

8. MPEG-2, Test model 5(TM5) Doc. ISO/IEC JTC1/SC29/WG11/93-225b, Test Model Editing Committee, Apr 1993.

9. ISO/IEC/MPEG'97: "MPEG-4 video verification model 8.0", Document N1996, July 1997.

10. ISO/IEC/MPEG'97: "MPEG-4 Requirement – Version 3", MPEG Requirements Group, Document N1682,April 1997.

11. P. Kauff., B. Makai., S. Rauthenberg., U. Golz, J. De Lameillieure, T. Sikora, "Functional coding of video using a shape-adaptive DCT algorithm and an object-based motion prediction toolbox", IEEE Transactions on Circuits & Systems in Video Technology-7, pp. 181-196, February 1997.

12. R. Schaafer, "MPEG-4: a multimedia compression standard for interactive applications and services", IEE Electronic & Communication Engineering Journal, Vol. 10, No. 6, pp. 253-262, 1998.

13. T. Sikora, "Low complexity shape-adaptive DCT for coding of arbitrarily shaped image segments", Signal Processing, Image Communications, Vol. 7, pp. 381-395, 1995.

14. D.T Hoang, E.L Linzer and J.S.Vitter "Lexicographic bit allocation for MPEG video", Journal of Visual Communication and Image Representation, Dec. 1997.

15. L.Qian, D.Jones, K.Ramchandran, S.Appadwedula "A General Joint Source-Channel Matching Method for Wireless Video Transmission", ICIP 99.

16. MPEG-4 Standards - MPEG97/N1796 - ISO/IEC JTC1/SC29/WG11- July 1997.

17. G.K.Wallace, "The JPEG Still Picture Compression Standard", IEEE Trans. On Consumer Electronics, December 1991.

18. Digital Compression and Coding of Continuous tone Still Images, Part 1, Requirements and Guidelines, ISO/IEC JTC1 Draft International Standard 10918-1, November 1991

19. Digital Compression and Coding of Continuous tone Still Images, Part 2. Compliance Testing, ISO/IEC JTC1 Committee Draft 10918-2, December 1991.

20. M.Nelson, Data Compression Book, M&T Books, 1991

21. D.A.Huffman, "A method for the Construction of Minimum-Redundancy Codes", Proc. of the Inst. Of Radio Engineers, Vol. 40, 1952, pp. 1098-1101.

22. ITU-T Recommendation H261: Video codec for audio-visual services at px64 kbits, Mar. 1993

23. Draft ITU-T Recommendation H263: Video Coding for Low bit rate communication, July 1995.

24. ITU-T/SG15, Video Codec Test Model, TMN7, Nice, Feb. 1997.

25. ITU-T/SG15, Video Codec Test Model, TMN8, Portland, Jun. 1998.

26. C.J. van den Branden Lambrecht and O.Verscheure, " A Working Spatio-Temporal model of the Human Visual System for Image Restoration and Quality Assessment Applications", in Proceedings of ICASSP, pp 2293-2296, Atlanta, GA, May 7 1996.

27. A.Watson, Handbook of perception and human performance, chapter 6, Temporal Sensitivity, John Wiley 1986.

28. I.A.Olzak and J.P.Thomas, Handbook of perception and human performance, chapter 7, Seeing Spatial Patterns, John Wiley, 1986.

29. C.J. van den Branden Lambrecht and O.Verscheure, "Efficient Spatio-Temporal Decomposition for Perceptual Processing of Video Sequences", in Proc. of ICIP, Lausanne, Switzerland, September 16-19, 1996

30. O.Verscheure, "Perceptual Video Activity Measure", Technical Report, Swiss Federal Institute of Technology, June 1996

31. W.B.Pennebaker and J.L.Mitchell, "JPEG Still Image Data Compression Standard", New York, Van Nostrand Reinhold, 1993.

32. C.S.Wen-Hsiung Chen and S.Fralick, " A fast computational algorithm for the discrete cosine transform", IEEE Trans. On Communications, 1997.

33. A.Ligtenberg and M.Vetterli, " A Discrete Fourier/Cosine Transform chip", IEEE Journal of Selected Areas in Communications",vol. SAC-4, pp 49-61, Jan. 1996.

34. Z.Wang, " Fast algorithms for the discrete wavelet transform and the discrete Fourier transform", IEEE Trans. On Signal Processing, vol ASSP-32, pp. 803-816, Aug. 1984

35. B.Lee, " A new algorithm to compute the discrete cosine transform", IEEE Trans on Signal Proc. vol ASSP-32, pp. 1243-1245, Dec. 1984

36. P.Duhamel and H.H.Mida, " New 2n DCT algorithms suitable for VLSI implementation", in Proc of ICASSP 87, (Dallas), p. 1805, Apr. 1987.

37. C.Loeffler, A.Ligtenberg and G.Moschytz, " Practical fast 1-D DCT with 11 multiplications", in Proc. of ICASSP 1989.

38. E.Feig and E.Linzer," Discrete Cosine Transform algorithms for image data compression", in Proc. of Electronic Imaging '90, p. 84, 1990.

39. M.Vetterli, "Tradeoffs in the computation of mono and multi-dimensional DCT's", tech report, Ctr. Of Telecommunications Research, Columbia University, June 1988.

40. E.Feig and S.Winograd, " On the multiplicative complexity of the discrete cosine transform", IEEE Trans. On Information theory, 1992.

41. H.R.Wu and Z.Man, " Comments on fast algorithms and implementation of 2-D recursive cosine transform", IEEE Trans. On Circuits and Systems for Video Technology, 1998.

42. N.I.Cho and S.U.Lee, " A fast 4*4 DCT algorithm for the recursive 2-D DCT", IEEE Trans. On Circuits and Systems for Video Technology, 1998.

43. A.Said and W.Pearlman, " A new fast and efficient image codec based on Set Partitioning in Hierarchical Trees", IEEE Trans. Circuits and Systems for Video Technology, vol. 6, June 3, 1996.

44. J.M.Shapiro, " Embedded image coding using zero-trees of wavelet coefficients", IEEE Trans. On Signal Proc., 41(12):3445-3462, Dec. 1993.

45. G.M.Davies and S.Chawla, " Image coding using optimised significance tree quantization", in Proc. Data Compression Conference (J.A.Storer and M.Cohn, eds) pp. 387-396, Mar. 1997.

46. M.Vetterli and J.Covacevic, Wavelets and Sub-band Coding, Prentice-Hall, Englewood Cliffs, NJ. 1995.

47. M.Vetterli, "Multi-dimensional sub-band coding: Some theory and algorithms", Signal Processing, vol. 6, pp. 97-112, 1984.

48. J.W.Woods and S.D.O'Neil, "Sub-band coding of images", IEEE Transactions on Acoustics, Speech and Signal Processing, vol. 32, no 5, pp. 1278-1288, Oct. 1986.

49. J.Covacevic, "Sub-band coding systems incorporating quantizer models", IEEE Transactions on Image Processing, vol 4, no 5, pp. 543-553, May 1995.

50. Still Picture Interchange File Format, ITU-T Recommendation T.84[ISO/IEC 10918-4].

51. B.G.Haskell, A. Puri, and A.N.Netravali, " Digital Video: An introduction to MPEG-2", New York, Chapman and Hall,1997.

52. ITU-T Recommendation, H324, "Line Transmission of non-telephone signals-Terminal for low bit rate multimedia communication".

53. A.Puri, R.Aravind and B.G.Haskell, "Adaptive frame/field motion compensated video coding", Signal Processing Image Communication, vol. 1-5, pp. 39-58, Feb. 1993.

54. Special Issue on MPEG-4, Signal Processing, Image Communication, vol. 9, May 1997.

55. Special Issue on MPEG-4, Signal Processing, Image Communication, vol. 10, July 1997.

56. International Committee for Standardisation, Final Committee draft ISO/IEC 14496-2, " Coding of Audio Visual Objects: Visual".

57. G.Privat and I.Le-Hin, " Hardware support for shape decoding from 2D region based image representations", in Multimedia Hardware Architectures 1997, Proc. SPIE, San Jose, CA, vol. 3021, 1997, pp. 149-159.

58. A. Ortega, K. Ramchandran and M. Vetterli. 'Optimal trellis-based buffered compression and fast approximations', IEEE Trans. Image Processing, Vol 3, Jan 1994, pp 26-40.

59. J. Choi and D. Park. 'A stable feedback control of the buffer state using controlled Lagrange multiplier method', IEEE Trans. Image Processing, Vol 3, Sept 1994, pp 546-558.

60. L.J. Lin and A. Ortega 'Bit-rate control using piecewise approximated rate-distortion characteristics' IEEE Trans. Circuits & Systems for Video Technology, Vol 8, No 4, August 1998, pp 446-459.

61. Y. Shoham and A. Gersho 'Efficient bit allocation for an arbitrary set of quantizers', IEEE Trans. Acoust., Speech, Signal Processing, Vol 36, Sept 1988, pp 1445-1453.

62. S.W Wu and A. Gersho 'Rate-constrained optimal block-adaptive coding for digital tape recording of HDTV' IEEE Trans. Circuits Syst. Video Technology, Vol 1, Mar 1991, pp100-112.

63. C.T Chen and A. Wong 'A self-governing rate buffer control strategy for pseudo-constant bit rate video coding', IEEE Trans. Image Processing, Vol 2, Jan 1993, pp 50-59.

64. C.Y Hsu, A. Ortega and A. Reibman 'Joint selection of source and channel rate for VBR video transmission under ATM policing constraints' IEEE J. Select. Areas Commun., Vol 15, Aug. 1997, pp 1016-1028.

65. G. Keesman, I. Shah and R. Klein-Gunnewiek 'Bit-rate control for MPEG encoders' Signal Processing, Image communication, Vol 6, pp 545-560, Feb 1995.

66. L.J Lin , A. Ortega and C.C.J Kuo 'Rate control using spline-interpolated R-D characteristics' Proc. SPIE Visual Commun. Image Processing'96, Orlando, FL., Mar. 1996, pp 111-122.

67. A. Reibman and B.G Haskell 'Constraints on variable bit-rate video for ATM networks', IEEE Trans. Circuits Syst. Video Technology, Vol 2, pp 361-372, Dec. 1992.

68. T. Wiegand, M. Lightstone, et al. 'Rate-distortion optimized mode selection for very low bit rate video coding and the emerging H.263 standard', IEEE Trans. Circuits Syst. Video Tech. Vol 6, Apr 1996, pp 182-190.

69. J. Zdepsky, D. Raychaudhuri and K. Joseph 'Statistically based buffer control policies for constant rate transmission of compressed digital video', IEEE Trans. Communication, Vol 39, No 6, June 1991, pp 947-957.

70. T.Sikora, "The MPEG-4 Video Standard Verification Model", IEEE Trans. CSVT. Vol. 7, No 1, Feb. 1997.

71. E.A.Edirisinghe, J.Jiang and C.Grecos, " A Novel Shape Padding Technique for improving MPEG-4 Compression Efficiency", IEE Electronics Letters, Vol. 35, No 17, Aug. 1999, pp. 1453-1454.

72. H.M Hang and J.J Chen "Source model for transform video coder and its application – part I: fundamental theory", IEEE Trans. Circuits and Systems for Video Technology, Vol 7, pp. 287-311, April 1997.

73. W.Ding and B.Liu, "Rate Control of MPEG video coding and recording by rate quantization modelling," IEEE Trans. Circuits Syst. Video Tech., vol. 6, no 1,pp. 12-20,Feb 1996.

74. K.Ramchandran, A.Ortega, and M.Vetterli, "Bit Allocation for dependent quantization with applications to multiresolution and MPEG video coders", IEEE Trans. Image Proc, vol 3, no 5,pp. 533-545,Sep. 1994.

75. D.W.Lin, M.H.Wang and J.J.Chen, "Optimal delayed coding of video sequences subject to a buffer size constraint", Proc. of SPIE Visual Communications and Image Processing, 1993, Cambridge, MA, November 1993,pp. 223-234.

76. J.Lee and B.W.Dickinson, "Joint optimization of frame type selection and bit allocation for MPEG video encoders", Proc. ICIP 1994, Austin, TX, 1994, vol 2, pp. 962-966.

77. J.R.Corbera, S.Lei, "Rate Control in DCT Video Coding for Low Delay Communications", IEEE Trans. Circuits Syst. Video Tech., vol. 9, no 1, pp. 172-185, Feb 1999.

78. G.Schuster, G.Melnikov, A.K.Katsaggelos, "A Review of the Minimum Maximum Criterion for Optimal Bit Allocation among Dependent Quantisers", IEEE Transactions on Multimedia, vol 1, no 1,pp 3-17, March 99.

79. A.Gersho, R.M.Gray, Vector Quantization and Signal Compression, Norwell, MA, Kluwer Academic, 1992.

80. S. Daly, K. Matthews and J.R.Corbera, "Face-based visually optimised image sequence coding", in Proc. IEEE Int. Conf. Image Processing (ICIP), Chicago, IL, Oct. 1998, vol. III, pp. 443-447.

81. L-J Lin and A.Ortega, "Perceptually based video rate control using pre-filtering and predicted rate-distortion characteristics", in ICIP 97, Santa Barbara, CA, Sept. 1997.

82. G.M.Schuster, A.K.Katsaggelos, "Fast and efficient mode and quantizer selection in the rate distortion sense for H263", Proceedings of Visual Communication and Image Processing,1996.

83. J. Jiang 'A low cost content adaptive and rate controllable near lossless image codec in DPCM domain' *IEEE Trans. On Image Processing,* Vol 9, No 4, 2000, pp543-554.

84. J. Jiang and M. Reddy ' An open-loop rate control scheme for JPEG-LS near lossless image compression' *IEE Electronics Letters,* Vol 35, No. 6, 1999, pp465-466.

85. M.J Weinberger, J.J Rissanen. and R.B Arps. 'Applications of universal context modeling to lossless compression of grey-level images' IEEE Trans. On Image Processing, Vol 5, No 4, 1996, pp 575-586.

86. M.J Weinberger, G.Seroussi, G.Sapiro 'LOCO-I: A low complexity, context-based, lossless image compression algorithm' Proceedings of Data Compression Conference, Utah, 1996, pp 140-149.

87. B.Guo, J.Jiang, S.Y.Yang 'Revision to Edge detection based prediction in JPEG-LS', Proceedings of SIP 2000,Las Vegas.

88. R.F Rice 'Some practical universal noiseless coding techniques: III' Tech. Report JPL, Vol 91-3, Jet Propulsion Laboratory, Pasadena, CA, November, 1991.

89. R.F Rice 'Some practical universal noiseless coding techniques' Tech. Report JPL, Vol 79-22, Jet Propulsion Laboratory, Pasadena, CA, March, 1979.

90. D.F.Frimout, J.Biemond and R.L.Lagendik, " Forward rate control for MPEG recording", in Proc. SPIE Visual Commun. Image Processing, Cambridge, MA, Nov. 93, pp. 184-194.

91. A.Nicoulin, M.Mattaveli, W.Li, A.Basso, A.Popat, and M.Kunt, " Image sequence coding using motion compensated sub-band decomposition", in Motion Analysis and Image Sequence Processing, M.I.Sezan and R.N.Lagendjik, Eds. Norwell, MA, Kluwer Academic, 1993, pp. 225-256.

92. B.Tao, H.A.Peterson and B.W.Dickinson, "A rate quantization model for MPEG encoders", in Proc. ICIP, Santa Barbara, CA, vol. 1, Oct. 1997, pp. 338-341.

93. T.Chiang and Y.Q.Zhang, "A new rate control scheme using quadratic rate distortion model", IEEE. Trans. Circuits and Systems for Video Technology, vol. 7, pp. 246-250, Feb. 1997.

94. A.Y.K.Yan and M.L.Liou, " Adaptive Predictive Rate Control Algorithm for MPEG videos by rate quantization method", in Proc. Picture Coding Symposium. Berlin, Germany, Sept. 1997, pp. 619-624.

95. D.A.Pierre, " Optimization Theory with Applications", New York, Dover, 1986.

96. K.M.Uz, J.M.Shapiro and M.Czigler, " Optimal bit allocation in the presence of quantizer feedback", Proc. ICASSP 93, Minneapolis, MN, Apr. 1993, vol. V, pp. 385-388.

97. D.LeGall, "MPEG: a video compression standard for multimedia applications", Communications of the ACM, vol 34, no, 4, pp. 46-58, April 1991.

98. J.Mitchell, W. Pennebaker, C.E. Fogg and D.J. LeGall, MPEG video compression standard, Chapman and Hall, New York, 1997.

99. J.Katto and M.Ohta, "Mathematical analysis of MPEG compression capability and its application to rate control", in Proc. of ICIP 95, Washington DC, 1995, vol. 2, pp. 555-559.

100. D.G.Lueberger, Linear and Nonlinear Programming, Addison Wesley 1984.

101. H.Everett, "Generalised Lagrange multiplier method for solving problems of optimum allocation of resources", Operations Research, vol. 11, pp. 319-417, 1963.

102. G.Dahlquist and A.Bjorck, Numerical Methods, Prentice-Hall, 1974.

103. J.E.Dennis and R.B.Schnabel, Numerical methods for unconstrained optimisation and non-linear equations, Prentice-Hall, Englewood Cliffs, NJ. 1993.

104. K.Ramchandran and M.Vetterli, "Best wavelet packet bases in a rate distortion sense", IEEE Trans. On Image Processing, vol.2, no.2, pp. 160-175, Apr. 1993.

105. A Ortega, " Optimal bit allocation under multiple rate constraints", In Proc. of DCC 96,Snowbird, Utah, Apr. 1996.

106. J.J.Chen and D.W.Lin, " Optimal Coding of Video Sequences over ATM networks", In Proc. ICIP 1995, vol. 1, Washington DC, pp.21-24, Oct. 1995.

107. A.J.Viterbi and J.K.Omura, Principles of Digital Communication and Coding, New York, McGraw-Hill, 1979.

108. G.D.Forney, " The Viterbi algorithm", Proc. IEEE, vol. 61, pp. 268-278, Mar. 1973.

109. A Ortega, Optimisation Techniques for adaptive quantization of image and video under delay constraints, Phd Thesis, Columbia University 1994.

110. T.G.Cover and J.A.Thomas, Elements of Information Theory, Ch. 13, John Wiley and sons, Inc. 1991.

111. ITU-T 81. Information Technology, Digital Compression and Coding of Continuous-Tone Still Images, Requirements and Guidelines. Recommendation T.81, ITU, 1992.

112. M.Schindler, "Practical Huffman Coding", http://compressconsult.com/huffman, October 1998.

113. G.G.Langdon, "An introduction to arithmetic coding", IBM.J.Res.Develop., 28, 135-149,1984.

114. J.J. Rissanen and G.G.Langton, "Arithmetic Coding", IBM.J.Res. Develop.",23, 149-162, March 1979.

115. R.M.Witten, I.H.Neal and J.G.Cleary, "Arithmetic Coding for Data Compression", Communications of the ACM, 30(6),520-540,June 1987.

116. N.S.Jayant, and P.Noll. "Digital Coding of waveforms: Principles and Application to Speech and Video", Prentice Hall, Englewood Cliffs, New Jersey, 1984.

117. M.Goldberg and H.Sun, " Frame adaptive vector quantization for image sequence coding", IEEE Trans. On Comm., COM-33:629-635, May 1998.

118. W-T Chen, R-F Chang, and J-S Wang, " Image sequence coding using adaptive finite state vector quantization", IEEE Trans. On Circuits and Sys. For Video Technology, 2(1):15-24,Mar. 1992.

119. R-F Chang, W-T Chen and J-S Wang, " Image Sequence Coding using adaptive non-uniform tree structured vector quantization", Journal of Visual Communication and Image representation, 2(2): 166-176, June 1991.

120. R-F Chang, W-T Chen and J-S Wang, " Image sequence coding using adaptive tree structured vector quantization with multipath searching", IEE Proc. I, 139(1): 9-14, Feb. 1992.

121. C.Constantinescu and J.A.Storer, " Online adaptive vector quantization with variable size codebook entries", In Proc. of the Data Compression Conference, pages 34-41, Mar. 1993.

122. A.N.Netravali and B.G.Haskell, Digital Pictures, Representation and Compression, Plenum Press, New York, 1988.

123. G.K.Wallace, "The JPEG still picture compression standard", Communications of the ACM, 34(4):30-44,April 1991.

124. JPEG technical specification: Revision (DRAFT), joint photographic experts group, ISO/IEC JTC1/SC2/WG8, CCITT SGVIII, August 1990.

125. Y.H.Kim and J.Modestino, " Adaptive entropy-coded sub-band coding of images", IEEE Trans. On Image Proc, 1(1):31-48,, Jan 1992.

126. P.H.Westerink, D.E.Boekee, J.Biemond and J.W.Woods, "Sub-band coding of images using vector quantization", IEEE Trans. On Comm, 36:713-719, 1989.

127. M.Antonini, M.Barlaud, P.Mathieu and I.Daubechies, " Image coding using wavelet transform", IEEE Trans. On Image Processing, 1(2):205-220, Apr. 1992.

128. A.Lewis and G.Knowles, " Image compression using the 2-d wavelet transform", IEEE Trans. On Image Processing, 1(2):244-250, Apr. 1992.

129. C.Chrysafis and A.Ortega, "Efficient context based entropy coding for lossy wavelet packet compression", In Proc. of DCC 97.

130. K.Ramchandran and M.Vetterli, " Rate distortion optimal fast thresholding with complete JPEG/MPEG decoder compatibility", IEEE Trans. On Image Processing, 1994.

131. K.Ramchandran and M.Vetterli, "Syntax constrained encoder optimization using adaptive quantization thresholding for JPEG/MPEG coders", in J.A.Storer and M.Cohn editors, Proc. of the Data Compression Conf., pages 146-155,Snowbird, Utah, March 1994.

132. Z.Xiong, N.P.Galatsanos and M.T.Orchard, " Marginal analysis prioritisation for image compression based on hierarchical wavelet decomposition", In Proc. of ICASSP '93, pages 546-549, Minneapolis, MN, Apr. 1993.

133. P.A.Chu, M.Effros, R.M.Gray, " A vector quantization approach to universal noiseless coding and quantization", IEEE Trans. On Info. Th, 1994.

134. M.Effros, P.A.Chu and R.M.Gray, " Variable dimension weighted universal vector quantization and noiseless coding", In Proc. of Data Compression, DCC'94, pages 2-11, Snowbird, Utah, Mar. 1994.

135. N.S.Jayant, "Adaptive quantization with a one word memory", Bell. Sys. Tech. J. 52(7):1119-1144, Sept. 1973.

136. S.Chrissafulli, R.B.Bitmead, " Adaptive quantization : solution via non-adaptive linear control", IEEE Trans. On Comm, 41(5): 7141-748,May 1993.

137. A.R.Calderbank, S.W.McLaughlin and D.F.Lyons, "A low complexity two stage adaptive vector quantizer", In Proc. of the 25th CISS, pages 582-587, Baltimore, MD, Mar. 1991.

138. D.J.Goodman and A.Gersho, Theory of adaptive quantizers", IEEE Trans. On Comm, COM-22(8):1037-1045,Aug. 1994.

139. T.C.Bell, J.C.Cleary and I.H.Witten, Text compression, Prentice Hall, Englewood Cliffs, NJ, 1990.

140. G.G.Langton and J.Rissanen, "Compression of black and white images with arithmetic coding", IEEE Trans. On Comm., COM-29(6):858-867,Jun. 1981.

141. W.B.Pennebaker, J.L.Mitchell, G.G. Langton and R.B.Arps, "An overview of the basic principles of the Q-codec adaptive binary arithmetic coder", IBM Journal of Research and Development 32(6):717-726, Nov. 1988.

142. W.B.Pennebaker and J.L.Mitchell, "Probability estimation of the Q-coder",IBM J.Res.Develop., 32(6):737-752,Nov. 1988.

143. J.G.Proakis, C.M.Rader, F.Link and C.L.Nikias, Advanced digital signal processing, Macmillan,New York, 1992.

144. R.S.Gallager, "Variations on a theme by Huffman", IEEE Trans. On Info. Theory, IT-24(6):668-674,Nov. 1978.

145. D.Knuth, "Dynamic Huffman Coding", Journal of Algorithms, (6):163-180, 1985.

146. J.S.Vitter, "Dynamic Huffman Coding", ACM Trans. On Math. Software, 15(2):158-167,1989.

147. H-C. Huang, J-L.Wu, "Windowed Huffman coding algorithm with size adaptation", IEE Proc. I,140(2):109-113,Apr. 1993.

148. J.Rissanen, "Universal coding, information, prediction and estimation", IEEE Trans. On Info. Theory, IT-30(4):629-636, 1984.

149. J.Rissanen, Stochastic complexity in statistical inquiry, World Scientific, Singapore, 1989.

150. K.Ramchandran, Z.Xiong, K.Asai and M.Vetterli, " Adaptive transformations for image coding using spatially varying wavelet packets", IEEE Trans. On Image Proc, 1996.

151. D.Taubman and A.Zakhor, " Multirate 3-D sub-band coding of video", IEEE Trans. On Image Proc., 1994.

152. H-J.Wang and C-C Kuo, " A multi threshold wavelet coder (MTWC) for high fidelity image compression", 1997.

153. J.Li and S.Lei, " An embedded still image coder with rate distortion optimization", IEEE Trans. On Image Proc., 1999.

154. B-B.Chai, J.Vass, X.Zhuang, "Significant-linked connected component analysis for wavelet image coding", IEEE Trans. On Image. Proc. 1999.

155. M.Crouse and K.Ramchandran, "Joint thresholding and quantizer selection for transform image coding. Entropy constrained analysis and applications to baseline JPEG", IEEE Trans. On Image Proc., 1997.

156. J.Li, J.Li and C-C. Kuo, "Layered DCT still image compression", IEEE Trans. On Circ. and Syst. For Video Tech., 1997.

157. G.J.Sullivan and R.L.Baker, " Efficient quad-tree coding of images and video", In Proc. of ICASSP '91, 1991.

158. S.Todd, G.G. Langton Jr. and J.Rissanen, "Parameter reduction and context selection for compression of the gray scale images", IBM Jl. Res. Develop., vol 29 (2) pp. 188-193, Mar. 1985.

159. G.G.Langton Jr., A.Gulati and E.Seiler, " On the JPEG model for lossless image compression" in Proc. 1992 DCC (Snowbird, Utah, USA), pp. 172-180, Mar. 1992.

160. G.Glangton Jr. and M.Mareboyana, "Centering of context dependent components of prediction error distributions of images", in Proc. SPIE, vol 2028, pp. 26-31, July 1993.

161. G.Glangton Jr and C.A.Haidinyak, "Experiments with lossless and virtually lossless image compression algorithms", in Proc. SPIE, vol 2418, pp. 21-27,Feb. 1995.

162. X.Wu and N.D. Memon, "Context-based, adaptive, lossless image coding", IEEE Trans. Commun. vol. 45(4), pp. 437-444, Apr. 1997.

163. B.Meyer and P.Tischer, "TMW – A new method for lossless image compression", in Proc. 1997 International Picture Coding Symposium (PCS 97), (Berlin, Germany), Sept. 1997.

164. A.Netravali and J.O.Limb, "Picture Coding: a review", Proc. IEEE, vol 68, pp. 366-406, 1980.

165. R.Li, B.Zeng and M.L.Liou, "A new three step search algorithm for block motion estimation", IEEE Trans. On Circuits and Systems for Video Technology, vol. 4, no 4, pp. 438-442, Aug. 1994.

166. L.Po and W.Ma, "A novel Four Step Search Algorithm for Fast Block Motion Estimation", IEEE Trans. On Circuits and Systems for Video Technology, vol. 6, no 3, pp. 313-317, June 1996.

167. T.Zahariadis and D.Kalivas, " A spiral search algorithm for fast estimation of block motion vectors", Signal Processing VIII, theories and applications, proceedings of the EUSIPCO 96, Eighth European Signal Processing Conference, p.3, pp. 1079-1082, vol 2.

168. J.Jain and A.Jain, "Displacement measurement and its application in interframe image coding", IEEE Trans. On Communications, vol. COM-29, pp. 1799-1808, Dec. 1981.

169. A.Puri, H.Hang and D.Schilling, "An efficient block matching algorithm for motion compensated coding", Proceedings IEEE ICASSP, pp. 25.4.1-24.4.4, 1987.

170. M.Ghanbari, " The Cross Search Algorithm for Motion Estimation". IEEE Trans. On Communications, vol. COM-38, no. 7, pp. 950-953, July 1990.

171. R.Sinivasan, K.Rao, "Predictive coding based on efficient motion estimation", International Conference on Communications, Part 1, pp. 521-526, 1988, Amsterdam.

172. A.Tourapis, G.Shen, M.Liou, O.Au, I.Ahmad , "A New Predictive Diamond Search Algorithm for Block Based Motion Estimation", VCIP 2000.

173. S.Zhou and K.K.Ma, " A new Diamond Search Algorithm for fast block matching motion estimation", Proc. of Int. Conf. Information, Communications and Signal Processing , vol 1, pp. 292-6, 1997.

174. J.Y.Tham, S.Ranganath, M.Ranganath and A.A.Kassim, "A Novel Unrestricted Center-Biased Diamond Search Algorithm for Block Motion Estimation", IEEE Transactions on Circuits and Systems for Video Technology Vol. 8, pp. 369-377, Aug. 1998.

175. M.Alkanhal, D.Turaga and T.Chen, " Correlation based Search Algorithms for Motion Estimation", Proc. of Picture Coding Symposium, Portland, OR, April 21-25, 1999.

176. A.M.Tekalp, Digital Video Processing, Prentice Hall, New York, 1995.

177. Y.Altunbasak, P.E.Eren and A.M.Tekalp, "Region-Based Parametric Motion Segmentation Using Color Information", In Journal of Graphical Models and Image Processing, vol. 60, No 1, January, pp. 13-23, 1998.

178. J.Y.A.Wang and E.H.Adelson, " Representing moving images with layers", IEEE Trans. Image Proc. 3(5), Sept. 1994, 625-638.

179. M.Bober and J.Kittler, "On combining the Hough transform and multi-resolution MRFs for the robust analysis of complex motion", in Proc. of Second Asian Conference on Computer Vision (ACCV), Dec. 1995.

180. J-M Odobez and P.Bouthemy, " Direct model based image motion segmentation for dynamic scene analysis", in Proc. of Second Asian Conference on Computer Vision (ACCV), Dec. 1995.

181. Y.Weiss and E.H.Adelson, " A unified mixture framework for motion segmentation: Incorporating spatial coherence and estimating the number of models", in Proc. IEEE Int. Conf. Computer Vision and Pattern Recognition, June 1996.

182. M.M.Chang, A.M.Tekalp and M.I.Sezan, " An algorithm for simultaneous motion estimation and scene segmentation", in Proc. IEEE ICASSP, Adelaide, Australia, April 1994.

183. J.R.Bergen, P.J.Burt and K.Hanna, "Dynamic multiple motion computation" in Journal of Artificial Intelligence and Computer Vision (Y.A.Feldman and A.Bruckstein Eds), pp. 147-156, Elsevier, Amsterdam, 1992.

184. M.Irani and S.Peleg, " Motion analysis for image enhancement: Resolution, Occlusion and Transparency", Journal of Visual Communication and Image Representation, 4(4), Dec. 1993, 324-335.

185. R.Mech and P.Gerken, "Automatic segmentation of moving objects", Doc. No ISO/IEC/JTC1/SC29/WG11 MPEG 96/1188, Sept. 1996.

186. G.Russo and S.Colonnese, "Automatic segmentation Techniques", Doc. No ISO/IEC/JTC1/SC29/WG11 MPEG 96/1181, Sept. 1996.

187. D.W.Murray and B.F.Buxton, " Scene segmentation from visual motion using global optimization", IEEE Trans. Pattern Anal. Machine Intel., 9(2) Mar. 1987, 220-228.